

**BIDIRECTIONAL METALATION OF HYDROBENZOIN:
DIRECT ACCESS TO NEW CHIRAL LIGANDS AND
AUXILIARIES**

by

Inhee Cho

B.Sc. Honours (Co-op), University of British Columbia, 2005

THESIS SUBMITTED IN PARTIAL FULFILLMENT OF
THE REQUIREMENTS FOR THE DEGREE OF

MASTER OF SCIENCE

In the
Department of Chemistry

© Inhee Cho 2009

SIMON FRASER UNIVERSITY

Summer 2009

All rights reserved. This work may not be
reproduced in whole or in part, by photocopy
or other means, without permission of the author.

APPROVAL

Name: Inhee Cho

Degree: Master of Science

Title of Thesis: Bidirectional Metalation of Hydrobenzoin: Direct Access to New Chiral Ligands and Auxiliaries

Examining Committee:

Chair

Dr. Erika Plettner
Associate Professor, Department of Chemistry

Dr. Robert A. Britton
Senior Supervisor
Assistant Professor, Department of Chemistry

Dr. Peter D. Wilson
Supervisor
Associate Professor, Department of Chemistry

Dr. Daniel B. Leznoff
Supervisor
Associate Professor, Department of Chemistry

Dr. Vance E. Williams
Internal Examiner
Associate Professor, Department of Chemistry

Date Defended/Approved: **May 25, 2009**



SIMON FRASER UNIVERSITY
LIBRARY

Declaration of Partial Copyright Licence

The author, whose copyright is declared on the title page of this work, has granted to Simon Fraser University the right to lend this thesis, project or extended essay to users of the Simon Fraser University Library, and to make partial or single copies only for such users or in response to a request from the library of any other university, or other educational institution, on its own behalf or for one of its users.

The author has further granted permission to Simon Fraser University to keep or make a digital copy for use in its circulating collection (currently available to the public at the "Institutional Repository" link of the SFU Library website <www.lib.sfu.ca> at: <<http://ir.lib.sfu.ca/handle/1892/112>>) and, without changing the content, to translate the thesis/project or extended essays, if technically possible, to any medium or format for the purpose of preservation of the digital work.

The author has further agreed that permission for multiple copying of this work for scholarly purposes may be granted by either the author or the Dean of Graduate Studies.

It is understood that copying or publication of this work for financial gain shall not be allowed without the author's written permission.

Permission for public performance, or limited permission for private scholarly use, of any multimedia materials forming part of this work, may have been granted by the author. This information may be found on the separately catalogued multimedia material and in the signed Partial Copyright Licence.

While licensing SFU to permit the above uses, the author retains copyright in the thesis, project or extended essays, including the right to change the work for subsequent purposes, including editing and publishing the work in whole or in part, and licensing other parties, as the author may desire.

The original Partial Copyright Licence attesting to these terms, and signed by this author, may be found in the original bound copy of this work, retained in the Simon Fraser University Archive.

Simon Fraser University Library
Burnaby, BC, Canada

ABSTRACT

In the last 30 years, the development of asymmetric reactions has become one of the most important pursuits within the field of organic chemistry. In this regard, hydrobenzoin has demonstrated utility as both an auxiliary and a ligand for a variety of asymmetric transformations including aldol reactions, Diels-Alder reactions, and Evans-Tishchenko reactions. Oftentimes, however, the optimization of these processes involves the use of *ortho*-functionalized hydrobenzoin derivatives, the syntheses of which are often lengthy and/or proceed without complete control of absolute chemistry, detracting from the utility of this catalyst/ligand system. This thesis reports the development of a novel synthesis of *ortho*-substituted hydrobenzoin derivatives via a one-step process that involves a bidirectional *ortho*-metalation of hydrobenzoin. Further exploitation of these hydrobenzoin derivatives via Pd-catalyzed cross coupling reactions further enhances the utility of this process and provides access to a wide range of novel chiral ligands and auxiliaries in optically pure form.

Keywords: asymmetric synthesis; hydrobenzoin ligands and auxiliaries; directed *ortho*-metalation

Subject Terms: asymmetric synthesis; organic chemistry; catalysis; ligands; auxiliaries

To JC - Je T'aime

ACKNOWLEDGEMENTS

I would not be here if it wasn't for God. I don't think I have ever believed that more than I do now. Thank you so much for everything – for being my saviour, my guide, a comforter, an unconditionally loving father, and a friend. Help me to understand more of Your character and to treat each day as a gift from You.

I would also especially like to thank my supervisor Dr. Rob Britton – I know that I wasn't the easiest person to work with these past 2.5 years but I really do appreciate your patience, enthusiasm and support. I have not met a professor who continually looks out for his student's needs more than you did. If I ever get rich, I will try to remember to buy you a chiral GC column (perhaps several!).

To the members of the Britton lab (past and present) – I wish you all the best and keep getting all those scholarships and publications. Special thanks to Elena, Hoda and Stan for making me laugh. I would also like to acknowledge Jason Draper for his help in obtaining references and spectra while I was overseas. Hongwen and Regine have also played a major part in helping me get results for my thesis with their remarkable expertise. I would also like to acknowledge and thank Mike Katz and the Leznoff group for their help with crystal structure determination.

I would also like to thank my committee members Drs. Danny Leznoff and Peter Wilson who have helped guide the progress of my master's work. Susie,

Yolanda, and Ken also have always been there to answer any administrative questions I had about graduate school. Carlotta Spino has been a great help in the days leading up to the completion of my thesis. I would also wish to thank Simon Fraser University (Graduate Fellowship) and Michael Smith Foundation for Health Research for their financial support.

GABO – thanks for all the coffee breaks and random talks. I hope that you get to graduate soon too! My brothers and sisters in Christ – thanks for all the prayer, the accountability, talks and fun times. You have truly loved me as yourselves.

My parents and Bubbles – thank you for being supportive in the way you know how. I love you very much and sorry for keeping you awake so often. Big dong – we don't talk often, but when we do, I'm reminded of how great a brother you are.

And finally JC (MMT, MGF, BGF) – thank you so much for your love and for not only enduring the good times with me but also the annoying, sad, depressing, frustrating, monotonous, and tiring times as well. Je T'aime, gros bisous!

TABLE OF CONTENTS

Approval	ii
Abstract	iii
Dedication	iv
Acknowledgements	v
Table of Contents	vii
List of Figures	x
List of Schemes	xi
List of Tables	xiv
Abbreviations	xv
1: Introduction	1
1.1 Chiral Ligands and Auxiliaries in Asymmetric Synthesis	1
1.2 Background - Hydrobenzoin as an Auxiliary.....	7
1.2.1 Diastereoselective Reduction of α -Keto Esters.....	7
1.2.2 Hydrobenzoin as an Auxiliary in <i>anti</i> -Selective Glycolate Aldol Additions	10
1.2.3 (<i>S,S</i>)-Hydrobenzoin as an Auxiliary in the Synthesis of Polyhydroxy- and Aminohydroxy-Compounds	11
1.2.4 Regio- and Diastereoselective S_N2' or S_N2'' Additions to Allylic Acetals using Hydrobenzoin as a Chiral Auxiliary.....	13
1.2.5 Diastereoselective Diels-Alder Reactions Involving (<i>R,R</i>)- Hydrobenzoin in the Partial Synthesis of the Immunosuppressant FK-506.....	14
1.2.6 Heterodiene Cycloadditions of C_2 -Symmetric 4,5- Disubstituted Ketene Acetals	16
1.2.7 Chiral Diol Systems Using Hydrobenzoin as an Auxiliary	19
1.3 Background – Hydrobenzoin as a Chiral Ligand	21
1.3.1 Chiral Hydrobenzoin•SnCl ₄ and its Derivatives in the Catalytic Enantioselective Allyl- and Crotylboration of Aldehydes	22
1.3.2 Catalytic Asymmetric Evans-Tischenko Reaction of Aldehydes and Aliphatic Ketones using Hydrobenzoin and its Derivatives.....	24

1.3.3	Hydrobenzoin as a Chiral Catalyst in the Asymmetric Addition of Organolithium Reagents to Arene Tricarbonylchromium Complexes.....	27
1.3.4	Hydrobenzoin as a Catalyst in the Enantioselective Conjugate Addition of an Organolithium to an α,β – Unsaturated Aldimine.....	29
1.4	Synthesis of <i>ortho</i> -Substituted hydrobenzoin.....	31
1.4.1	Literature Procedures for Synthesis of <i>ortho</i> -Substituted Hydrobenzoin.....	31
1.4.2	Background to this Thesis.....	34
1.4.3	Thesis Proposal – New Efficient Synthesis of <i>ortho</i> -Substituted Hydrobenzoin.....	36
	2: Bidirectional metalation of Hydrobenzoin and applications	38
2.1	Directed <i>ortho</i> -Metalation (DoM) Reactions	38
2.1.1	General Characteristics and Mechanistic Aspects.....	38
2.1.2	<i>Ortho</i> -Metalation Reactions Involving a Benzyl Alcohol or α -Methylbenzyl Alcohol.....	46
2.1.3	Optimization of the Bidirectional <i>ortho</i> -Lithiation of (<i>R,R</i>)-Hydrobenzoin.....	50
2.1.4	Optimization of Bidirectional Metalation of Hydrobenzoin.....	52
2.1.5	Confirmation of Optical Purity	59
2.1.6	Screening of Electrophiles in the Bidirectional Metalation of (<i>R,R</i>)-Hydrobenzoin.....	59
2.1.7	<i>Ortho</i> -Substituted Hydrobenzoin Derivatives from Diiodo 198 and <i>bis</i> -Benoxaborol 204	77
2.1.8	Buchwald-Hartwig Couplings to form Azepines.....	80
2.1.9	Intramolecular Cross-Coupling Reactions.....	82
2.1.10	<i>ortho</i> -Pyridine Substituted Hydrobenzoin.....	85
2.2	Conclusion	88
	3: Future Direction.....	90
	4: General Conclusion	93
	5: Experimental.....	97
5.1	General	97
5.2	Verification of Optical Purity (GC) of Tetraanion after treatment with H ₂ O.....	99
5.3	Butane Gas Evolution Studies.....	99
5.4	Procedure for Deuterium Quench.....	100
5.5	Preparation of Hydrobenzoin Derivatives	101
5.5.1	Preparation of (<i>1R,2R</i>)-1,2-di- <i>o</i> -tolylethane-1,2-diol 194	101
5.5.2	Preparation of (<i>1R,2R</i>)-1,2- <i>bis</i> -(2-iodophenyl)-ethane-1,2-diol 178	102
5.5.3	Preparation of (<i>1R,2R</i>)-1,2- <i>bis</i> -(2-bromophenyl)-ethane-1,2-diol 83	103
5.5.4	Preparation of the <i>bis</i> -lactone 195	105

5.5.5	Preparation of <i>bis</i> -benzoxaborol 196	106
5.5.6	Preparation of the <i>bis</i> -siloxane 197	108
5.5.7	Preparation of (4 <i>R</i> , 5 <i>R</i>)-4,5- <i>bis</i> -(2-iodophenyl)-2,2-dimethyl-1,3-dioxolane 212	110
5.5.8	Preparation of silepine 235	111
5.5.9	Preparation of (4 <i>R</i> ,5 <i>R</i>)-4,5- <i>bis</i> -(2-trimethylsilylphenyl)-2,2-dimethyl-1,3-dioxolane 236	112
5.5.10	Preparation of 4,5- <i>bis</i> -biphenyl-2-yl-2,2-dimethyl-[1,3]-dioxolane 237	113
5.5.11	Preparation of (1 <i>R</i> ,2 <i>R</i>)-1,2-di(biphenyl-2-yl)ethane-1,2-diol 239	115
5.5.12	Preparation of (1 <i>R</i> ,2 <i>R</i>)-1,2- <i>bis</i> (2-(<i>E</i>)-cyclooctenylphenyl)ethane-1,2-diol – Vivol precursor 134	116
5.5.13	Preparation of (1 <i>R</i> ,2 <i>R</i>)- 1,2- <i>bis</i> (2-hydroxyphenyl)ethane-1,2-diol 240	117
5.6	Selected ¹ H and ¹³ C NMR Spectra.....	119
5.7	Crystal Structure Data for Compound 197	131
References		141

LIST OF FIGURES

Figure 1. Examples of diol ligands.	5
Figure 2. Increased selectivity of L-selectride [®] mediated reduction with <i>o</i> -methoxy groups.	9
Figure 3. Preferred conformation 74a of the ketene acetals versus 74b	19
Figure 4. Stacked conformation of Vivol.	24
Figure 5. <i>O,N</i> -Donor ligands screened for the Evans-Tischenko reaction.	27
Figure 6. Proposed transition state for the enantioselective addition of an organolithium to an α,β -unsaturated aldimine.	31
Figure 7. Partial bond formation in transition state for kinetically enhanced metalation mechanism.	42
Figure 8. Arenes studied by Collum <i>et al.</i>	44
Figure 9. A: ¹ H NMR of (<i>R,R</i>)-hydrobenzoin. B: ¹ H NMR of deuterated hydrobenzoin.	51
Figure 10. Gas (butane) evolution studies. Reaction conditions: 0.47 mmol of (<i>R,R</i>)-hydrobenzoin in mixture of 2:1 hexane-ether ([25]=0.08M), 6.0 equiv of <i>n</i> -BuLi.	54
Figure 11. Percentage of hydrobenzoin 25 , monodeuteriohydrobenzoin 176 and dideuteriohydrobenzoin 177 following treatment of a refluxing solution of 25 and <i>n</i> -BuLi (6 equiv) with D ₂ O after various reaction times. The crude product following D ₂ O quench was concentrated repeatedly from CH ₃ OH, to ensure complete exchange of OH for OD. The ratio of 25 : 176 : 177 for these products, respectively, was determined by mass spectroscopy.	55
Figure 12. ORTEP plot of the crystal structure of <i>bis</i> -siloxane 197 . We thank Michael J. Katz (Leznoff laboratory, Department of Chemistry, Simon Fraser University) for solving this crystal structure.	63
Figure 13. Summary of <i>ortho</i> -substituted hydrobenzoin derivatives synthesized.	96

LIST OF SCHEMES

Scheme 1. Example of a Diastereoselective Synthesis with Chiral Auxiliaries	2
Scheme 2. Evans Boron-Mediated Aldol Reaction Using Chiral Oxazolidinones	3
Scheme 3. Reduction of Acetophenone with Modified (<i>R</i>)-BINAL-H 24	4
Scheme 4. Asymmetric Reduction of Enamides Using DIOP Ligands.....	6
Scheme 5. L-Selectride [®] -Mediated Reduction of Phenylglyoxylate and Cleavage	8
Scheme 6. Conformational Analysis of L-Selectride [®] Mediated Reduction of Phenylglyoxylates.....	9
Scheme 7. Glycolate Aldol Reactions	11
Scheme 8. Synthesis of (+)-Polyoxamic Acid and D-Sorbitol Using (<i>S,S</i>)-Hydrobenzoin as a Source of Chirality	12
Scheme 9. Addition of Phenylcuprate to Allylic Hydrobenzoin Acetals	14
Scheme 10. Diels-Alder Reaction Using (<i>R,R</i>)-Hydrobenzoin as an Auxiliary.....	15
Scheme 11. Conformation of the <i>Bis</i> -Acrylate Reaction Complex	15
Scheme 12. Diastereoselective Cycloaddition of a Hydrobenzoin-Derived Acetic Acid Ester Enolate and an α,β -Unsaturated Carbonyl Compound.....	17
Scheme 13. Model Used to Explain Increased Selectivity in Cycloaddition Reactions of Ketene Acetal 70	18
Scheme 14. Nucleophilic Additions Proceeding <i>via</i> the Intermediate 75	21
Scheme 15. Postulated Mechanism of Evans-Tischenko Reaction	25
Scheme 16. Enantioselective Evans-Tischenko Reaction	26
Scheme 17. Addition of RLi and Propargyl Amine in the Presence of Chiral Catalysts to an Arene Cr(CO) ₃ Complex	28
Scheme 18. Asymmetric Addition of Organolithiums into a Prochiral Arene Complex	28

Scheme 19. Addition of <i>n</i> -Butyllithium to Aldimine 108 Using Hydrobenzoin Derived Chiral Diether 105	29
Scheme 20. Typical Procedure for the Synthesis of <i>ortho</i> -Substituted Hydrobenzoin Derivatives.....	32
Scheme 21. Synthesis of Vivol.....	34
Scheme 22. Diastereoselective Mukaiyama Aldol Reaction in Water	35
Scheme 23. First Attempted Synthesis of Chiral Borinic Acid 139	36
Scheme 24. Proposed Direct Access to <i>ortho</i> -Substituted Hydrobenzoin Derivatives.....	37
Scheme 25. Directed <i>ortho</i> -Metalations.....	39
Scheme 26. General Concept of CIPE	40
Scheme 27. Directed Metalation of 148 through Complexation with <i>s</i> -BuLi Tetramers	41
Scheme 28. An Example of Intra- and Intermolecular Isotope Effects of Directed Metalations.....	43
Scheme 29. Proposed Mechanism of Urea Metalation Reaction.....	44
Scheme 30. Triple-ion Based Model of DoM Reactions, X = OMe, F	45
Scheme 31. Synthesis of Hypervalent Iodine Compound 172 via Seebach Method	49
Scheme 32. Synthesis of Iodosobenzoic Acids Using <i>ortho</i> -Lithiation.....	49
Scheme 33. Kilogram Scale Synthesis of (<i>R,R</i>)- or (<i>S,S</i>)- Hydrobenzoin	50
Scheme 34. Reaction of Organolithium Reagents (B) with Tetrahydrofuran.....	52
Scheme 35. Possible Mechanism for Observed Side Product 184	56
Scheme 36. <i>Ortho</i> -Lithiation Through an Alkoxide Intermediate.....	57
Scheme 37. Rearrangement of <i>bis</i> -Indane 188 to <i>cis</i> -Decalin-like Structure 189	57
Scheme 38. Bridged Complex 191 in Lithiation of Diphenylacetylene	58
Scheme 39. Potential Mechanism for Second <i>ortho</i> -Deprotonation.....	58
Scheme 40. Reaction Mechanism of Tetraanion with Iodine	62
Scheme 41. Reaction of Tetraanion 189 with TMSCl	64
Scheme 42. Formation of Six-membered Ring in Reaction of Tetraanion with SiMe ₂ Cl ₂	65
Scheme 43. Protection of Diiodo Hydrobenzoin Derivative 178	66
Scheme 44. Reaction of Digrynard 215 with Exogenous Oxygen.....	67

Scheme 45. Distinguishing Between the Borinic Acid 139 and the <i>bis</i> -Benzoxaborol 196	70
Scheme 46. Addition of Carbanions to Carbonyls by Electron-transfer Mechanism (D = donor, A = acceptor).....	73
Scheme 47. Reaction of Tetraanion with Carbonyl Compounds.....	73
Scheme 48. Reaction of Benzyl Chloride with Itself under Basic Conditions	74
Scheme 49. Synthesis of <i>ortho</i> -Substituted Hydrobenzoin Derivatives from Acetonide 212	78
Scheme 50. <i>cis</i> -4b,9b-Dihydrobenzofuro[3,2-b]-benzofuran, Product Obtained from Pd(0) Catalyzed Coupling of Diiodo Hydrobenzoin 178	78
Scheme 51. Cross Coupling of <i>bis</i> -Benzoxaborol with Aryl Halides and Vinyl Triflates.....	79
Scheme 52. Oxidation of <i>bis</i> -Benzoxaborol to Give <i>bis</i> -Phenol 240	80
Scheme 53. Attempted Buchwald-Hartwig Couplings.....	81
Scheme 54. Coupling of 4-Iodotoluene with Benzylamine	82
Scheme 55. Proposed Synthesis of Dihydrophenanthrene 246	82
Scheme 56. Examples of Reactions Using Copper Thiophene Carboxylate	84
Scheme 57. Synthesis of Copper Thiophene Carboxylate.....	84
Scheme 58. Example of Coupling of Aryl Halide with Pyridine <i>N</i> -Oxide	86
Scheme 59. Serendipitous Reductive Cyclization Using Pyridine <i>N</i> -Oxide and Palladium.....	86
Scheme 60. Reductive Elimination of Pd(II) Species to Give Coupled Product 255	87
Scheme 61. Reductive Elimination of Ethane via Pd(IV) Species with Bipyridine Ligand.....	87
Scheme 62. Hetero-Diels-Alder Reaction Using <i>ortho</i> -Silylated Derivative (<i>R</i>)- 264	91
Scheme 63. Asymmetric Mannich Reaction using BINOL	92

LIST OF TABLES

Table 1. Selected Examples of the Diastereoselective Synthesis of 1,2-Substituted Diols using Hydrobenzoin as an Auxiliary.....	20
Table 2. Results of Allylboration Reaction with Different <i>ortho</i> -Substituted Diols	23
Table 3. Enantioselective Conjugate Addition of an Organolithium to an α,β – Unsaturated Aldimine under Different Conditions.....	30
Table 4. Hierarchy of Carbon Based DMGs.....	47
Table 5. The <i>ortho</i> -Lithiation of Benzyl Alcohol.....	48
Table 6. Bidirectional Metalation of (<i>R,R</i>)-Hydrobenzoin	52
Table 7. Optimum Equivalents of <i>n</i> -BuLi for the Diiodination of Hydrobenzoin	53
Table 8. Synthesis of Hydrobenzoin Derivatives.....	60
Table 9. Incorporation of Silicon in the <i>ortho</i> -Positions of Hydrobenzoin	64
Table 10. Attempts to Incorporate Boron <i>via</i> the Acetonide Protected Diiodo Hydrobenzoin Derivative 212	67
Table 11. Attempted Syntheses of Dimethoxy Boronic Acid 141	68
Table 12. Direct Functionalization of Hydrobenzoin with Boron	69
Table 13. Addition of Carbon Electrophiles to the Tetraanion	72
Table 14. Results from Transmetalation of Tetraanion with Zn and Mg.....	75
Table 15. Carbon-carbon Bond Formation Reactions with Benzaldehyde	76
Table 16. Attempted Syntheses of <i>ortho</i> -Amino Hydrobenzoin Derivatives	81
Table 17. Results of Oxidative Couplings	83
Table 18. Synthesis of Diiodohydrobenzoin Derivative 187 with Copper Thiophene Carboxylate	85

ABBREVIATIONS

Å	angstrom
Ac	acetyl
AD	asymmetric dihydroxylation
Ar	aryl (substituted aromatic ring)
BINAL-H	2,2'-dihydroxy-1,1'-binaphthyl lithium aluminium hydride
BINAP	2,2'- <i>bis</i> (diphenylphosphino)-1,1'-binaphthyl
BINOL	1,1'-bi-2-naphthol
Bn	benzyl
Bu (ⁿ Bu)	<i>n</i> -butyl
c-hex	cyclohexyl
CIPE	complex induced proximity effect
COD	cyclooctadiene
CuTC	copper(I) thiophene-2-carboxylate
DCE	dichloroethane
DCM	dichloromethane
de	diastereomeric excess
DIC	diisopropyl carbodiimide
DIOP	4,5- <i>bis</i> -[(diphenylphosphanyl)methyl]-2,2-dimethyl-[1,3]dioxolane
DIPEA (Hünig's base)	<i>N,N</i> -diisopropylethylamine
(DHDQ) ₂ PHAL	1,4- <i>bis</i> (dihydroquininyl)phthalazine
DMAP	<i>N,N</i> -dimethylaminopyridine
DMDO	dimethoxydioxirane
DME	dimethoxyethane
DMF	<i>N,N</i> -dimethyl formamide
DMG	directing metal group
DoM	directed <i>ortho</i> -metalation

dppe	1,2- <i>bis</i> (diphenylphosphino)ethane
dr	diastereomeric ratio
E	electrophile
ee	enantiomeric excess
EI	electron impact
equiv	equivalents
er	enantiomeric ratio
ESI	electrospray
Et	ethyl
FAB	fast atom bombardment
GC	gas chromatography
h (hrs)	hour (hours)
HMPA	hexamethylphosphoramide
HPLC	high performance liquid chromatography
HOESY	heteronuclear Overhauser effect spectroscopy
Hünig's base (DIPEA)	<i>N,N</i> -Diisopropylethylamine
Hz	Hertz
IR	infrared spectroscopy
<i>iso</i> -butyl	2-methylpropyl
KEM	kinetically enhanced metalation
LAH	lithium aluminum hydride
LBA	Lewis acid Brønsted acid
L-selectride	lithium triisobutylhydroborate
M	metal (generic)
Me	methyl
min	minute(s)
mol	mole(s)
MS	mass spectrometry
NMI	<i>N</i> -methylimidazole
NMR	nuclear magnetic resonance spectroscopy
<i>n</i> -Pr	<i>n</i> -propyl
Nu	nucleophile

o/n	overnight
Ph	phenyl
Pr	propyl
quant	quantitative
s-Bu	<i>sec</i> -Butyl
SET	single electron transfer
SM	starting material
TADDOL	(-)- <i>trans</i> - α,α' -(dimethyl-1,3-dioxolane-4,5-diyl)bis(diphenylmethanol)
TBDMS	<i>t</i> -Butyl dimethyl silyl
<i>t</i> -Bu	<i>tert</i> -Butyl
Tf	triflate
THF	tetrahydrofuran
TMS	trimethylsilyl
Tosyl	toluene-sulfonyl
Ts	See <i>Tosyl</i>

1: INTRODUCTION

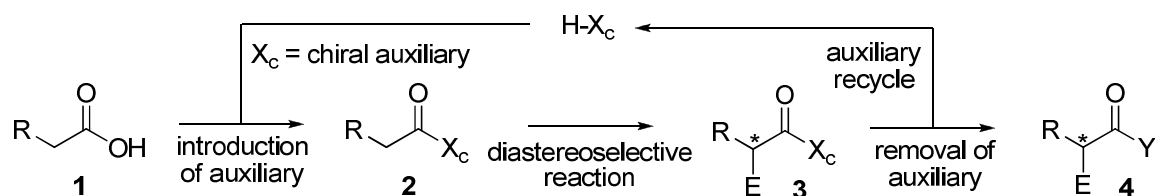
This thesis concerns the development of efficient syntheses of hydrobenzoin-derived auxiliaries and ligands that have been shown to catalyze a variety of important asymmetric reactions. A background to the literature concerning the use of hydrobenzoin as an auxiliary and ligand will also be surveyed with a special focus on its *ortho*-functionalized derivatives.

1.1 Chiral Ligands and Auxiliaries in Asymmetric Synthesis

The abundance of chirality in natural products as well as pharmaceuticals, agrochemicals, fragrances, and flavour chemicals¹ continues to drive the development of new methods for introducing asymmetry into molecules. Nowhere is this more important than in the pharmaceutical industry, where one enantiomer of a drug may elicit the desired biological effect whereas the other enantiomer displays no activity or causes adverse side effects.² Thus, over the past 30 years, the development of highly efficient, practical and enantioselective synthetic processes has been the focus of many researchers and recently the subject of the Nobel Prize in chemistry.³

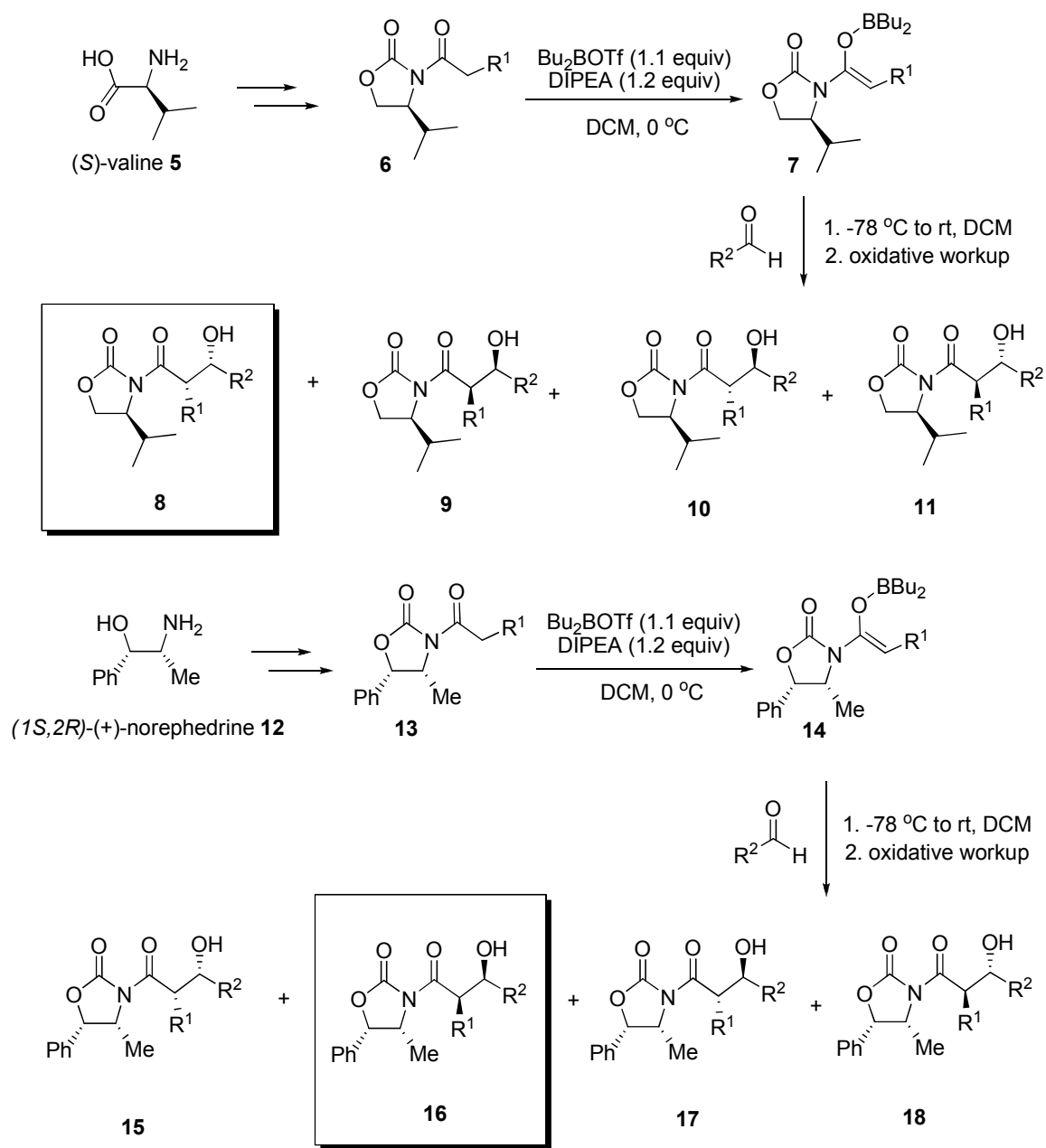
The most common method for introducing asymmetry in a synthetic process involves the use of chiral auxiliaries, which bias an otherwise non-selective reaction towards the formation of one diastereomer. As indicated below in Scheme 1, removal of the chiral auxiliary then unveils an optically pure product

and oftentimes the chiral auxiliary itself can be recycled to improve the economics of the process.



Scheme 1. Example of a Diastereoselective Synthesis with Chiral Auxiliaries

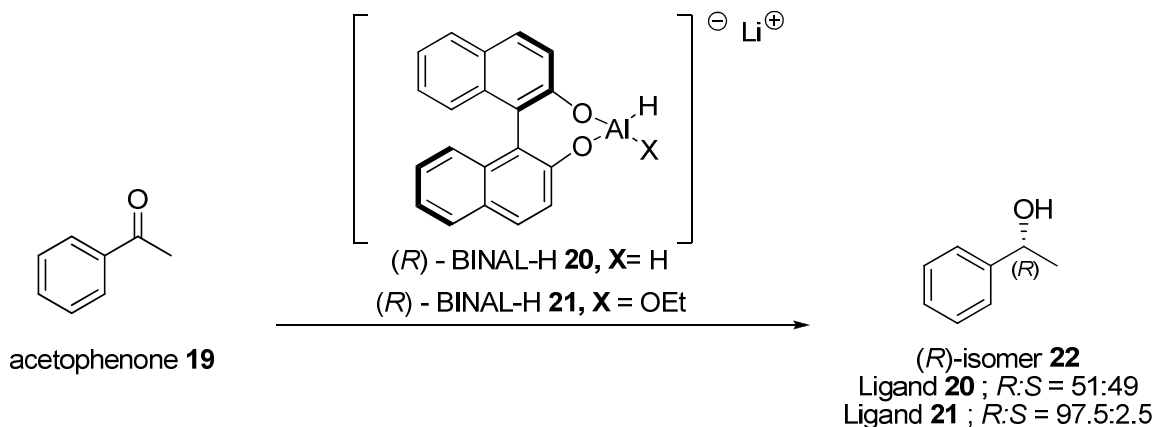
In general, the criteria for selecting a chiral auxiliary include cost, ease with which it can be incorporated and removed from the substrate, and its effectiveness at imparting diastereoselectivity in a desired synthetic process. Not surprisingly, many auxiliaries are derived from inexpensive and naturally occurring members of the chiral pool or chiral building blocks produced in unrelated industrial processes. For example, the oxazolidinone based auxiliaries developed by the Evans group⁴ are made from the natural amino acid (*S*)-valine (Scheme 2, **5** → **6**) or the commercially available (*1S,2R*)-norephedrine (Scheme 2, **12** → **13**). After enolization with dibutylboron triflate (e.g., **7** and **14**) and subsequent coupling with an aldehyde, the (*S*)-valine derived oxazolidinone affords almost exclusively the *syn* aldol product **8** while the (*1S,2R*)-norephedrine derived oxazolidinone provides the enantiomeric *syn* aldol product **16**. In both cases, the production of *anti*-aldol products **10-11** or **17-18** never exceeds 1% of the overall yield. After separation of the desired diastereomer from the minor stereoisomers and removal of the auxiliary, these processes afford optically pure *syn*-aldol products in excellent overall yield.



Scheme 2. Evans Boron-Mediated Aldol Reaction Using Chiral Oxazolidinones

A classic example of an asymmetric reaction using chiral reagents involves the reduction of prochiral ketones with (*R*)-BINAL-H **20** (Scheme 3).⁵ In this case it was found that the reducing agent - prepared by mixing an equimolar

amount of LiAlH_4 and (*R*)-BINOL in THF – effectively reduced acetophenone to provide the corresponding secondary alcohol **22** in low enantiomeric excess (e.r. = 51:49). However, it was later shown⁵ that simply replacing one of the hydrogen atoms in BINAL-H with an ethoxide (e.g., **21**, Scheme 3) afforded an effective reagent for the enantioselective reduction of prochiral ketones. For example, using this modified reducing agent the reduction of acetophenone gave a 97.5:2.5 selectivity for the (*R*)-isomer **22** over the corresponding (*S*)-isomer.



Scheme 3. Reduction of Acetophenone with Modified (*R*)-BINAL-H **24**

While there are clear advantages associated with the use of chiral auxiliaries, their use also necessitates additional appendage and removal steps, and stoichiometric amounts of chiral reagents are required. These added steps often lead to lower overall yields and increases to both the cost of a synthetic process and amount of byproducts produced, the latter of which also detracts from the environmental appeal of a reaction sequence. In addition, during the removal of the chiral auxiliary from the product, care must be taken to avoid destruction of the newly introduced stereogenic centres.⁶ On the basis of these concerns, there has been an exponential growth in the development of *catalytic*

asymmetric reactions over the past 30 years. In a catalytic process, a ligand that is present in sub-stoichiometric quantities, coordinates to the prochiral material in a non-covalent manner prior to the stereoselective reaction and thus precludes both the appendage and removal steps required with chiral auxiliaries. The transfer of asymmetry in these reactions is often fine-tuned by the choice of metal and/or chiral ligand; widely used chiral ligands include various diols,⁷ as well as diamines,⁸ and diphosphines (Figure 1).⁹

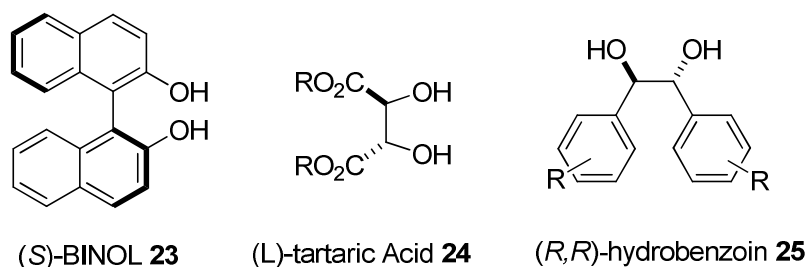
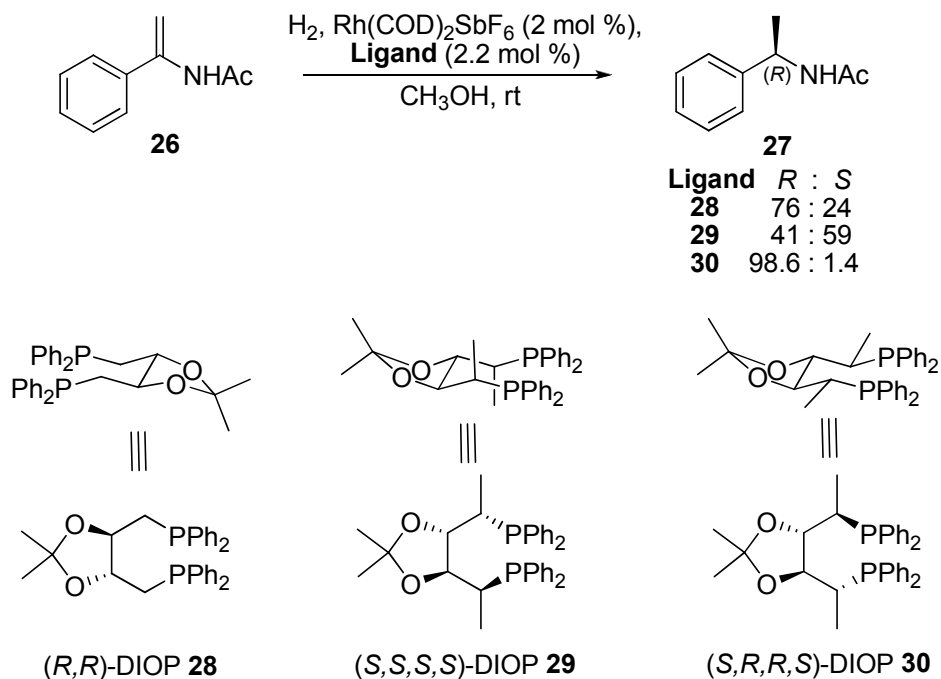


Figure 1. Examples of diol ligands.

Zhang has reported a catalytic asymmetric hydrogenation reaction that exploits Kagan's C_2 symmetric DIOP ligand **28** (Scheme 4).¹⁰ Thus, the hydrogenation of enamide **26**, with (*R,R*)-DIOP (**28**) afforded a 76:24 mixture of enantiomeric amines favouring the (*R*)-enantiomer **27**. This modest selectivity was attributed to the lack of rigidity of the complex, which consequently permits equilibration between the chair and boat conformations of a six-membered ring chelate. To verify this supposition, methyl groups were introduced in the α -positions of the diphenylphosphino groups through the synthesis of the modified DIOP **29**. However, this alteration decreased the enantioselectivity of this reaction and afforded a 41:59 ratio of *R*:*S* enantiomeric amines. Conformational analysis of the ligands (Scheme 4) revealed a mismatch between

the carbon backbone and the axial methyl groups, an observation that prompted the synthesis of the diastereomeric ligand **30**, in which the methyl groups preferentially adopt equatorial positions. Indeed, employing this modified DIOP ligand **30**, the (*R*)-isomer (e.r. = 98.6:1.4) was the predominant product of the enamine reduction, further confirming the importance of ligand modification in catalytic asymmetric synthesis.



Scheme 4. Asymmetric Reduction of Enamides Using DIOP Ligands

As evidenced by these examples, both chiral auxiliaries and ligands have proven useful in many synthetic transformations and the development of new ligands/auxiliaries continue to broaden the scope of many asymmetric processes. Oftentimes, however, the general utility of these auxiliaries or ligands is hampered by their cost, complexities associated with their synthesis or their sole

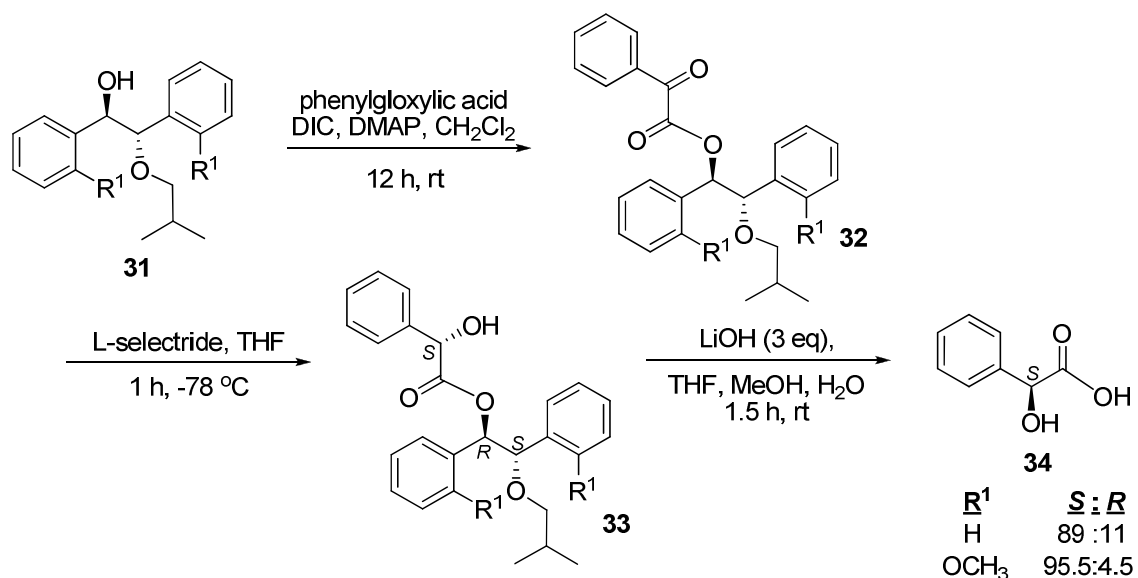
availability as a single enantiomer.¹¹ Consequently, the identification of cheap or readily accessible chiral scaffolds is an important pursuit.

1.2 Background - Hydrobenzoin as an Auxiliary

Discussed below are examples in which hydrobenzoin has been used as an auxiliary in asymmetric transformations. In particular, *ortho*-substituted hydrobenzoin derivatives will be discussed in more detail to emphasize the need for efficient syntheses of these substances.

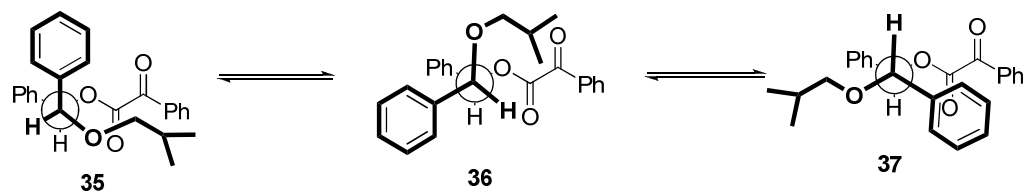
1.2.1 Diastereoselective Reduction of α -Keto Esters

The L-selectride[®]-mediated reduction of α -keto esters using *meso*-hydrobenzoin as an auxiliary has been reported by Gaertner (Scheme 5).¹² In this work, hydrobenzoin derivatives were first desymmetrized through protection of one of the alcohol functions to provide the *iso*-butyl ethers **31**. Phenylglyoxylic acid was then coupled to the remaining free hydroxyl group to afford the keto ester **32**, which was subsequently reduced with L-selectride[®] to the corresponding α -hydroxyketone **33**. In this work, it was found that when $R^1 = H$, reduction favoured the formation of the (*S,R,S*) diastereomer **33** (d.r. = 89:11). Introduction of a methoxy group in the *ortho* positions on both aromatic rings ($R^1 = OCH_3$) of the hydrobenzoin auxiliary led to an improvement in the diastereoselectivity of the reduction reaction, which afforded a 95.5:4.5 mixture. Following purification of the hydroxy ester **33** and hydrolytic cleavage of the hydrobenzoin auxiliary, the mandelic acid **34** was produced in good overall yield as a single enantiomer.



Scheme 5. L-Selectride[®]-Mediated Reduction of Phenylglyoxylate and Cleavage

In this work, it was reasoned that the preferential addition of hydride to the *re* face of the ketone function in **32**, observed when $\text{R}^1 = \text{H}$, occurs as a result of steric shielding of the ketone function by the ether or aryl moiety (Scheme 6). In the ^1H NMR spectrum of **32** ($\text{R}^1 = \text{OMe}$), a small coupling constant between the benzylic protons ($J = 3.5 \text{ Hz}$) suggested that the dominant conformation for this molecule can be described by either of the Newman projections **35** or **36**. In the former conformer, the approach of the hydride to the β -face of the ketone function would be blocked by the *iso*-butyl group, which is consistent with the observed preferential formation of the (*S,R,S*)-enantiomer **33** (Scheme 5).



Scheme 6. Conformational Analysis of L-Selectride[®] Mediated Reduction of Phenylglyoxylates

The enhanced diastereoselectivity that was observed when the *o*-methoxy derivative was employed (i.e., **32**, R¹ = OMe) was explained through consideration of additional coordinative effects. As shown in Figure 2, lithium can coordinate between the *iso*-butyl ether, the carbonyl and one of the *o*-methoxy substituents, leading to a more rigid intermediate in which there is more extensive shielding of the *si* face of the ketone function. However, attempts to increase this rigidity with other Lewis acids (e.g., ZnCl₂) or through the introduction of additional coordinating groups on the ether function did not translate into an increase in diastereoselectivity.

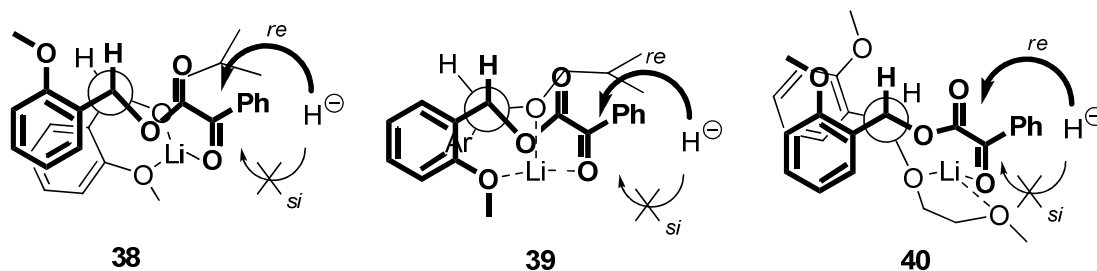
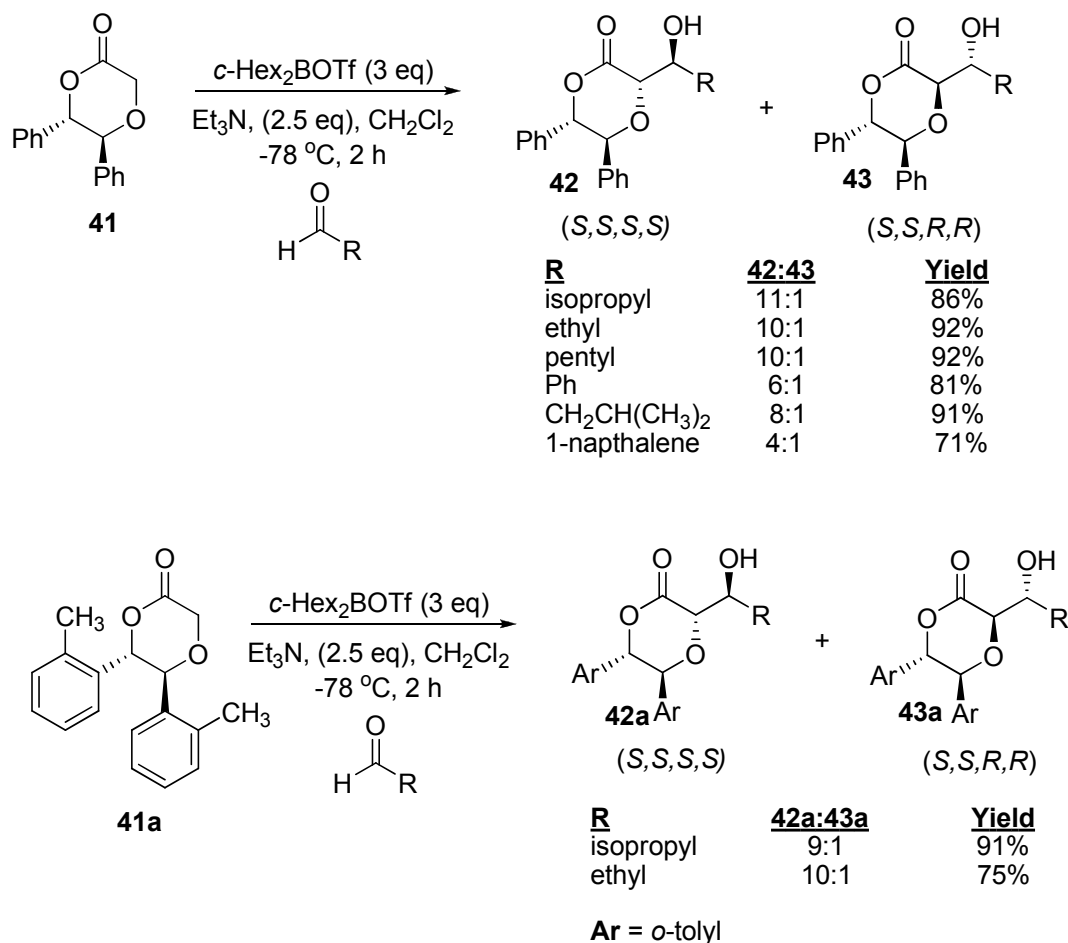


Figure 2. Increased selectivity of L-selectride[®] mediated reduction with *o*-methoxy groups.

1.2.2 Hydrobenzoin as an Auxiliary in *anti*-Selective Glycolate Aldol Additions

(*S,S*)-Hydrobenzoin has also found use as an auxiliary in glycolate aldol additions (Scheme 7).¹³ In this work, the hydrobenzoin-derived pyrone **41** was synthesized in order to constrain the geometry of the boron enolate formed through its reaction with (cyclohexyl)₂BOTf. Coupling of the boron enolate derived from **41** with various aldehydes preferentially afforded the 1,2-*anti* aldol adducts **42** and **43**. Using the optimized conditions shown in Scheme 7, a variety of aldehydes engaged in useful coupling reactions with **41**. For example, straight chain and branched aldehydes such as isobutyraldehyde (R = isopropyl), acetaldehyde (R = ethyl), and valeraldehyde (R = pentyl) gave good yields as well as good selectivity. However, in reactions with benzaldehyde (R = Ph) or isovaleraldehyde (R = CH₂CH(CH₃)₂), the selectivity decreased (6:1 and 8:1 respectively), and little selectivity was observed when R = 1-naphthalene (d.r = 4:1).

When the *ortho*-functionalized hydrobenzoin auxiliaries were employed in these reactions a decrease in selectivity or yield was observed. Thus, reaction of isobutyraldehyde with the *ortho*-substituted auxiliary **41a** gave an improved yield (91%) but a decrease in diastereoselectivity (**42a:43a** = 9:1). Conversely, in reactions with acetaldehyde the diastereoselectivity remained constant but the yield decreased to 75%. Consequently, no other *ortho* substituted hydrobenzoin auxiliaries were investigated.

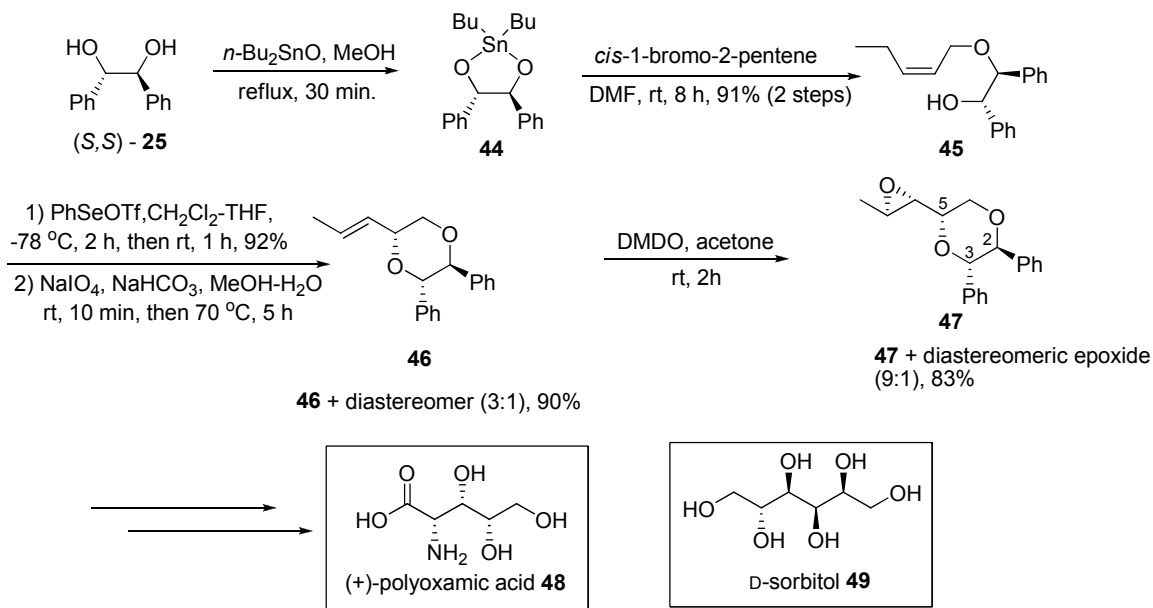


Scheme 7. Glycolate Aldol Reactions

1.2.3 (*S,S*)-Hydrobenzoin as an Auxiliary in the Synthesis of Polyhydroxy and Aminohydroxy Compounds

In their synthesis of (+)-polyoxamic acid, Kim and co-workers successfully employed (*S,S*)-hydrobenzoin as a chiral auxiliary during the functionalization of *cis*-1-bromo-2-pentene (Scheme 8).¹⁴ In this work, (*S,S*)-hydrobenzoin **25** was converted into the stannylene acetal **44**, which displaced the bromine atom in *cis*-1-bromo-2-pentene, affording the allylic alcohol **45**. Conversion of this allylic alcohol into oxyselenides and subsequent oxidation provided the (*2S,3S,5S*)-olefin **46** and its diastereomer (not shown) in a 3:1 ratio. Presumably,

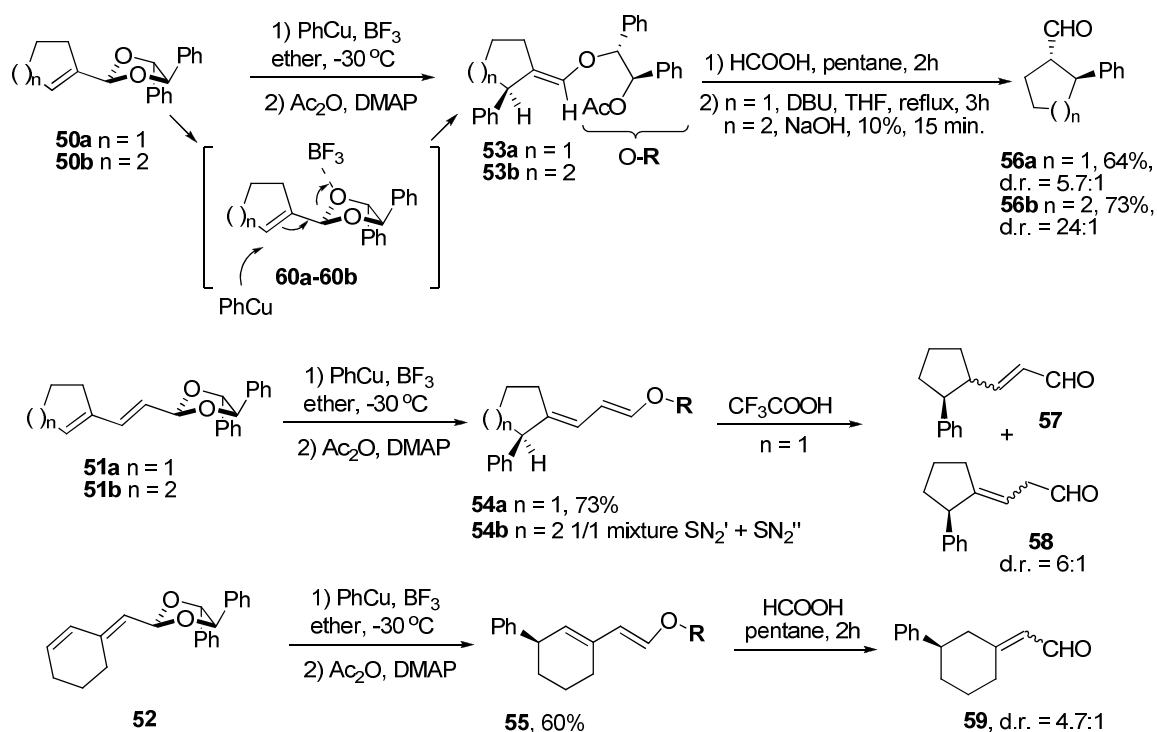
electrophilic addition to the selenium reagent on the olefin to form a selenonium ion is reversible and the intramolecular attack of the hydroxyl group was favoured when the 1-propenyl group is situated in an equatorial position. Separation of these diastereomers by flash chromatography followed by dimethyldioxirane oxidation of diastereomer **46** afforded epoxide **47** in 83% yield and in good diastereoselectivity (d.r. = 9:1). Further functional group manipulations led to the target compound, (+)-polyoxamic acid **48**. Notably, in this example, the chiral hydrobenzoin auxiliary could not be recycled since hydrobenzoin was also used as a source of oxygen atoms. This methodology was also applied to the synthesis of D-sorbitol (**49**, see inset) by employing *trans*-1-iodo-2-hexene instead of *cis*-1-bromo-2-pentene.



Scheme 8. Synthesis of (+)-Polyoxamic Acid and D-Sorbitol Using (S,S)-Hydrobenzoin as a Source of Chirality

1.2.4 Regio- and Diastereoselective S_N2' or S_N2'' Additions to Allylic Acetals using Hydrobenzoin as a Chiral Auxiliary

The stereoselective addition of organocopper reagents to allylic acetals derived from (*R,R*)-hydrobenzoin has also been reported.¹⁵ As indicated in Scheme 9, a phenyl copper reagent was added to the acetals **50-52** in the presence of BF₃•OEt₂ to afford enol ethers derived from S_N2' or S_N2'' additions. In this work, it was found that reactions of acetals **50a** and **50b** yielded the S_N2' enol ethers **53a** and **53b** with (*E*) stereochemistry and acetal **51a**, derived from a dienal, gave product **54a** consistent with a S_N2'' addition and (*E*) geometry of both double bonds. In contrast, the cyclohexene analogue **51b** did not show any regioselectivity and gave a mixture of enol ethers resulting from both S_N2' or S_N2'' reactions. Hydrolysis of the enol ethers **53a** and **53b** using formic acid gave a mixture of *cis* and *trans* isomers that were epimerized under basic conditions (DBU or NaOH) to afford the substituted *trans*-cycloalkanes **56a** and **56b**. Attempts to hydrolyze **54a** and **54b** using the same conditions (HCOOH, pentane) resulted in a complex mixture. However, treatment of **54a** with trifluoroacetic acid yielded a 1:1 mixture of *cis* and *trans* aldehyde **57** and β,γ-unsaturated aldehyde **58**. Unfortunately, complex mixtures were obtained from the hydrolysis of the conjugated dienes **54b** and **55**. Analysis of the absolute stereochemistry and facial preference of the addition reactions to **50-52** indicates substitution occurs in an *anti* fashion (intermediates **60a** and **60b**, Scheme 9). This conformational proclivity was rationalized by the selective complexation of BF₃•OEt₂ to one of the oxygens of the hydrobenzoin acetal prior to reaction with the phenyl copper reagent.

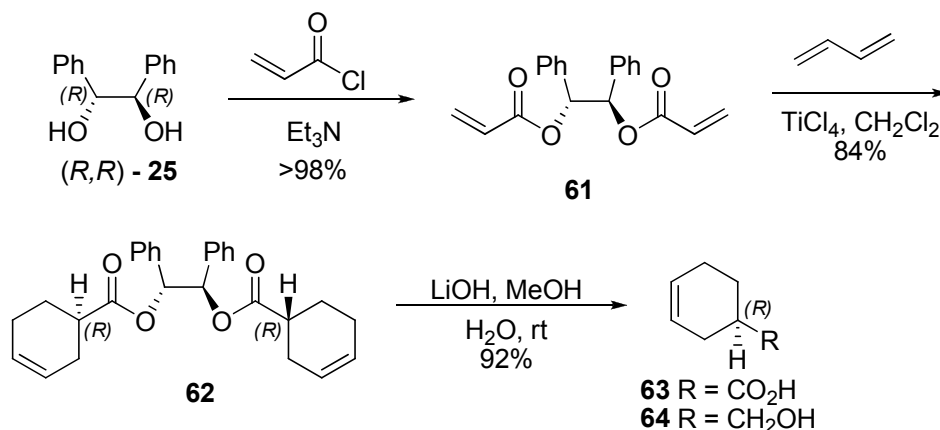


Scheme 9. Addition of Phenylcuprate to Allylic Hydrobenzoin Acetals

1.2.5 Diastereoselective Diels-Alder Reactions Involving (*R,R*)-Hydrobenzoin in the Partial Synthesis of the Immunosuppressant FK-506

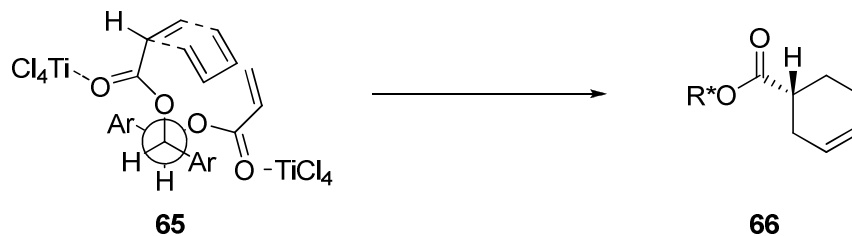
In their efforts directed towards the synthesis of the immunosuppressant natural product FK-506, Marshall and Xie reported a diastereoselective Diels-Alder reaction using (*R,R*)-hydrobenzoin as a chiral auxiliary (Scheme 10).¹⁶ In this example, (*R,R*)-hydrobenzoin (**25**) was esterified with acryloyl chloride to give the *bis*-acrylate **61** in excellent yield (>98%). Subsequent reaction of the *bis*-acrylate with butadiene in the presence of TiCl₄ afforded the *bis*-cyclohexene **62**, which was saponified to afford the acid **63** in 92% yield with 93% of the auxiliary recovered. The enantiomeric excess of the acid **63** was found to be 95% in

favour of the (*R*)-enantiomer, which was determined through reduction of acid **63** to the known alcohol **64**.¹⁷



Scheme 10. Diels-Alder Reaction Using (*R,R*)-Hydrobenzoin as an Auxiliary

To rationalize the high degree of diastereoselectivity observed in this process, it was proposed that the phenyl substituents on the *bis*-acrylate would adopt an *anti* orientation to minimize steric interactions. Also, calculations reported by Houk suggested that in the preferred conformation **65**, approach of the diene towards the α -face of the acrylate is blocked by the phenyl group of the hydrobenzoin auxiliary (Scheme 11).¹⁸



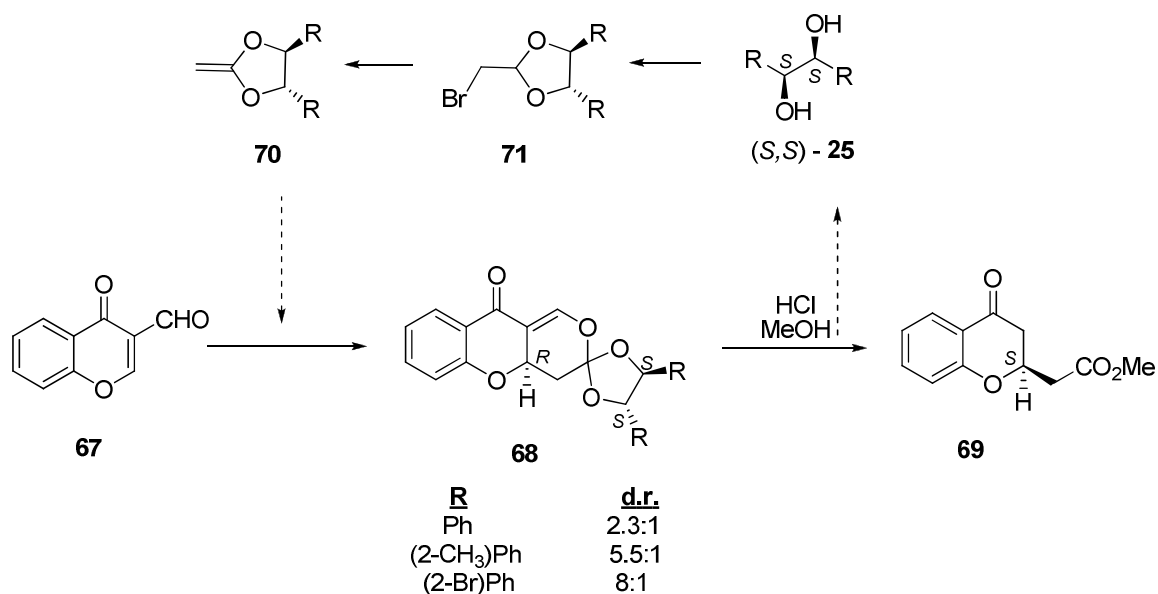
Scheme 11. Conformation of the *Bis*-Acrylate Reaction Complex

Isoprene and 1,3-cyclopentadiene also engaged in highly enantioselective Diels-Alder reactions with the *bis*-acrylate **61** (e.r. = 19:1 and e.r. = 24:1,

respectively). On the other hand, reactions of the *bis*-methacrylic or crotonic ester derivatives of **61** with butadiene showed poor enantioselectivity and low yields. In these later cases it was proposed that the additional methyl group introduces new detrimental steric interactions (e.g., **65**). Importantly, this diastereoselective Diels-Alder reaction became one of the key steps used in the partial synthesis of the immunosuppressant FK-506.

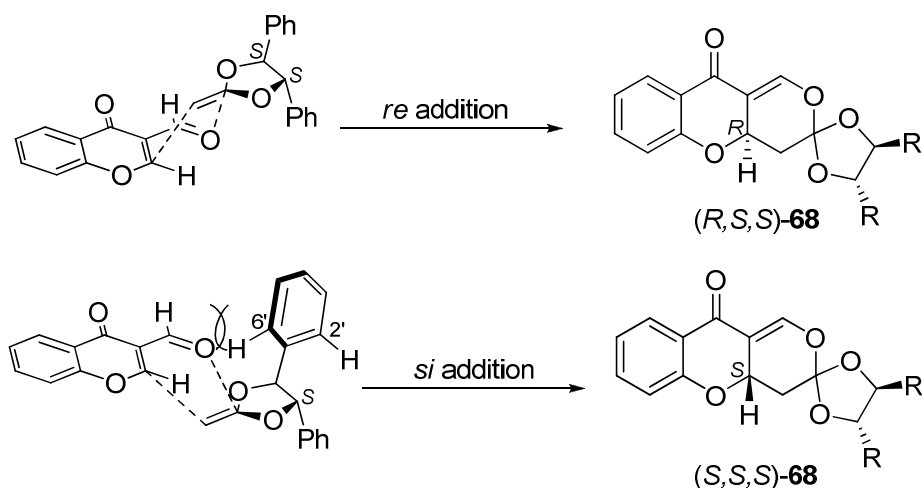
1.2.6 Heterodiene Cycloadditions of C_2 -Symmetric 4,5-Disubstituted Ketene Acetals

The utility of hydrobenzoin as an auxiliary in the asymmetric conjugate addition of an acetic acid ester enolate to the 3-formylchromone has been reported by Wallace (Scheme 12, **67** → **69**).¹⁹ In this work, cycloaddition of ketene acetals **70** with the chromone **67** gave *ortho* esters **68**, which were transformed to **69** by acid promoted methanolysis and decarbonylation. When R=Ph, the diastereomeric ratio favouring the (*R,S,S*) isomer **68** was 2.3:1 with an isolated overall yield of 61% for both diastereomers. In contrast, when an *ortho*-substituent was introduced on the aromatic rings of the hydrobenzoin auxiliary, the diastereoselectivity increased. Thus, *ortho*-substitution with a methyl group afforded **68** in a diastereomeric ratio of 5.5:1 and when bromine was introduced at the *ortho* position, this ratio increased to 8:1.



Scheme 12. Diastereoselective Cycloaddition of a Hydrobenzoin-Derived Acetic Acid Ester Enolate and an α,β -Unsaturated Carbonyl Compound

As depicted below in Scheme 13, the preferential formation of (*R,S,S*) diastereomer **68** in the cycloaddition step (Scheme 12, **67** \rightarrow **68**) was rationalized based on steric interactions between the hydrogen on the 2' or 6' position of the ketene acetal and the chromone in the transition structure that would lead to the diastereomeric product. However, this model fails to provide a basis for the increase in selectivity observed when *ortho*-substituted ketene acetals were employed, as rotation of the C-aryl bond would lead to a transition structure in which the hydrogen is oriented towards the reacting centres.



Scheme 13. Model Used to Explain Increased Selectivity in Cycloaddition Reactions of Ketene Acetal **70**

To gain a further appreciation for the increased diastereoselectivity observed with *ortho*-substituted ketene acetals, cyclic carbonates derived from these hydrobenzoin analogues were crystallized. Based on X-ray crystal analysis and molecular modeling calculations, it was construed that the carbonates (and accordingly the ketene acetals) preferred a conformation in which the *ortho* substituent at the 2' position is eclipsed by the H₅ benzylic hydrogen (e.g., **70a**, Figure 3) by approximately 8.5 kJ mol⁻¹, a result that is in good agreement with the Houk model.²⁰ While this may impart a certain degree of rigidity to the ketene acetal **70a**, this does not explain how *ortho* substitution affects the diastereochemical outcome of these reactions, as the group that is nearest to the π-bond in the cycloaddition step should be the hydrogen atom. Thus, the enhanced selectivity is more likely the result of “structural effects which may include the precise location of this hydrogen atom, [and] other (e.g. polar)

interactions prior to or during bonding."¹⁹ The *ortho*-substituents seem to inflect stereoselectivity not by direct steric blockage but by distorting the angle of the hydrogen atom on the 6' position and giving conformational rigidity to the ketene acetals, and consequently preferential reaction on the *re* face.

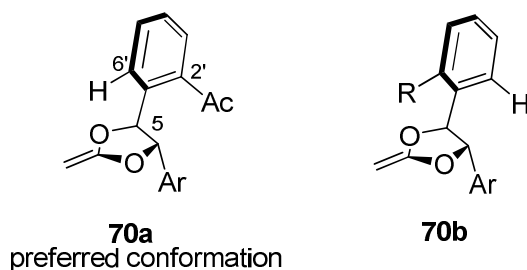
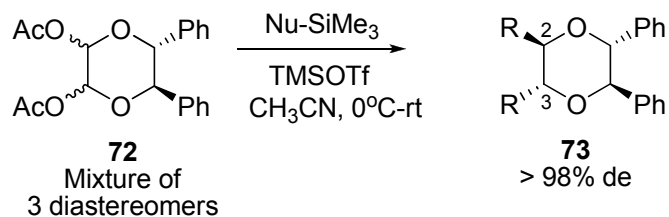


Figure 3. Preferred conformation **74a** of the ketene acetals versus **74b**.

1.2.7 Chiral Diol Systems Using Hydrobenzoin as an Auxiliary

Fujioka and Kita have shown that through sequential nucleophilic additions to diastereomeric mixtures of the (*5R,6R*)-2,3-diacetoxy-5,6-diphenyl-1,4-dioxane **72**, the product **73** is produced in greater than 99:1 diastereomeric ratios (Table 1).²¹ Synthesis of the dioxane **72** involved coupling of hydrobenzoin with glyoxal using a catalytic amount of *p*-TsOH and azeotropic removal of water followed by acetylation. When this dioxane was reacted with a variety of carbon nucleophiles, this process afforded the doubly substituted dioxane **73**. While the highest yield was obtained from the addition of allyltrimethylsilane (75%, Table 1, entry 1), a diversity of nucleophiles that included α -alkynyltrimethylsilanes (entry 3) and the cyclobutenediol derivative (entry 4) also engaged in useful reactions with **72**. The most surprising aspect of these additions is that regardless of the choice of nucleophile, the stereoselectivity of the process remained constant .

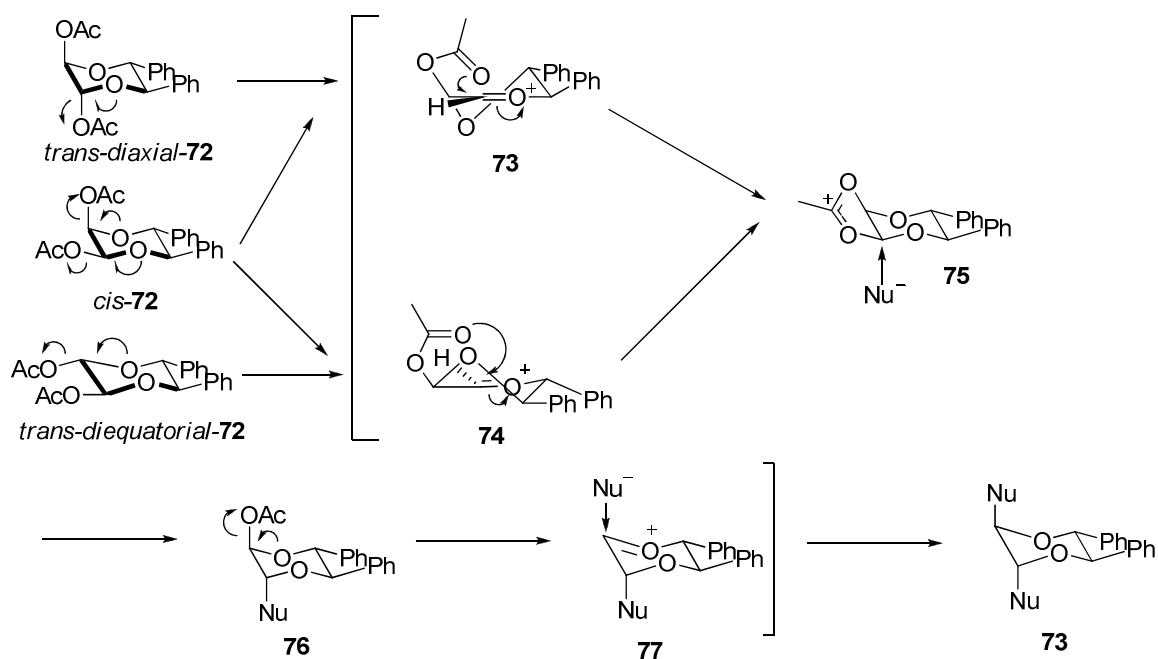
Table 1. Selected Examples of the Diastereoselective Synthesis of 1,2-Substituted Diols using Hydrobenzoin as an Auxiliary.



entry	Nu-SiMe ₃	product	yield(%)
1		R =	75%
2		R =	57%
3	Bu-C≡C-SiMe ₃	R =	30%
4		R =	74%
5		R =	61%

The consistent formation of the (2R,3R) stereoisomer **73** regardless of the nucleophile suggests that each reaction proceeds via the same intermediate. Thus, it was proposed that each of the diastereomeric dioxanes **72** undergo transformation to the same 1,3-dioxolane-2-ylum ion intermediate **75** *in situ*, and that the subsequent nucleophilic addition is controlled by stereoelectronic factors (Scheme 14). After elimination of the second acetoxy group, a second equivalent of a nucleophile attacks from an axial direction on the *re*-face of the oxonium ion

77 to afford *trans*-diaxial product **73**. The stereoselectivity of this addition process is the result of the favourable formation of a chair-like transition state (vs boat-like for equatorial addition) during the addition of the nucleophile.



Scheme 14. Nucleophilic Additions Proceeding *via* the Intermediate **75**

1.3 Background – Hydrobenzoin as a Chiral Ligand

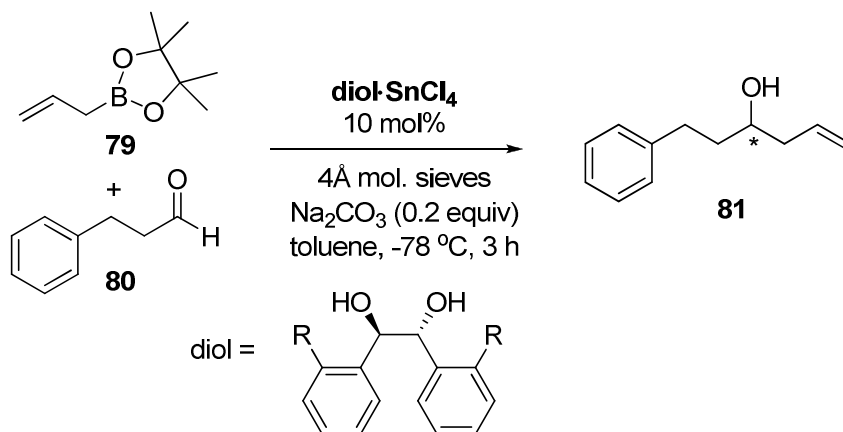
This section will highlight the use of hydrobenzoin as a chiral *ligand* in recent literature with particular emphasis on the use of *ortho*-substituted hydrobenzoin derivatives as ligands.

1.3.1 Chiral Hydrobenzoin·SnCl₄ and its Derivatives in the Catalytic Enantioselective Allyl- and Crotylboration of Aldehydes

One of the most extensive studies describing the importance of *ortho* substituted hydrobenzoins as a ligand was recently reported by Hall who discovered that these ligands impart good to excellent levels of enantioselectivity in the allylboration of cinnamaldehyde (Table 2).²² Having established that SnCl₄ was the optimal Lewis acid to use in conjunction with hydrobenzoin-derived Brønsted acids, the effects of *ortho*-substitution on the aromatic rings of hydrobenzoin were investigated. Initial studies indicated that hydrobenzoin (i.e. no *ortho*-substituent) was unable to impart useful levels of enantioselectivity in the allylboration reaction (Table 2, entry 1). However, a screen of hydrobenzoin derivatives that bear substituents of differing polarity in the *ortho*-position indicated that non-polar alkyl groups such as *iso*-propyl (Table 2, entry 4) increased the enantiomeric ratio and gave higher selectivity than polar substituents such as bromine or methoxy groups (entries 2-3). Furthermore, increasing the steric bulk of the non-polar groups from propyl to *t*-butyl (entry 5) led to low levels of conversion and poor enantiomeric ratios, possibly as a result of lack of accessibility of the activated proton in the active catalyst (c.f. Figure 4). Based on this result, it was concluded that the optimal substituent on the aryl ring would be a bulky, non-polar group that possesses at least one benzylic proton. Thus, a series of aliphatic ring substituted hydrobenzoins were screened (entries 6-7) and indeed these ligands proved to be excellent catalysts for this reaction. Of these, the diol that imparted the highest degree of enantioselectivity (e.r. =

28:1) and conversion (100%) proved to hydrobenzoin with *ortho* cyclooctyl groups, which was subsequently named Vivol (entry 7).

Table 2. Results of Allylboration Reaction with Different *ortho*-Substituted Diols



entry	R (Diol)	yield (%)	e.r. (<i>R</i> : <i>S</i>)
1	H (25)	75%	1.7:1
2	OCH ₃ (82)	75%	5.4:1
3	Br (83)	94%	7.7:1
4	<i>iso</i> -propyl (84)	71%	8.5:1
5	<i>tert</i> -butyl (85)	18%	1.2:1
6	cyclohexyl (86)	100%	10:1
7	cyclooctyl (Vivol 87)	100%	28:1

An understanding of the facial preference imparted by this Lewis acid Brønsted acid (LBA) system was obtained through analysis of a crystal structure of a 1:1 mixture of Vivol **87** and SnCl₄. Figure 4 shows the catalyst's preference towards a stacked conformation, in which each of the cyclooctyl groups are in

close proximity to the other aryl group. Thus, the two acidic protons are pointed outward in a pseudoequatorial direction from the 5-membered ring chelate structure, which portrays a lack of orientational flexibility. Edges of the cyclooctyl ring and the apical chlorine atoms also block certain areas around the activated protons and thus are able to translate stereochemical information to the Brønsted acid. The cyclooctyl groups are also believed to direct the angle of the aryl groups, a critical aspect of the transition state assembly. Thus, the highly disymmetric nature of the Vivol catalyst and its ability to translate enantioselectivity could potentially lend itself to other applications which require the use of LBA catalysts.

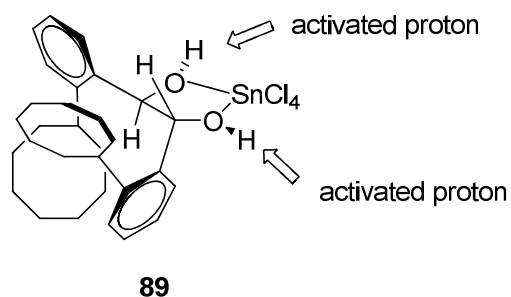
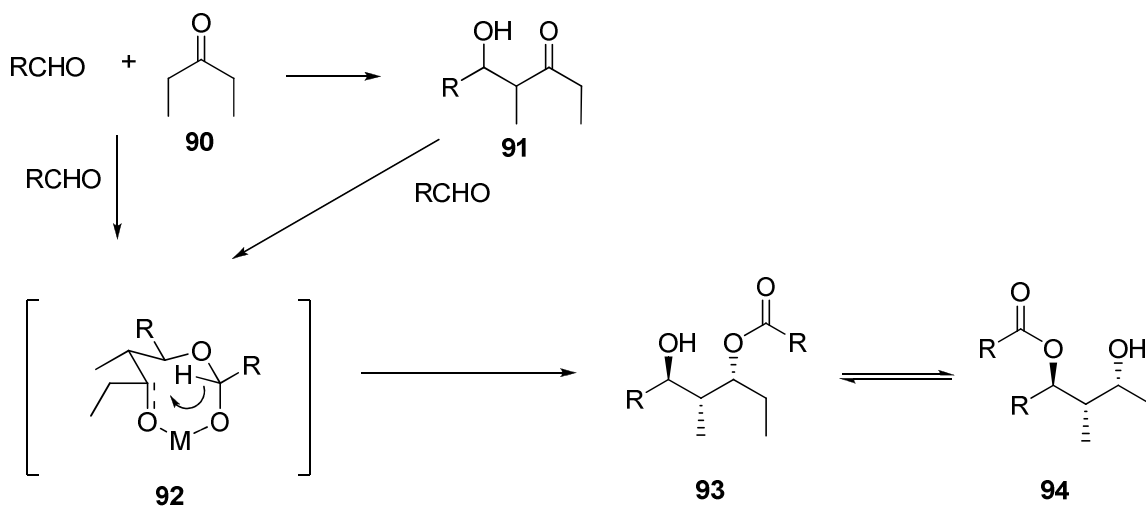


Figure 4. Stacked conformation of Vivol.

1.3.2 Catalytic Asymmetric Evans-Tischenko Reaction of Aldehydes and Aliphatic Ketones using Hydrobenzoin and its Derivatives

Hydrobenzoin has also proven useful in promoting an enantioselective variant of the Evans-Tishchenko reaction (Scheme 15).²³ Based on the high *anti*-selectivity observed in this reaction, it is apparent that the 6-membered cyclic transition state **92** favours a conformation in which the substituents on the pseudo-six membered ring are oriented equatorially. Mlynarski and Mitura sought

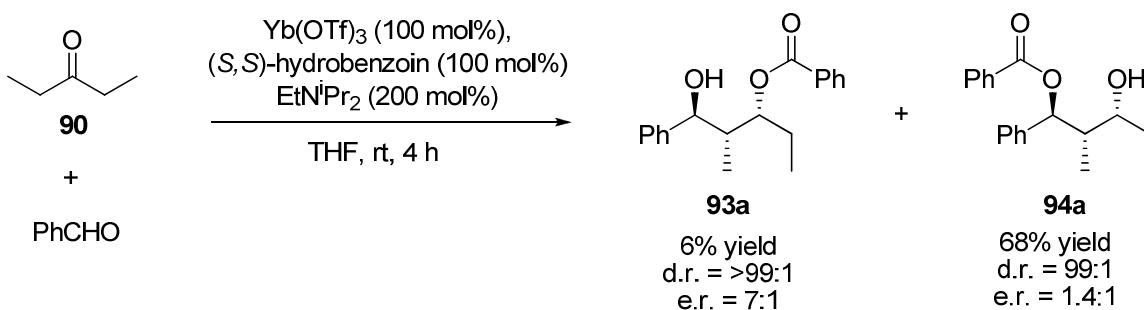
to exploit this preference by developing a metal-based catalyst that could impart *enantioselectivity* to this widely used reaction.²³ If successful, hydrolysis of the 1,3-diol monoesters **93** and **94** would afford a product that contains three contiguous stereogenic centres favouring that with the 1,2- and 1,3-*anti* configuration, a useful building block for polyketide synthesis.²⁴



Scheme 15. Postulated Mechanism of Evans-Tischenko Reaction

Among a variety of catalysts screened for this reaction, it was found that a combination of (*S,S*)-hydrobenzoin, ytterbium(III) triflate, and a tertiary amine (Hünig's base) gave the best results in the reaction of benzaldehyde with 3-pentanone (Scheme 16). Under these conditions, the regioisomers **93a** and **94a** were formed in 6% (e.r. = 7:1) and 68% (e.r. = 1.4:1) yields respectively. As expected with the Evans-Tischenko reaction, the diastereoselectivity was high and only traces of the 1,2-*syn*-1,3-*anti* isomer (< 3%) were present. Other common diol ligands such as TADDOL failed to promote this reaction and use of other metals led to significant amounts of the *anti* and *syn* aldol product **91**

(Scheme 15) but not the desired Evans-Tischenko product **93**. It was also shown that the amine played an integral part in these reactions, and that reaction in which *N*-methylimidazole was used as the base gave the highest levels of enantioselectivity (e.r. = 4.9:1 for **93a** based on 20 mol% loading), while those with triethylamine gave the lowest (e.r. = 3.6:1 for **93a** based on 20 mol% loading). Hünig's base was chosen due to its comparable selectivity to *N*-methylimidazole (e.r. = 3.7:1 for **93a**) and higher chemical yields observed with its use. Although the yields and enantioselectivities are modest at best, this enantioselective variant of the Evans-Tischenko reaction is the first example of its kind.



Scheme 16. Enantioselective Evans-Tischenko Reaction

In related work,²⁵ Mlynarski and coworkers continued to explore this catalytic system through the preparation of *O,N*-donor ligands based on (*S,S*)-hydrobenzoin core (**95-97**, Figure 5). They assumed that these pincer structures would impart a greater stability and also increase the reactivity of the catalyst through Lewis base activation of the metal.²⁶ In this study, the best results were obtained by using Yb(OTf)_3 and ligand **96** with 20% catalyst loading (97% yield of

93a and **94a**, e.r. = 1.6:1). The diether **95** gave no enantioselectivity and ester **97** failed to promote the desired reaction. While the diester **98** proved to be an effective catalyst for this process (84% yield), the lack of enantioselectivity imparted by this ligand suggests that the phenyl substituents present in hydrobenzoin are key.

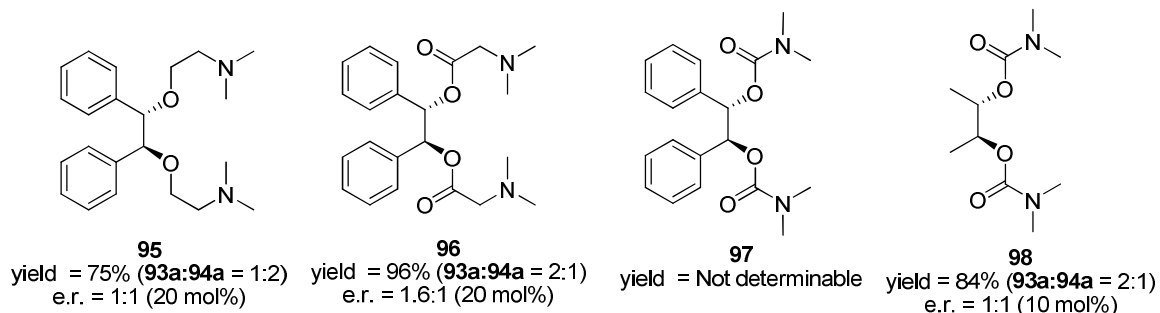
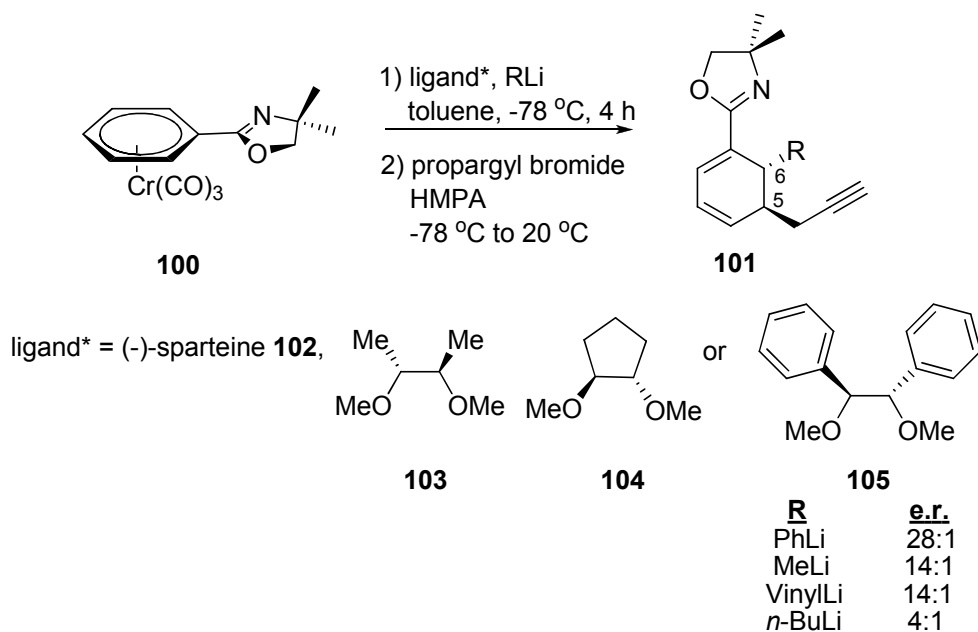


Figure 5. *O,N*-Donor ligands screened for the Evans-Tischenko reaction.

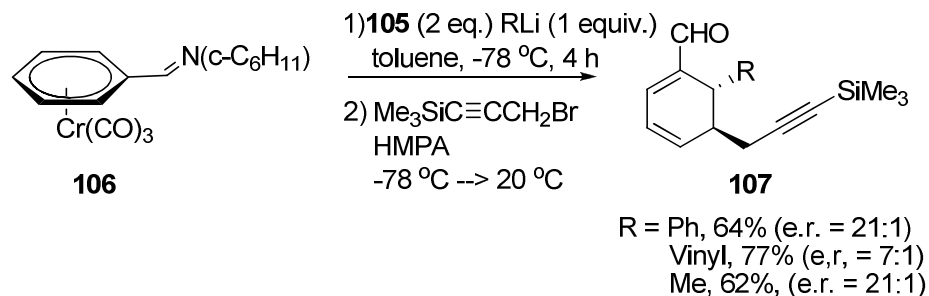
1.3.3 Hydrobenzoin as a Chiral Catalyst in the Asymmetric Addition of Organolithium Reagents to Arene Tricarbonylchromium Complexes.

The enantioselective addition of an organolithium reagent to a prochiral arene $\text{Cr}(\text{CO})_3$ complex followed by reaction of the resultant anion with propargyl bromide was described by Kundig and co-workers (Scheme 17).²⁷ In this work, the four ligands **102-105**, were screened in reactions with phenyllithium, vinylolithium, methyllithium and *n*-BuLi and it was found that the dimethoxyhydrobenzoin **105** imparted the highest degree of enantioselectivity for this reaction (phenyllithium e.r. = 28:1; vinylolithium and methyllithium, e.r. = 14:1; *n*-BuLi, e.r. = 4:1).



Scheme 17. Addition of RLi and Propargyl Amine in the Presence of Chiral Catalysts to an Arene Cr(CO)₃ Complex

This methodology was also extended to the imine complex **106** (Scheme 18). As indicated in Scheme 18, the ligand **105** promoted the enantioselective addition of both phenyllithium and methyllithium to the imine **106** to afford, following subsequent reaction with trimethylsilylpropargyl bromide, the dienals **107** in good to excellent enantiomeric ratios.

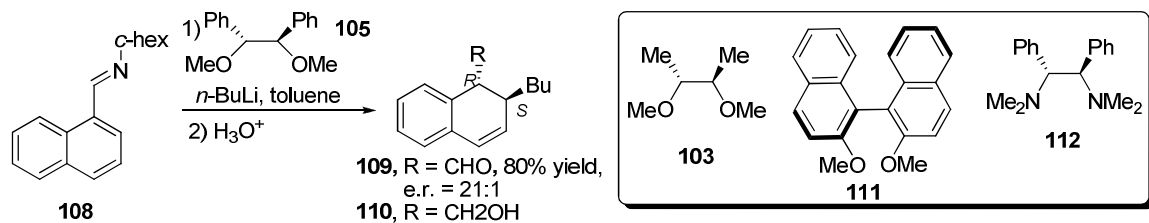


Scheme 18. Asymmetric Addition of Organolithiums into a Prochiral Arene Complex

1.3.4 Hydrobenzoin as a Catalyst in the Enantioselective Conjugate Addition of an Organolithium to an α,β – Unsaturated Aldimine.

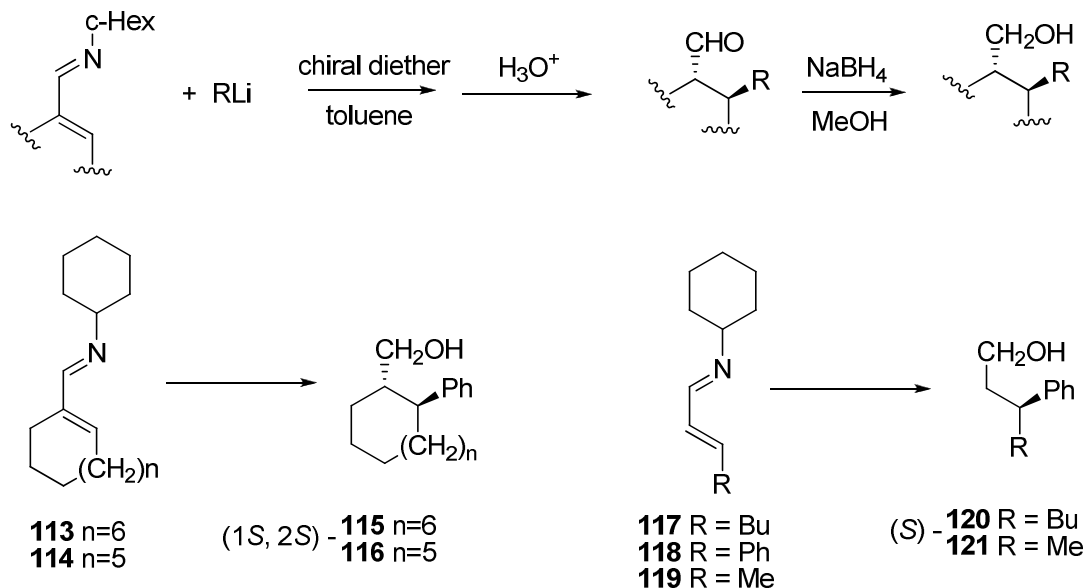
The C_2 -symmetric chiral diether **105** was also employed in the enantioselective conjugate addition of an organolithium to an α,β -unsaturated aldimine (e.g., **108** \rightarrow **109**, Scheme 19).²⁸ Thus, it was found that addition of *n*-BuLi to the aldimine **108** in the presence of **105** (1.4 equivalents) provides the aldehyde **109** in 80% yield (e.r. = 21:1). It was noted that the catalyst was recovered in quantitative yield.

Again, compared with ligands **103** and **111-112** (Scheme 19, see inset), the hydrobenzoin-derived ligand **105** imparted the highest level of enantioselectivity in the addition of alkylolithiums to aldimine **108**. As shown in Table 3, a comparison of ligands **103**, **105**, and **111-112** (entries 1-4) indicates that the hydrobenzoin-derived ligand **105** gave an enantiomeric ratio six times higher than the next best ligand. Surprisingly, the BINOL-based ligand **111** showed the poorest facial differentiation. A variety of other aldimines including those containing aliphatic rings were also good substrates for this reaction (entries 5-9).



Scheme 19. Addition of *n*-Butyllithium to Aldimine **108** Using Hydrobenzoin Derived Chiral Diether **105**

Table 3. Enantioselective Conjugate Addition of an Organolithium to an α,β – Unsaturated Aldimine under Different Conditions



entry	imine	RLi	chiral diether	temp (°C)	product	e.r.	yield (%)
1	108	Bu	(<i>R,R</i>) - 105	-78	(1 <i>R</i> ,2 <i>S</i>) - 110	21:1	80
2	108	Bu	(<i>R,R</i>) - 103	-78	(1 <i>R</i> ,2 <i>S</i>) - 110	3.2:1	92
3	108	Bu	(<i>S</i>) - 111	-78	(1 <i>R</i> ,2 <i>S</i>) - 110	1.1:1	46
4	108	Bu	(<i>S,S</i>) - 112	-78	(1 <i>R</i> ,2 <i>S</i>) - 110	1.2:1	26
5	113	Ph	(<i>R,R</i>) - 105	-45	(1 <i>S</i> ,2 <i>S</i>) - 115	49:1	61
6	114	Ph	(<i>R,R</i>) - 105	-45	(1 <i>S</i> ,2 <i>S</i>) - 116	99:1	59
7	117	Ph	(<i>R,R</i>) - 105	-78	(<i>S</i>) - 120	>99:1	58
8	118	Ph	(<i>R,R</i>) - 105	-78	(<i>R</i>) - 120	10:1	40
9	119	Bu	(<i>R,R</i>) - 105	-78	(<i>S</i>) - 121	>99:1	48

A model as shown in Figure 6 was used to rationalize stereochemical induction in the reactions mediated by ligand **105**. It was assumed the organolithium would form a five-membered chelate with the hydrobenzoin-derived ether **105** and that, on the basis of steric interactions, the methyl

substituents on ligand **105** would adopt a *trans* arrangement. In this favourable conformation (e.g., **122**), the *N*-cyclohexyl bond is *syn* to the Li-O1 bond; a conformation that promotes the addition of the R group to the aldimine from the α -face (as shown). The alternative conformation **123**, in which the *N*-cyclohexyl bond is oriented *syn* to the Li-O2 bond, should be disfavoured due to steric interactions between the O2-CH₃ and cyclohexyl and the R group and the aldimine.

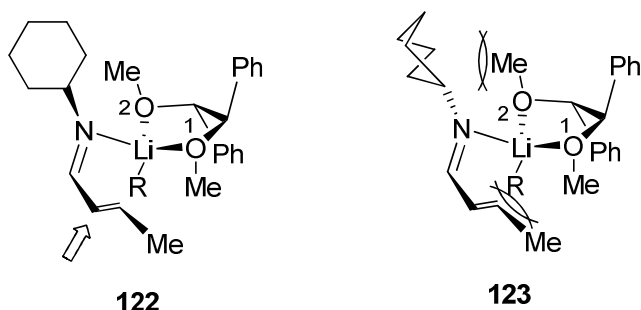


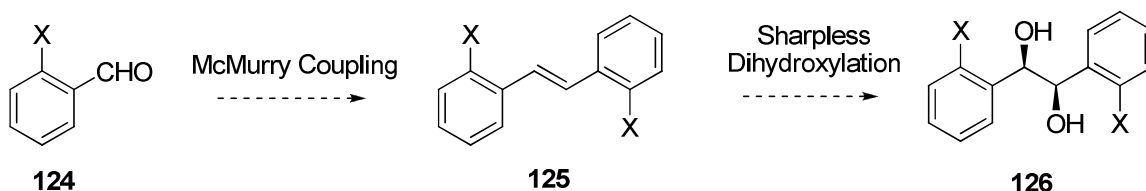
Figure 6. Proposed transition state for the enantioselective addition of an organolithium to an α,β -unsaturated aldimine.

1.4 Synthesis of *ortho*-substituted hydrobenzoin.

1.4.1 Literature Procedures for Synthesis of *ortho*-Substituted Hydrobenzoin.

As evidenced by both the number and diversity of examples discussed above, it is clear that hydrobenzoin and its derivatives are essential tools in asymmetric synthesis. Whether as an auxiliary or ligand, hydrobenzoin has been used in many reactions including aldol reactions, Diels-Alder reactions, substitution reactions, and Evans-Tischenko reactions. However, the current range of synthetic methodology available to efficiently generate functionalized

hydrobenzoin derivatives, especially those with *ortho*-substitution, is lacking. Thus, the preparation of these substances requires multiple-steps and eventual derivitization to verify the compound's optical purity. For example, to generate an *ortho*-substituted derivative of hydrobenzoin, the typical procedure involves McMurry coupling of an *ortho*-substituted aldehyde followed by a Sharpless asymmetric dihydroxylation (Scheme 20).



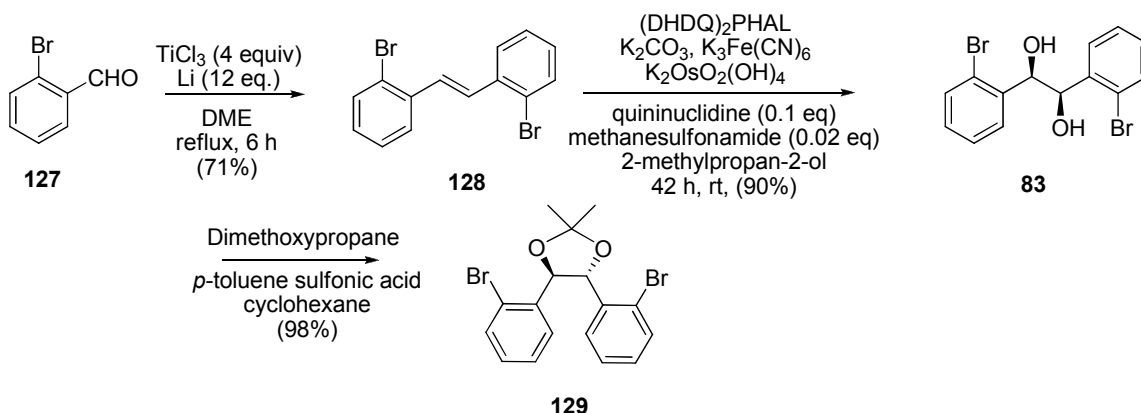
Scheme 20. Typical Procedure for the Synthesis of *ortho*-Substituted Hydrobenzoin Derivatives

The McMurry coupling involves the homo-coupling of an aldehyde to produce symmetrical alkene **125** using a low valent titanium complex.²⁹ The low valent titanium complex is often made *in situ* by mixing a high valent titanium (III or IV) compound (i.e. TiCl_3 or TiCl_4) with a reducing agent such as LiAlH_4 , Li, Na, Mg, Zn or Zn-Cu. The disadvantages of this methodology as pertaining to the synthesis of hydrobenzoin derivatives are: 1) a mixture of *E:Z* olefinic isomers is often obtained and thus an isomerisation step is necessary prior to the Sharpless dihydroxylation; 2) the desired *ortho*-substituted aldehyde may not be commercially available or may be costly; 3) the reagents required for the McMurry coupling (TiCl_3 , reducing agent) are not easily handled due to their air sensitivity.

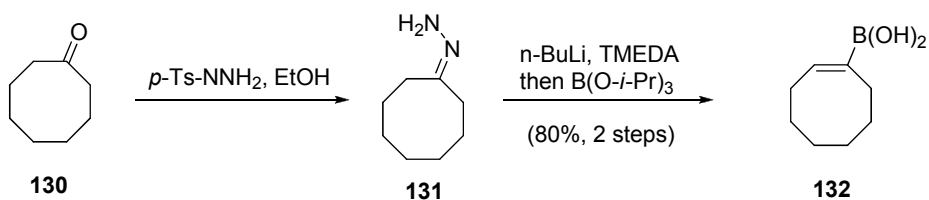
The Sharpless asymmetric dihydroxylation reaction of *trans*-stilbenes allows for the formation of either the (*S,S*)- or the (*R,R*)-enantiomer **126** by the addition of AD-mix α or AD-mix β , respectively.³⁰ This was found to be one of the most efficient and practical ways to make *ortho*-substituted derivatives of hydrobenzoin and allowed the synthesis of derivatives with CH₃, CF₃, I, Br, isopropylene and isopropyl substitutions.²² However, with bulkier substituents such as larger alkyl groups or a trimethylsilyl group, the dihydroxylation often fails to yield the desired derivative of diol **126**. A more general convergent approach designed by the Hall group,²² permitted the synthesis of these derivatives. Scheme 21 outlines the Hall approach which employs the dibromo acetone **129** as a building block that undergoes cross-coupling with a variety of boronic acids (e.g., **132**) or lithium-halogen exchange for reaction with electrophiles.

Although this route is capable of generating a variety of *ortho*-substituted hydrobenzoin derivatives in modest yield, it involves considerable work. Also, for each substrate the optical purity must be determined, as the Sharpless asymmetric dihydroxylation reaction does not always proceed with 100% enantiomeric selectivity. As a result, *ortho*-substituted hydrobenzoin derivatives are not often considered during ligand or auxiliary screening.

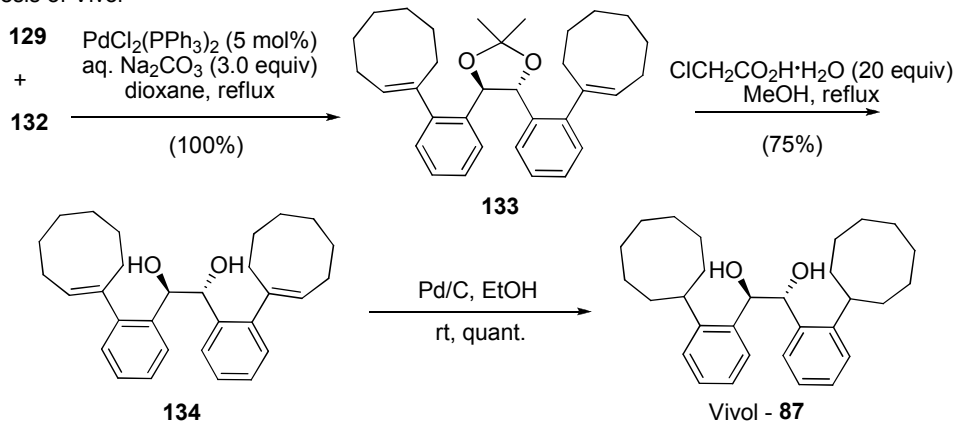
Synthesis of (4*R*, 5*R*)-4,5-bis(2-bromophenyl)-2,2-dimethyl-1,3-dioxolane



Synthesis of Cyclooctenylboronic acid



Synthesis of Vivol

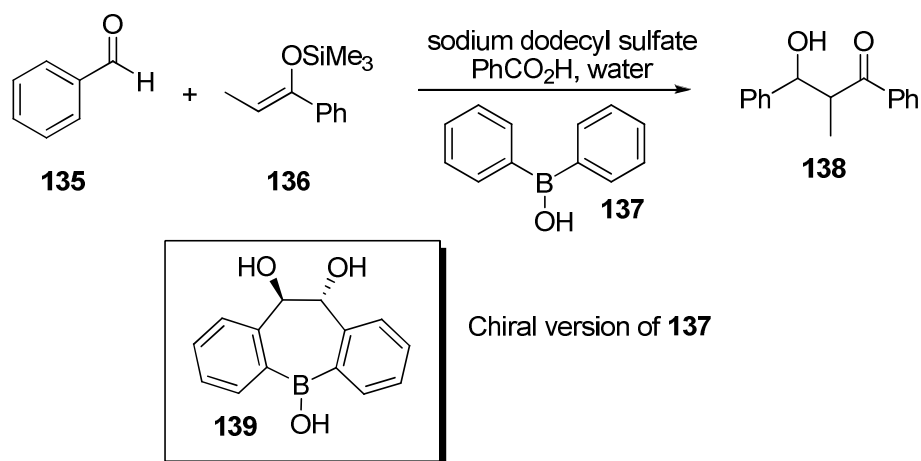


Scheme 21. Synthesis of Vivol

1.4.2 Background to this Thesis

Former members of the Britton group became interested in the synthesis of chiral boronic acids that may promote enantioselective Mukaiyama aldol reactions in water (Scheme 22).³¹ In 2001, Kobayashi reported a 94:6 *syn:anti* selectivity for the aldol products derived from reaction of the *Z*-enol silyl ether **136**

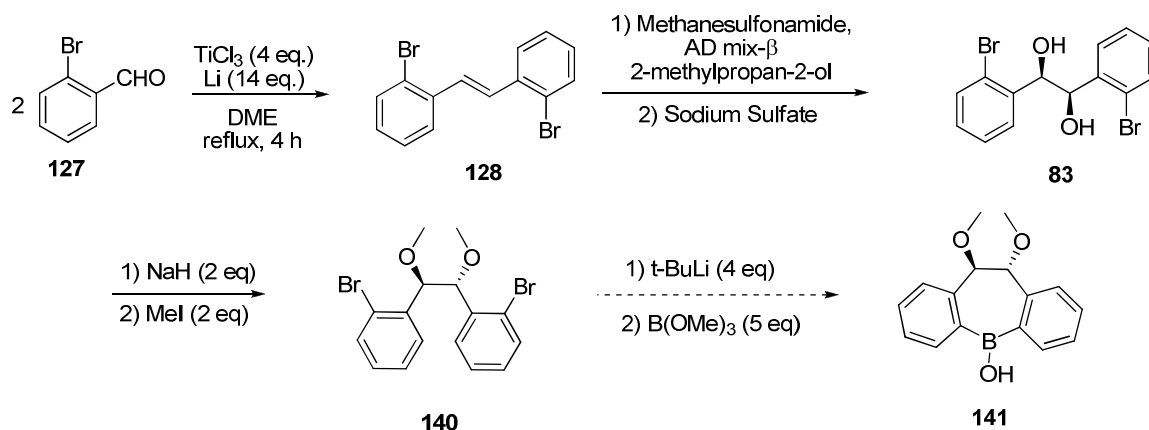
with benzaldehyde (**135**), catalytic amounts of diphenylborinic acid (**137**), and a surfactant (sodium dodecyl sulphate). As this reaction represents the first example of a boron aldol reaction that is catalytic in boron, it was envisaged that a chiral borinic acid may impart enantioselectivity to this process, and in so doing, represent the first catalytic asymmetric boron aldol reaction.³² Along these lines, we endeavoured to synthesize the chiral hydrobenzoin derived borinic acid **139** (Scheme 22).



Scheme 22. Diastereoselective Mukaiyama Aldol Reaction in Water

Initial efforts by a previous student in the Britton lab involved repetition of the established routes discussed above, which employ the *ortho*-substituted aldehyde **127** to give access to the dibromohydrobenzoin **83** (Scheme 23). Unfortunately, during these investigations, it proved difficult to incorporate a borinic acid into the substrate. A variety of organolithium reagents were employed for this reaction (e.g., *n*-BuLi, *s*-BuLi, *t*-BuLi) with no success. Moreover, access to the dibromohydrobenzoin **83** *via* the route presented below in Scheme 23 was low yielding, costly and time consuming (e.g., the

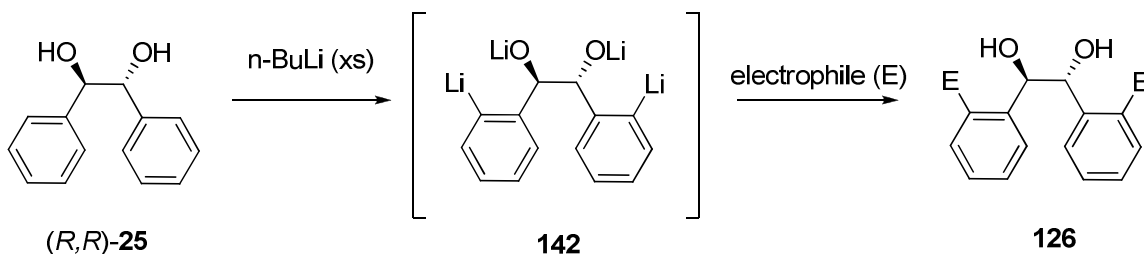
dihydroxylation reaction required several days). Thus, we endeavoured to develop a more direct synthesis of the dibromo intermediate **83** that could potentially afford borinic acid **139** without the need for protecting groups.



Scheme 23. First Attempted Synthesis of Chiral Borinic Acid **139**

1.4.3 Thesis Proposal – New Efficient Synthesis of *ortho*-Substituted Hydrobenzoins.

Based on precedent for directed *ortho*-metalations, we envisioned that commercially available (*R,R*)- or (*S,S*)-hydrobenzoin could itself be directly functionalized by consecutive directed *ortho*-metalations. This would lead to the novel tetraanion **142** which could be treated with various electrophiles to provide *ortho*-substituted hydrobenzoin derivatives **126** and the desired borinic acid **139** (Scheme 24).



Scheme 24. Proposed Direct Access to *ortho*-Substituted Hydrobenzoin Derivatives

Indeed, it was discovered that upon refluxing (*R,R*)-hydrobenzoin in a mixture of hexane-ether with excess *n*-BuLi, (*R,R*)-hydrobenzoin gradually dissolves to form a deep red solution and that subsequent addition of electrophiles to this mixture led to hydrobenzoin derivatives functionalized in both *ortho*-positions in modest yield. Remarkably, in one step, this process permits the functionalization of both *ortho* positions with complete regioselectivity (*vide infra*). In Chapter 2, background into directed *ortho*-metalations (DoM) and the efforts required to develop, optimize, and extend this new, useful, and efficient methodology are discussed. In Chapter 3, future directions of this methodology are discussed and in Chapter 4 the general conclusions of this thesis are summarized. Chapter 5 provides a detailed experimental with spectral data.

2: BIDIRECTIONAL METALATION OF HYDROBENZOIN AND APPLICATIONS

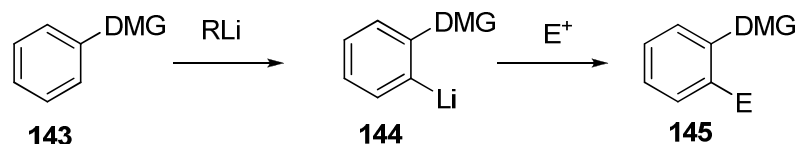
The methodology employed in our work has its roots in the rich history of directed *ortho*-metalation reactions.³³ Thus, a brief description of the general characteristics of this reaction and its application to benzyl alcohols is warranted.

2.1 Directed *ortho*-Metalation (DoM) Reactions

2.1.1 General Characteristics and Mechanistic Aspects.

Independent reports by Gilman and Bebb³⁴ and Wittig and Fuhrman³⁵ in 1939-1940 described the *ortho*-deprotonation of anisole by *n*-BuLi, which laid the foundation for exploration of this new area of aromatic substitution chemistry. However, it was not until the 1970s, when alkyllithium bases became commercially available,³⁶ that this process became more widely exploited. The comprehensive review by Gschwend and Rodriguez in 1979³⁷ also promoted the application of this methodology by highlighting its potential.

A simplistic view of this reaction is depicted below in Scheme 25 in which deprotonation with an alkyllithium base *ortho* to a heteroatom-containing directing metal group (DMG) gives the *ortho*-lithiated species **144**. Treatment of the resultant anion with different electrophiles affords 1,2-disubstituted aromatics **145**.

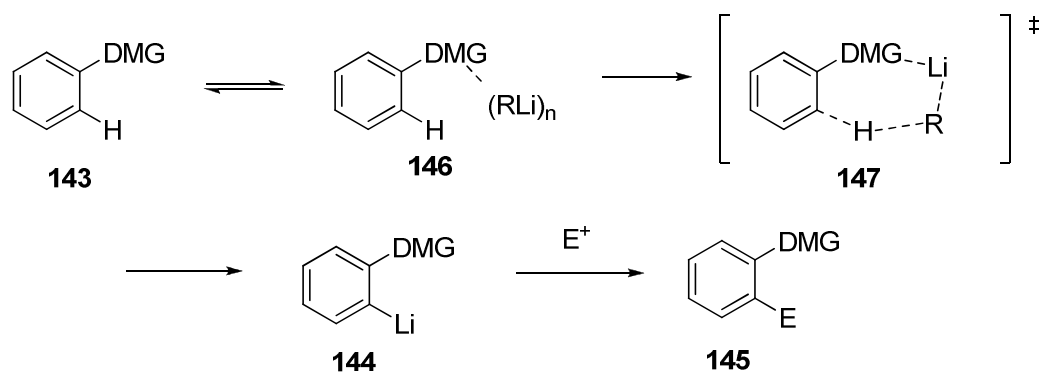


Scheme 25. Directed *ortho*-Metalations

While the full mechanistic nuances of this reaction remain elusive due to its complexity, it is agreed that successful deprotonations must involve good sites for coordination on the DMG and that the DMG must not be susceptible to nucleophilic attack by a strong base.³³ Some examples of successful and synthetically useful DMGs include the *o*-carbamates and *o*-sulfamates developed by the Snieckus group.³³

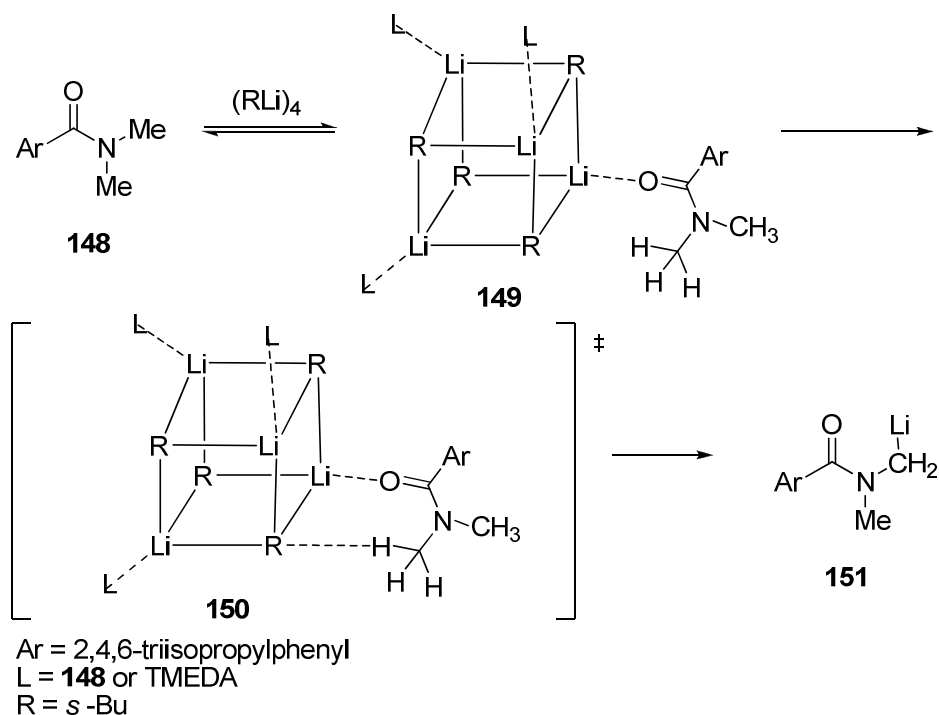
Although controversy exists with regards to the exact mechanism of this reaction, three proposals have been put forward: the complex induced proximity effect (CIPE), the kinetically enhanced metalation (KEM), and the inductive effect.

As implied by its name, CIPE conceptually involves the formation of a pre-coordinated complex as the key component prior to α -lithiation (Scheme 26). Thus, reaction of **143** with an alkyllithium forms complex **146**, which then directs the subsequent deprotonation leading to **144**.



Scheme 26. General Concept of CIPE

CIPE implies a two-step mechanism and is used to explain the regioselectivity seen in directed *ortho*-metalations. Support for pre-complexation of the alkyllithium to the DMG was given by the work of Beak and co-workers³⁸ who directly observed a complexed species upon reaction of the dimethyl carboxamide **148** with *s*-BuLi in cyclohexane using stopped-flow IR spectroscopy (Scheme 27). It was shown that the *s*-BuLi tetramer **149**, which was formed in rapid equilibrium with **148**, is a thousand times more reactive compared to differentially complexed tetramers. The formation of this complex would be followed by deprotonation via transition state **150** to give the deprotonated species **151**. One of the more interesting observations made during this study was that the addition of TMEDA did not break up the tetrameric species **149**. Thus, in contrast to the existing dogma that associates TMEDA with increasing the rate of a reaction by breaking up the lithium aggregates, it was proposed that TMEDA actually aided in releasing the carbanion in the transition state **150** for deprotonation.



Scheme 27. Directed Metalation of **148** through Complexation with *s*-BuLi Tetramers

In contrast to this two-step mechanism, Hommes and Schleyer suggested replacing CIPE with a one-step mechanism that they termed “kinetically enhanced metalation”.³⁹ Based on calculations, this mechanism postulates a single transition structure where complexation and proton abstraction occur simultaneously. Schleyer also pointed out the discrepancy between the CIPE mechanism, in which reactions should proceed more slowly owing to the free energy (ΔH) of the complexation that must be overcome, and the experimental evidence that showed a higher reactivity towards *ortho*-lithiation.⁴⁰ The kinetically enhanced metalation model attributes the increased rate to two factors: the favourable charge distribution and the shorter distance of Li-DMG (DMG = electronegative groups such as alkoxy, Fluorine) (Figure 7).

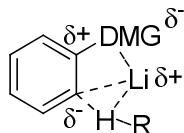
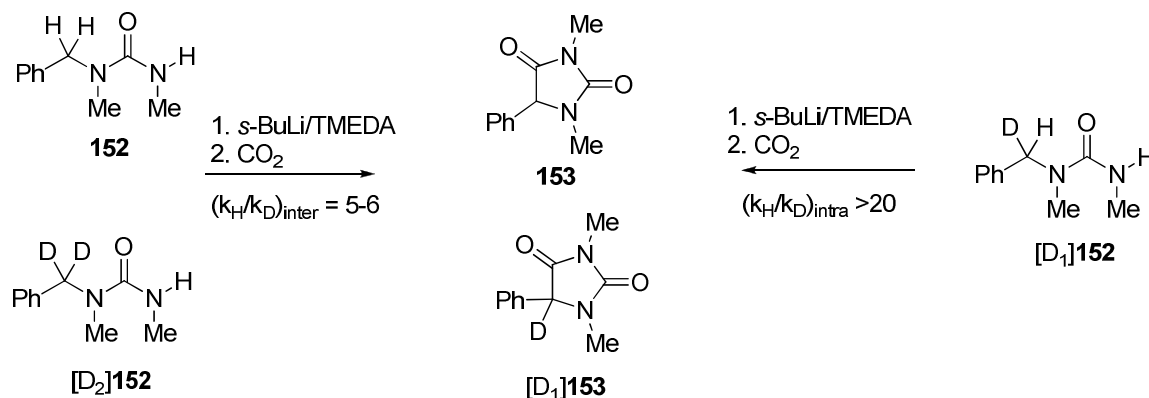


Figure 7. Partial bond formation in transition state for kinetically enhanced metalation mechanism.

Other circumstantial evidence pointing towards this model includes reports of an unreactive anisole•*n*-BuLi species in the directed metalation of anisole. Although this species was detected by $^6\text{Li}, ^1\text{H}$ -heteronuclear Overhauser effect spectroscopy (HOESY), upon addition of TMEDA and procession of the *ortho*-lithiation of anisole, this complex was no longer detectable. Thus, the observance of a complex may not indicate that the reaction proceeds *via* that intermediate. This particular reaction, instead, was thought to proceed through a complex that involves (*n*-BuLi) $_2$ •TMEDA•anisole. The observation of agostic metal hydrogen interactions in these species by Saa and coworkers⁴¹ also suggest that DoM reactions could involve kinetically enhanced metalation mechanisms.

In order to definitively determine whether the directed metalation reactions occur through a one-step (kinetically enhanced metalation) or two-step mechanism (CIPE), the protium/deuterium isotope effects of the urea **152** (Scheme 28) were investigated by Beak's group in 1999.⁴² In this work, **152**, [D₁]**152**, and [D₂]**152** were treated with *s*-BuLi•TMEDA followed by treatment with CO₂ to provide **153** or [D₁]**153**. If the reaction proceeded by a one-step mechanism without pre-complexation, the ratio of **153**/[D₁]**153** from both the intermolecular reaction (e.g., between **152** and [D₂]**152**) and the intramolecular

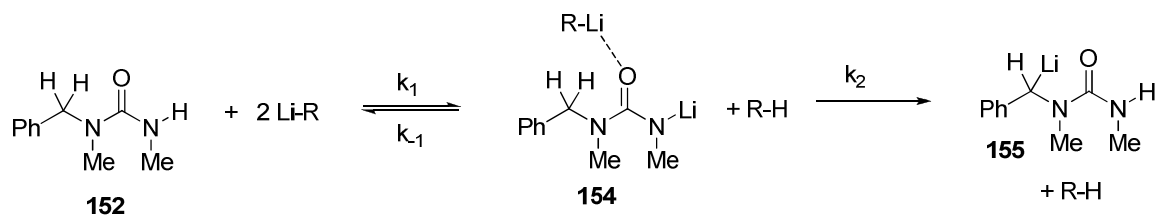
reaction (e.g., $[D_1]152$) would be similar since both experiments would involve the same primary isotope effects in the product determining step. In contrast, if the mechanism involved two steps, two different product ratios would be expected. The simplest case would afford a ratio of $153/[D_1]153$ of 1 for the intermolecular experiment since after irreversible complexation, which is assumed to be unaffected by labelling, deprotonation/deuteration will necessarily occur for **146** to convert into **144** (Scheme 26). Thus, in an intermolecular reaction, the base does not have a choice between the deuterium and the protium after the formation of a complex but for the intramolecular case, the product ratio should be determined by a primary isotope effect as the base has a choice between the protium or deuterium after irreversible complexation.



Scheme 28. An Example of Intra- and Intermolecular Isotope Effects of Directed Metalations

Measurement of k_H/k_D for the intermolecular reaction gave a value of 5-6 and the k_H/k_D for the intramolecular case gave an isotope effect >20 . The two differing values thus point towards a two-step mechanism. Beak also suggested

that a largely irreversible complexation followed by a slow deprotonation provided the best description of the mechanism (Scheme 29).



Scheme 29. Proposed Mechanism of Urea Metalation Reaction

Collum proposed yet another mechanism based on inductive effects where pre-complexation is minor or insignificant in the rate-limiting transition state.⁴³ The *n*-BuLi/TMEDA-mediated arene *ortho*-lithiations of **156** to **162** (Figure 8) revealed a substrate-independent rate law for all cases and implies a common mechanism for these reactions. The idealized rate law and mechanism are given by *equations 1* and *2* that shows first order dependence on the [arene] and [BuLi] but are independent of [TMEDA].

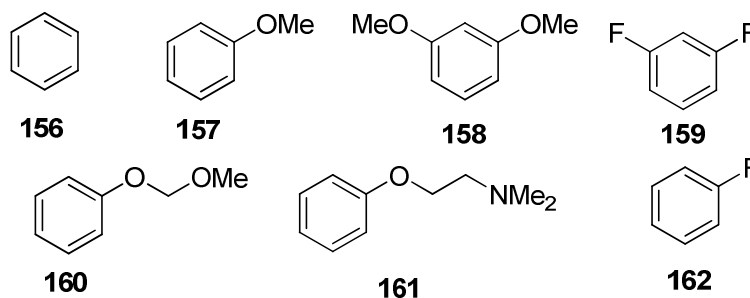
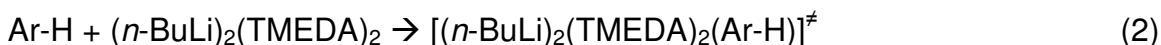


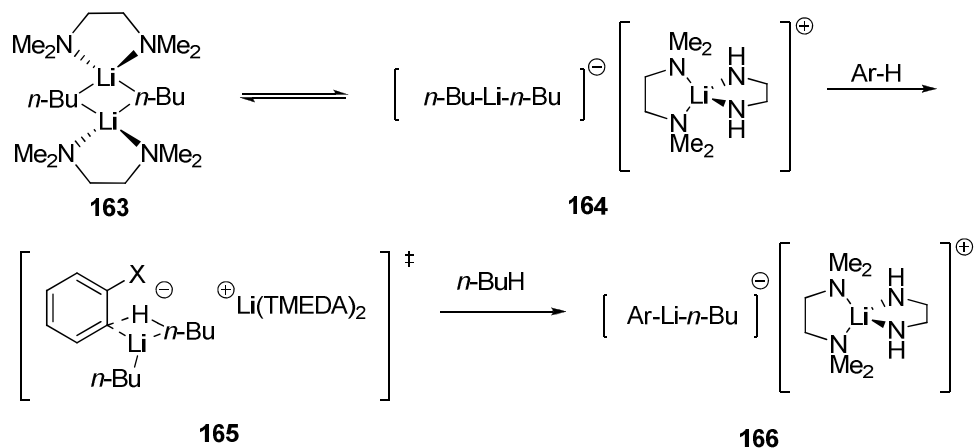
Figure 8. Arenes studied by Collum *et al.*

$$-d[\text{Ar-H}]/dt = k'[\text{ArH}]^1[\text{BuLi}]^1[\text{TMEDA}]^0 \quad (1)$$



Based on this result, Collum proposed a triple-ion based model consistent with rate law equation 2 depicted in Scheme 30. Thus, the *n*-BuLi and TMEDA dimer **163**⁴⁴ is in equilibrium with **164** prior to transformation into the lithiated species **166** via the triple ion transition state **165**. Based on *ab initio* calculations it was concluded that this model was more consistent for arenes bearing electronegative OMe and F groups than the CIPE model.

The general concept of inductive effects influencing DoM reactions warrants some comment. Collum based his assumptions largely on the inductive effects reported by Schlosser and co-workers,⁴⁵ who had previously set out to detail the additive effects, if any, of repetitive introduction of the same substituent into an aryl ring. An unbalanced addition of these additive effects is often observed; for example, the decreasing pKa values with the addition of fluorines to acetic acid is typical - the first halogen causes a decrease of 2.2, the second, a decrease of 1.7 and the third, a decrease of 1.1.



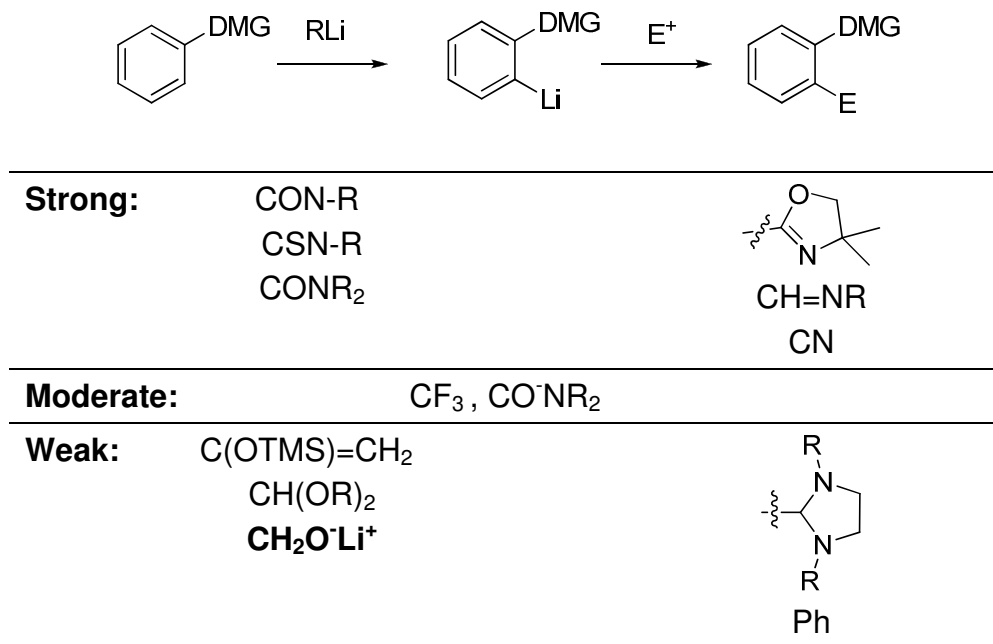
Scheme 30. Triple-ion Based Model of DoM Reactions, X = OMe, F

The trend observed in Schlosser's studies indicated that the gas phase acidities of fluorinated arenes is largely dependent on the location of the fluorine atoms. With respect to the site of deprotonation, each additional *ortho*-substituted fluorine gave the largest decrease in acidity; *meta*- and *para*-substituted fluorines did not reduce the acidity of the site of deprotonation by as large of a factor. Thus, by this model, purely inductive effects contributed to the regioselectivity and high rates of *ortho* metalation in DoM reactions.

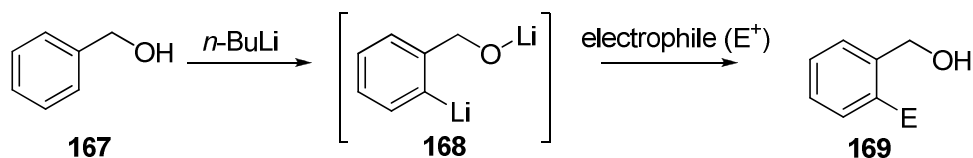
The recent computational and empirical evidence seems to lean towards the CIPE or inductive model to explain "directed" lithiation reactions versus the kinetically enhanced metalation model. However, it is not clear whether or not the mechanism of DoM reactions is also a function of reaction conditions, including solvent, base, or DMG, and consequently the KEM model cannot be entirely ruled out.

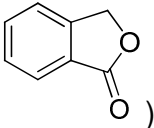
2.1.2 *Ortho*-Metalation Reactions Involving a Benzyl Alcohol or α -Methylbenzyl Alcohol.

Although directed *ortho*-metalations (DoM) have become a common means to functionalize aromatic rings, there are few examples in which a benzyl alcohol or α -methylbenzyl alcohol functions as a DMG in DoM reactions. According to Snieckus,³³ the lithiobenzyl alkoxide is a weak directing group in the hierarchy of carbon based *ortho*-directing substituents (Table 4)

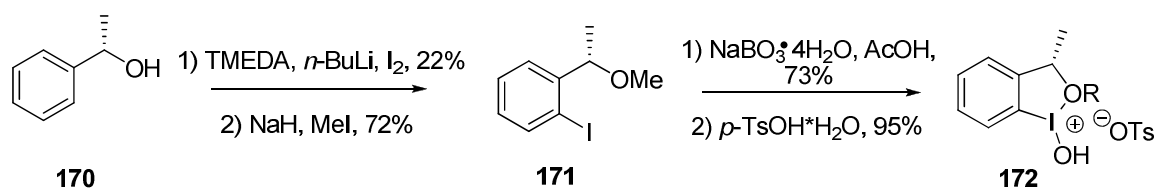
Table 4. Hierarchy of Carbon Based DMGs

Although the lithiobenzyl alkoxide has not been widely explored as a DMG, Seebach and Meyer demonstrated the scope and synthetic utility of this functionality as early as 1978.⁴⁶ In this work, it was demonstrated that heating benzyl alcohol in the presence of *n*-BuLi and tetramethylethylenediamine (TMEDA), followed by addition of an electrophile, led to *ortho*-functionalized benzyl alcohols. Examples of electrophiles reported in this study included methyl iodide, cyclohexanone, benzaldehyde and CO₂ (Table 5). In general, addition of carbonyl electrophiles such as benzaldehyde (entry 6), cyclohexanone (entry 5), and formaldehyde (entry 7) led to higher yields of the *ortho*-functionalized benzyl alcohol. In contrast, alkyl halides such as methyl iodide (entry 1) and butyl iodide (entry 2) gave poor yields.

Table 5. The *ortho*-Lithiation of Benzyl Alcohol

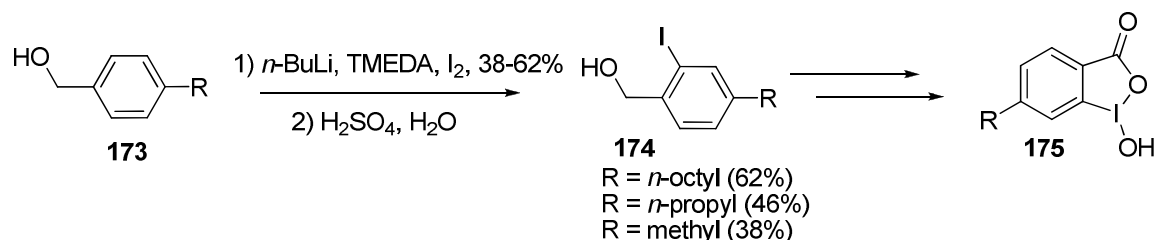
entry	electrophile	yield (%)
1	methyl iodide (E = CH ₃)	30%
2	butyl iodide (E = <i>n</i> -C ₄ H ₉)	trace
3	butyl bromide (E = <i>n</i> -C ₄ H ₉)	21%
4	iodine (E = I)	58%
5	cyclohexanone (E = C(OH)(CH ₂) ₅)	71%
6	benzaldehyde (E = CH(OH)C ₆ H ₅)	95%
7	formaldehyde (E = CH ₂ OH)	70%
8	carbon dioxide (Product = )	50%

DoM reactions that exploit benzyl alcohol or α -methylbenzyl alcohols as the DMG have also been used for the synthesis of chiral hypervalent iodine compounds in an effort to develop an asymmetric dioxytosylation of styrene and α -oxytosylation of propiophenone (Scheme 31).⁴⁷ To access these compounds, an *ortho*-lithiation reaction of (*S*)-1-phenylethanol **170** was carried out with *n*-BuLi followed by subsequent treatment with iodine and methylation to yield the α -iodo arene **171** in 22% yield. Oxidation of this substance afforded the optically pure hypervalent iodine compound **172**.



Scheme 31. Synthesis of Hypervalent Iodine Compound **172** via Seebach Method

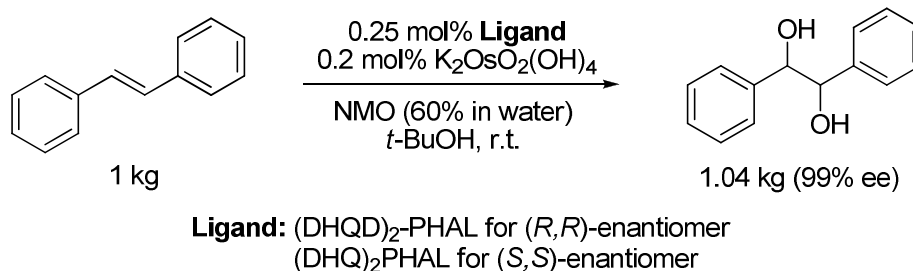
In a similar fashion, a series of 4-alkyl-2-iodosobenzoic acids **175**, were synthesized as catalysts for the hydrolysis of phosphorous esters.⁴⁸ Employing the method developed by Seebach⁴⁶ iodine was incorporated into the *ortho* position of *p*-alkylbenzyl alcohol. Depending on the length of the alkyl chain, the yields for these reactions ranged from 38-62% (Scheme 32).



Scheme 32. Synthesis of Iodosobenzoic Acids Using *ortho*-Lithiation

While it is clear that the benzyl alcohol function is not an ideal directing group for DoM reactions, we were encouraged by the results discussed above and the potential to directly functionalize both aromatic rings in hydrobenzoin using DoM chemistry. Furthermore, hydrobenzoin is readily synthesized on kilogram scale as either the (*S,S*) or (*R,R*) enantiomer from *trans*-stilbene using Sharpless dihydroxylation conditions (Scheme 33)⁴⁹ or is available commercially and is relatively inexpensive. For example, the current Aldrich price for (*R,R*)-hydrobenzoin is \$2.11 CDN/mmol making it approximately eight times cheaper

than one of the more widely used diol ligands, (*R*)-BINOL (\$16.35 CDN/mmol). Our efforts towards the development of a bidirectional metalation of hydrobenzoin are discussed in detail below.



Scheme 33. Kilogram Scale Synthesis of (*R,R*)- or (*S,S*)- Hydrobenzoin

2.1.3 Optimization of the Bidirectional *ortho*-Lithiation of (*R,R*)-Hydrobenzoin.

Although the hydroxymethyl group has received limited use in directed *ortho*-metalation (DoM) reactions, a former member of the Britton group discovered that refluxing (*R,R*)-hydrobenzoin for 8 hours in a 4:1 mixture of hexane:Et₂O followed by treatment with D₂O resulted in 75% of the expected deuterium incorporation for **177** (Table 6, entry 1). As **176** and **177** (Table 6) proved to be indistinguishable by ¹H, ¹³C, or ²D-NMR, the deuterium incorporation was calculated from integration of the ¹H NMR spectra of crude reaction products using *formula 3* (Figure 9):

$$\text{Deuterium incorporation} = |([\textit{ortho} \text{ protons}]/2 - 2)| \times 100\% \quad (3)$$

Examples of calculations using spectra from Figure 9:

Deuterium incorporation for hydrobenzoin (Figure 9, **A**) =

$$|(4.0/2)-2| \times 100\% = 0.0\% \quad (4)$$

Deuterium incorporation for hydrobenzoin after D₂O quench (Figure 9, **B**) =

$$|(2.3/2)-2| \times 100\% = 85\% \quad (5)$$

A: 0% incorporation

B: 85% incorporation

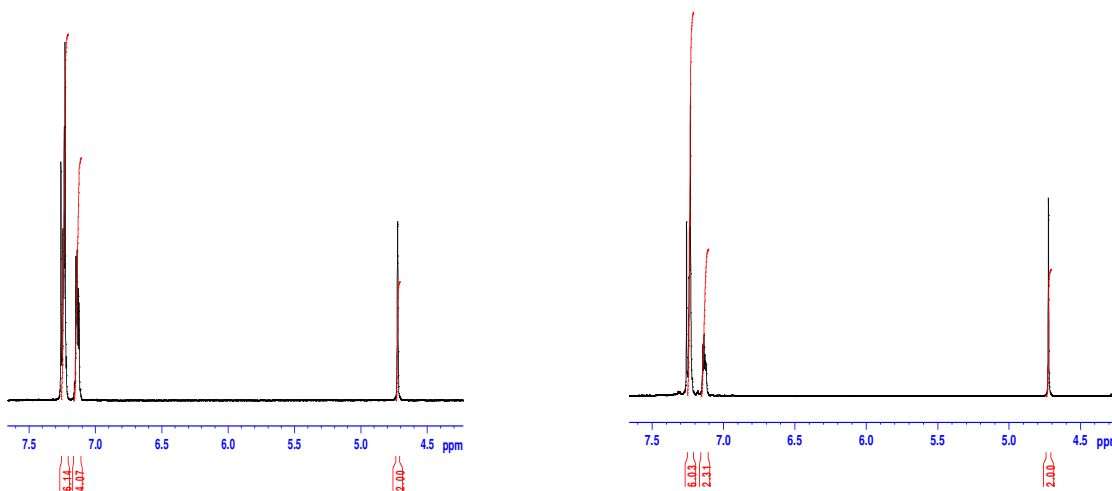
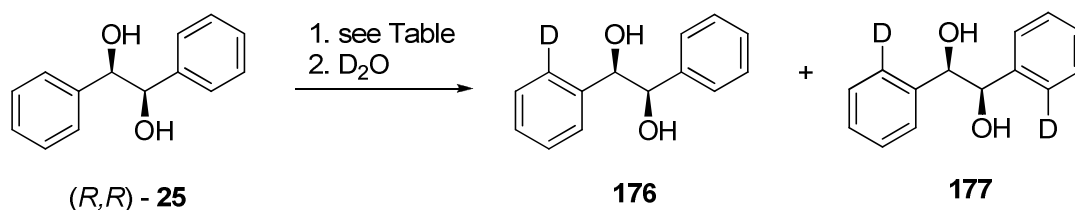


Figure 9. A: ¹H NMR of (*R,R*)-hydrobenzoin. B: ¹H NMR of deuterated hydrobenzoin.

While the use of *s*-BuLi (Table 6, entry 2) or addition of TMEDA to the *n*-BuLi reactions⁴⁶ failed to improve the level of deuterium incorporation, a slight increase in deuterium incorporation was observed when the reaction time was increased to 24h (entry 3). The optimal ratio of hexane-Et₂O was also investigated and found to be 2:1 (entries 4-6). This result is not unexpected as *n*-BuLi is known to exist as a hexamer in hexane³³ and the addition of a coordinating solvent such as ether most likely enhances the reactivity by dissociation of the hexamer and formation of more reactive tetramers or dimers.³³ Although tetrahydrofuran (THF) has also been shown to promote this dissociation,⁵⁰ THF also reacts with organolithium reagents, especially at higher

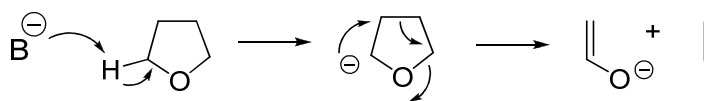
temperatures, which precluded its consideration during the initial investigation of this reaction (Scheme 34).⁵¹

Table 6. Bidirectional Metalation of (*R,R*)-Hydrobenzoin



entry ^a	alkyl lithium (equiv)	hexane:Et ₂ O ^b	time (h)	% deuterium incorporation
1	<i>n</i> -BuLi (8)	4:1	8	75
2	<i>s</i> -BuLi (8)	4:1	8	65
3	<i>n</i> -BuLi (8)	4:1	24	82
4	<i>n</i> -BuLi (8)	3:1	8	73
5	<i>n</i> -BuLi (8)	2:1	8	83
6	<i>n</i> -BuLi (8)	1:1	8	78
7	<i>n</i> -BuLi (6)	2:1	16	92

^a Entry 1-6 performed by former member of the Britton group. Entry 7 performed by the this thesis' author. ^b Reactions carried out on 0.5 mmol scale at reflux, [**25**] = 0.08 M



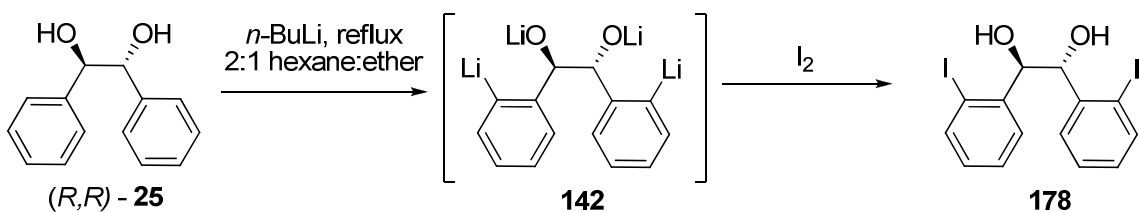
Scheme 34. Reaction of Organolithium Reagents (B) with Tetrahydrofuran

2.1.4 Optimization of Bidirectional Metalation of Hydrobenzoin

The remainder of this thesis discusses experimental results obtained by the author. Building on these preliminary results identified above in Table 6, another study exploring the optimal *equivalents* of *n*-BuLi was performed concurrently by the author in which iodine (instead of deuterium) was employed as the electrophile (Table 7). Although eight equivalents of *n*-BuLi provided the

optimal yield (Table 7, entry 1), to avoid production of unwanted by-products and decrease the necessary equivalents of electrophile, six equivalents of *n*-BuLi were chosen as the standard amount of alkyllithium reagent for this study. As evidenced in the previous studies (Table 6), where longer reaction times resulted in increased levels of deuterium incorporation, using only 6 equivalents of *n*-BuLi but extending the reaction time to 16 hours provided results comparable to those obtained with 8 equivalents of *n*-BuLi (Table 7, entry 4-5).

Table 7. Optimum Equivalents of *n*-BuLi for the Diiodination of Hydrobenzoin



entry	<i>n</i> -BuLi equivalents	reflux period (h)	I ₂ equivalents	isolated yield of 178 (%)
1	8	8	12	53%
2	4	16	5	19%
3	5	16	6	34%
4	6	16	7	51%
5	8	17	9	53%

Monitoring the formation of the tetraanion **142** by measurement of butane gas evolution indicated that rapid (20 min) deprotonation of the two alcohol functions is followed by slow (16h) removal of the two *ortho* protons (Figure 10).

Gas Evolution Studies

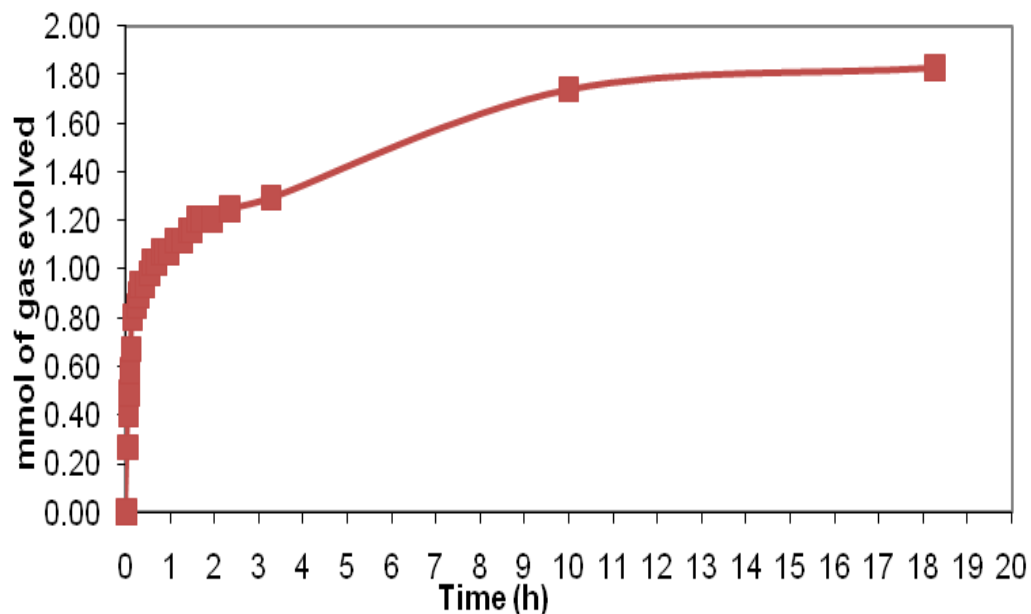


Figure 10. Gas (butane) evolution studies. Reaction conditions: 0.47 mmol of (*R,R*)-hydrobenzoin in mixture of 2:1 hexane-ether ($[25]=0.08\text{M}$), 6.0 equiv of *n*-BuLi.

The progress of the reaction of (*R,R*)-hydrobenzoin with *n*-BuLi under the optimized conditions (Table 6, entry 7) was also studied by mass spectrometry following D_2O quench, and ^1H NMR spectroscopy following reaction with methyl iodide. Interestingly, Figure 11 shows that slow removal of the first *ortho* proton is followed by a relatively fast removal of the second proton to generate the tetraanion **142**. Unfortunately, ^3Li and ^1H spectroscopy did not allow for additional insight into the nature and aggregation of intermediates involved in the production of the intermediate **142**.

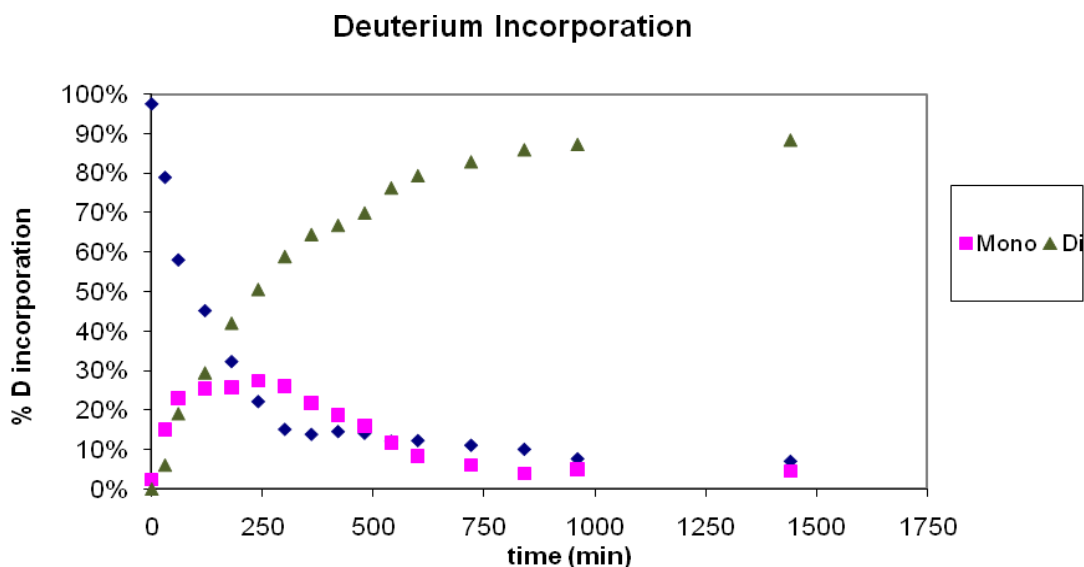
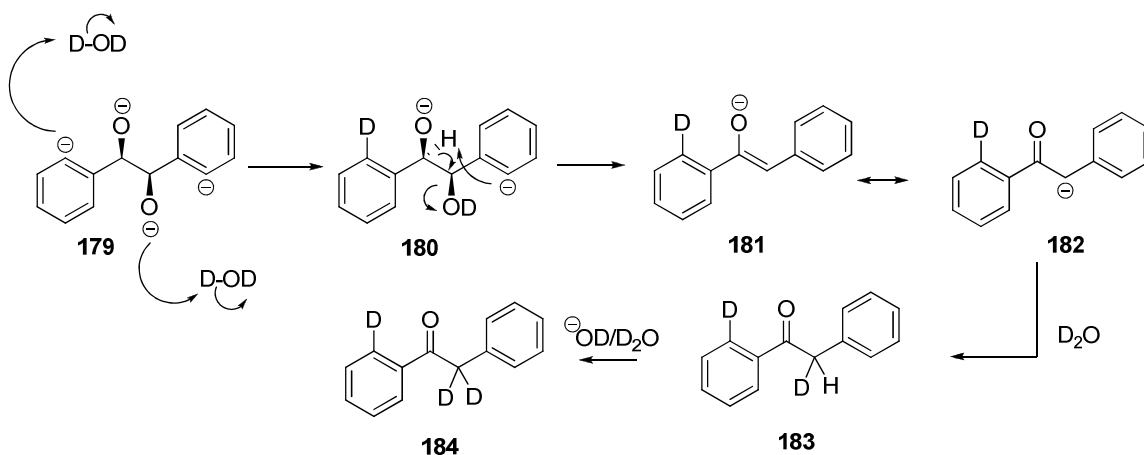


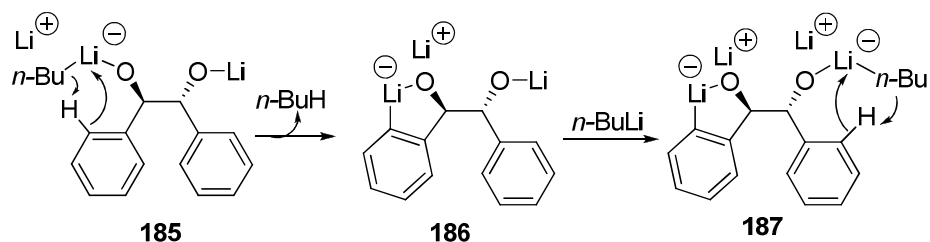
Figure 11. Percentage of hydrobenzoin **25**, monodeuteriohydrobenzoin **176** and dideuteriohydrobenzoin **177** following treatment of a refluxing solution of **25** and *n*-BuLi (6 equiv) with D₂O after various reaction times. The crude product following D₂O quench was concentrated repeatedly from CH₃OH, to ensure complete exchange of OH for OD. The ratio of **25**:**176**:**177** for these products, respectively, was determined by mass spectroscopy.

The deuterium quench studies also revealed the formation of a minor amount of the ketone product **184** (Scheme 35), obtained from competitive quench of a lithium alkoxide with D₂O. Presumably, an intramolecular deprotonation (E₂) elimination of OD occurs to give **183**, which in a basic solution of D₂O undergoes further exchange of the benzylic proton to give **184**.



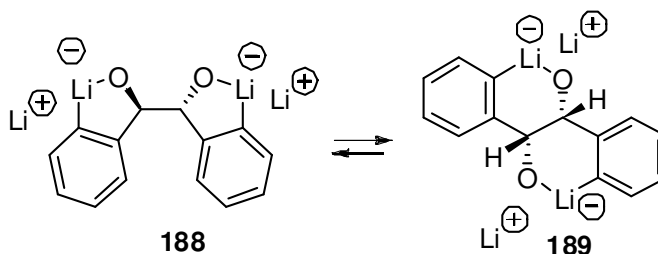
Scheme 35. Possible Mechanism for Observed Side Product **184**

Although further studies regarding the stoichiometry and rate of the reaction are needed to conclusively comment on the mechanism, it is possible to construct some hypotheses in this regard. It is well known that both lithium alkoxides and organolithium compounds exist as oligomeric species in hydrocarbon solvents and that mixed aggregates result from a combination of the two.⁵² The fact that TMEDA, which is known to increase the reactivity of organolithium species by breaking up oligomeric structures and polarizing the carbon-metal bond, has virtually no effect on the outcome of the deprotonation reaction indicates that addition of this diamine does not play any role in altering aggregation. Thus, we can speculate that the activation of the organometallic species occurs *via* the intermediacy of a lithium alkoxide complex (Scheme 36). This would be in agreement with a CIPE- type process, in which the new carbon-lithium bond is generated through a metathesis-like reaction after complexation with *n*-BuLi.

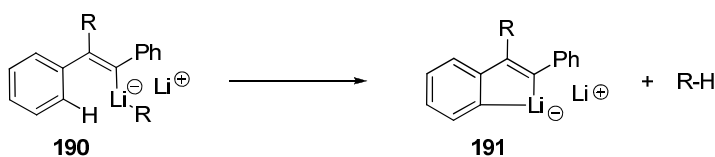


Scheme 36. *Ortho*-Lithiation Through an Alkoxide Intermediate

For simplicity, an intramolecular deprotonation is depicted in Scheme 36, however the *n*-BuLi could also come from a remote site in a complex aggregate. The second deprotonation would follow a similar mechanism leading to the *bis*-indane **188** (Scheme 37). This compound could then rearrange to a *cis*-decalin type structure **189**. Structures similar to **188** and **189** have been reported during the reaction of diphenylacetylene with organolithium reagents (Scheme 38).⁵³ In this work, a lithiated diphenylacetylene **190** was proposed to complex internally with the *ortho* (deprotonated) carbon on the aromatic ring creating a bridged structure **191** in the presence of excess of alkyllithium.

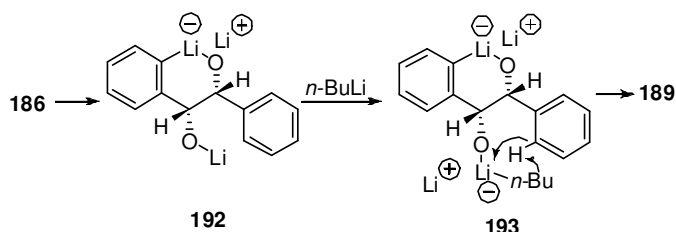


Scheme 37. Rearrangement of *bis*-Indane **188** to *cis*-Decalin-like Structure **189**



Scheme 38. Bridged Complex **191** in Lithiation of Diphenylacetylene

The kinetic data (Figure 11) suggests that the second aromatic deprotonation is faster than the first, indicating that the reaction manifold between the first and second deprotonation differs. However, according to the mechanism above, there is no evident reason why **187** should be deprotonated faster than **185** since the aggregation states in these two intermediates are similar. In fact, from the outset, we had expected the second deprotonation to be more challenging, as this introduces a fourth negative charge onto the molecule. A possible mechanism that explains the ease of formation of the tetraanion, born from discussions with Professor Victor Snieckus (Department of Chemistry, Queens University), involves rearrangement of **186** to the six-membered ring complex **192** (Scheme 39). In this case, the *cis* relationship between the lithium alkoxide and the phenyl ring and the consequent proximity of *n*-BuLi to the *ortho* proton may explain the enhanced rate for the second aromatic deprotonation. Unfortunately, attempts to crystallize the presumed “tetraanion” to gain further insight into the aggregation and structure of this intermediate proved futile.



Scheme 39. Potential Mechanism for Second *ortho*-Deprotonation

While further studies are warranted to fully probe the mechanism of the deprotonation, fortunately, this does not deter from the synthetic utility of this reaction. Although the exact nature of the reaction intermediate has not been confirmed, the term “tetraanion” will be used in the following sections in which the exploitation of this new tetraanion as a synthetic interemediate is discussed in detail.

2.1.5 Confirmation of Optical Purity

While it is unlikely that any epimerization of (*R,R*)-hydrobenzoin could occur during the reaction, the optical purity of (*R,R*)-hydrobenzoin recovered from the treatment of tetraanion **142** with H₂O was confirmed by chiral GC analysis (see experimental section). In addition, the ¹H NMR spectrum of the crude product contained none of the corresponding *meso*-hydrobenzoin, which can be differentiated from the *dl*-hydrobenzoin by the chemical shift of the benzyl protons (¹H NMR (CDCl₃) δ: 4.72 ppm (*dl*-hydrobenzoin); 4.80 ppm (*meso*-hydrobenzoin)).⁵⁴

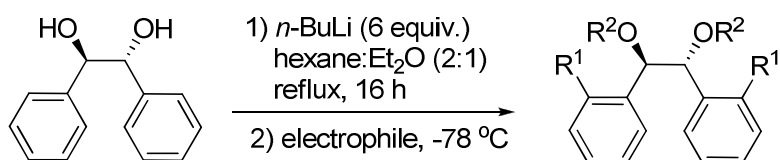
2.1.6 Screening of Electrophiles in the Bidirectional Metalation of (*R,R*)-Hydrobenzoin.

With the optimized conditions for the deprotonation established (Table 6, entry 7), we initiated a large screen of a variety of electrophiles in an effort to exploit the reactive tetraanion **142** for the direct synthesis of *ortho*-substituted hydrobenzoin derivatives. Electrophiles that gave reasonable yields of the corresponding *ortho*-functionalized hydrobenzoin derivatives are summarized in Table 8. Thus, CH₃I, I₂, dibromoethane, CO₂, B(OCH₃)₃, and Si(CH₃)₂Cl₂ afforded

the desired product along with minor amounts of the products resulting from *ortho*-functionalization of only one of the aromatic rings and recovered starting material, all of which could be separated by flash chromatography or recrystallization. For example, the crude ^1H NMR of the reaction between the tetraanion and methyl iodide (entry 1) revealed a ratio of 5:1:1 of the di-methylated hydrobenzoin, mono-methylated hydrobenzoin and starting material.

Unfortunately, we were unable to translate the high level of deuterium incorporation of the DoM step (>90%) to the reaction of the tetraanion with a broader array of electrophiles. This result may be attributed to the basic nature of the phenyl lithium and/or the steric bulk of the tetraanion and aggregation of this substance.

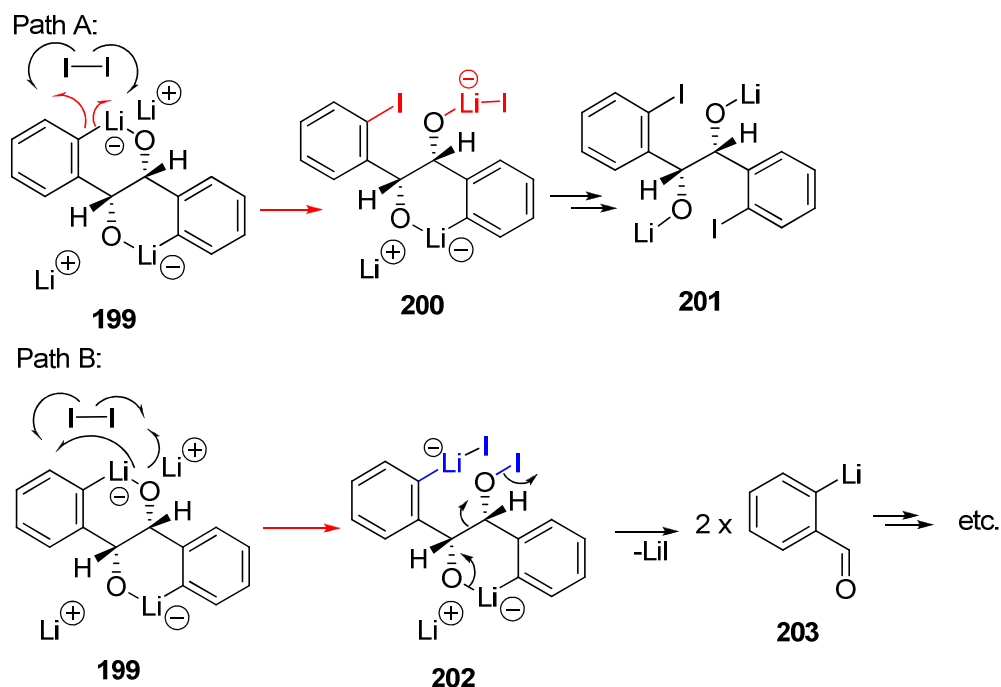
Table 8. Synthesis of Hydrobenzoin Derivatives



entry	electrophile ^a	R ¹	R ²	ratio of products ^b	product (% yield) ^c
1	CH ₃ I	CH ₃	H	5:1:1	194 (53)
2	I ₂	I	H	6:2:1	178 (53)
3	(CH ₂ Br) ₂	Br	H	5:3:1	83 (33)
4	CO ₂		CO ^{d,e}	ND ^f	195 (40)
5	B(OCH ₃) ₃ ^g		B(OH) ^d	10:2:5	196 (42)
6	Si(CH ₃) ₂ Cl ₂		Si(CH ₃) ₂ ^d	8:2:3	197 (36)

^a 7 equiv of electrophile. ^b Ratio of disubstituted hydrobenzoin: monosubstituted hydrobenzoin: recovered hydrobenzoin determined by analysis of ^1H NMR spectra of crude reaction mixtures. ^c Isolated Yield. ^d Unambiguous assignment of a five- or six-membered ring was not possible using NMR spectroscopy. ^e Product isolated by recrystallization. ^f B(OCH₃)₃ was added at 0 °C.

The reaction conditions leading to the results in Table 8 merit more comment. The addition of TMEDA (6.0 equiv) to the reaction of CH₃I with the tetraanion (Table 8, entry 1) afforded a lower yield of 2,2'-dimethylhydrobenzoin (**194**) (e.g., 2:2:1 of dimethylhydrobenzoin: monomethylhydrobenzoin: hydrobenzoin). Unfortunately, an increase in temperature from -78 °C to room temperature and longer reaction times also did not improve on this result. In the synthesis of the diiodo derivative **178** (entry 2), it was observed that subliming or grinding the iodine prior to its addition to the reaction mixture increased the yield. It can be presumed that sublimation and/or grinding increases the surface area of the iodine and consequently increases its solubility in the reaction mixture. However, attempts to pre-dissolve the iodine in THF before adding it to the reaction mixture failed to improve the yield of this process. A mechanism for the iodination reaction is outlined in Scheme 40. Organolithium reagents, especially poly anions such as **199**, are good reducing agents⁵⁵ and thus, the tetraanion, in the presence of iodine, can fragment via two distinct pathways. In Path A, a phenyl radical is formed that is able to trap the iodine radical to form a carbon-iodine bond. Alternatively, complex **199** can dissociate to form an oxygen-iodine bond that can further fragment to give decomposition products such as the *ortho*-lithiated aldehyde **203**. Side reactions such as those indicated in Scheme 40 may account for the poor mass recovery in the reactions of the tetraanion with I₂.



Scheme 40. Reaction Mechanism of Tetraanion with Iodine

Treatment of the tetraanion with bromine or dibromoethane led to similar yields of the dibromo derivative **83** (entry 3), however, the latter electrophile was preferable due to the fact that it is easier to handle experimentally. The reaction of the tetraanion with carbon dioxide (entry 4) was performed by heating solid CO₂ and bubbling the gas through a drying tube then directly into the reaction mixture. The formation of a lactone was detected using mass spectroscopy and the formation of a γ -lactone (versus a δ -lactone) was verified by IR spectroscopy (1770 cm⁻¹).⁵⁶

Table 9 summarizes the initial conditions attempted to functionalize the *ortho*-positions of hydrobenzoin with silicon. Surprisingly, chlorotrimethylsilane (TMSCl) failed to react with the tetraanion and afforded only starting material.

Triethylsilane⁵⁷ and TBDMSCl afforded predominantly the methyl ketone product **205**⁵⁸, presumably via a mechanism similar to that discussed above in which SiR₃ replaces deuterium in the initial intermediate **180** (Scheme 35). This result is not entirely surprising given the oxophilicity of silicon.⁵⁹ Fortunately, reaction of the tetraanion with dichlorodimethylsilane afforded the *bis*-siloxane **197** in 36% yield. The 6-membered ring structure (versus the 5-membered) was confirmed by crystal structure analysis (Figure 12).

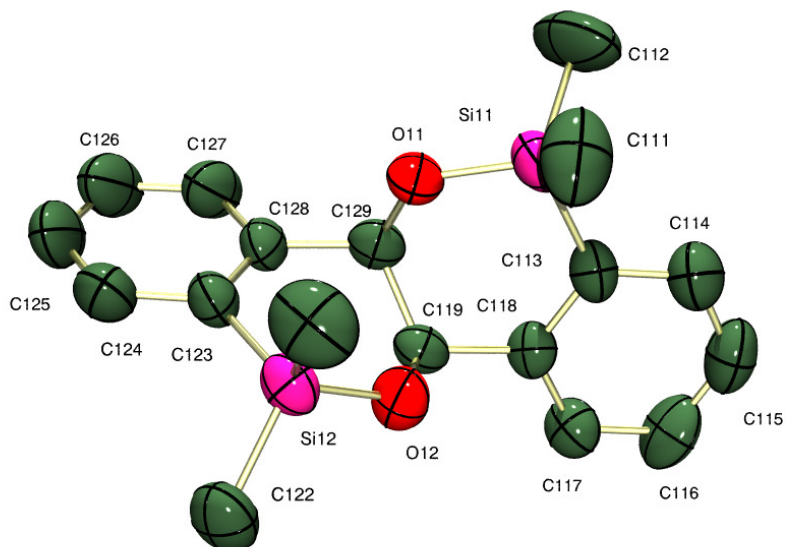
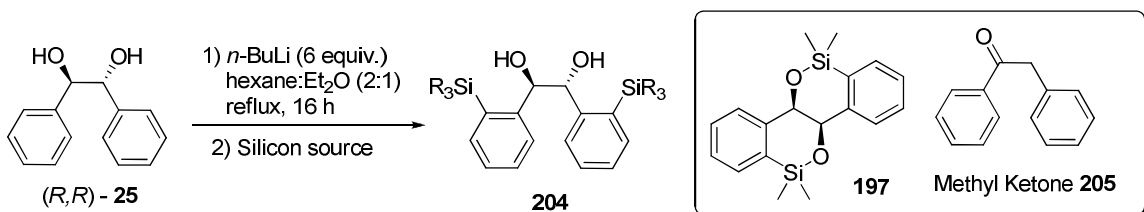


Figure 12. ORTEP plot of the crystal structure of *bis*-siloxane **197**. We thank Michael J. Katz (Leznoff laboratory, Department of Chemistry, Simon Fraser University) for solving this crystal structure.

A possible explanation for the failure of the reaction between the tetraanion and trimethylsilyl chloride is outlined in Scheme 41. Thus, a metathesis between the lithiated complex **189** and TMSCl may lead to the silicate **206**, which is incapable of further reaction with TMSCl. Upon aqueous work-up, the silicate **206** would undergo protonation and subsequent hydrolysis of the

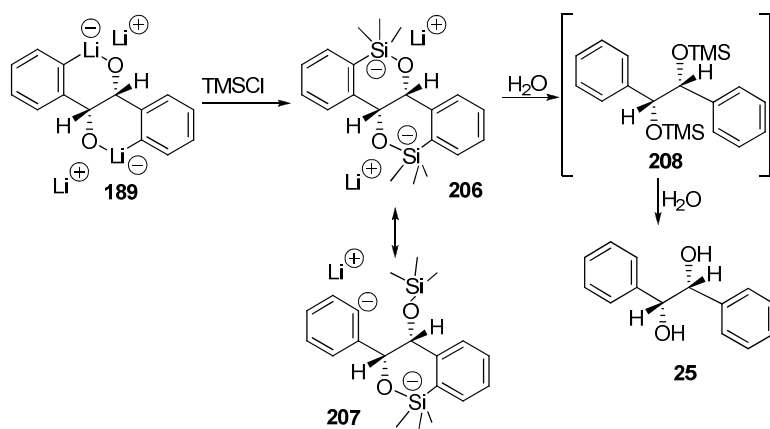
trimethylsilyl ether to afford hydrobenzoin. That starting material was not recovered from the reactions of the tetraanion with TBDMSCl suggests that, as a result of increased steric bulk relative to TMSCl, the intermediates in these reactions are incapable of forming ate complexes akin to **206**.

Table 9. Incorporation of Silicon in the *ortho*-Positions of Hydrobenzoin



entry	silicon source	result
1	TMSCl in THF	SM ^a
2	HSiEt ₃ in THF	methyl ketone ^b
3	HSiEt ₃ (reverse addition) ^c	methyl ketone
4	TBDMSCl (reverse addition)	methyl ketone
5	SiMe ₂ Cl ₂	36% of 197

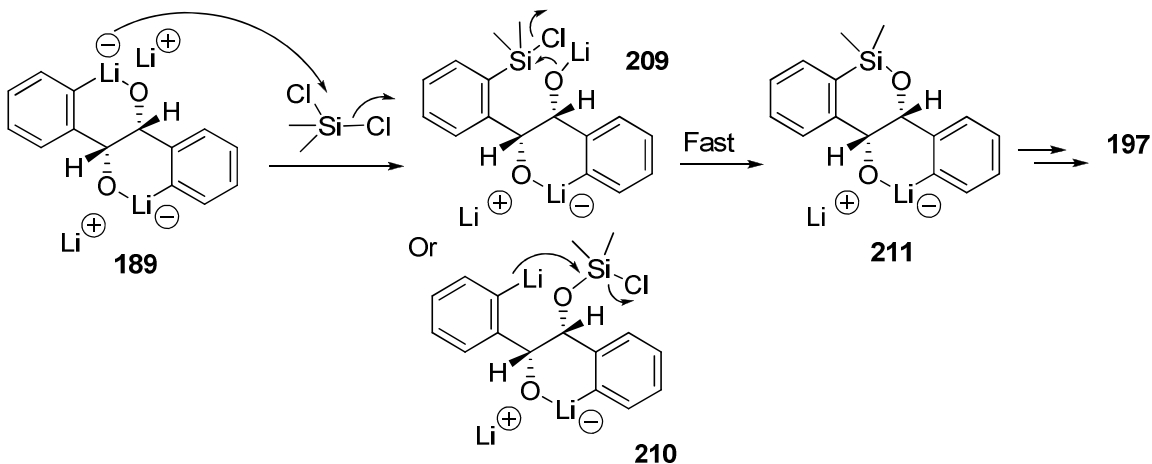
^a SM = starting material. ^b Methyl ketone obtained from side reaction shown in Scheme 35. ^c Addition of tetraanion to the silicon source in contrast to the addition of the silicon source to the tetraanion.



Scheme 41. Reaction of Tetraanion **189** with TMSCl

An interesting feature of the reaction of the tetraanion with SiMe₂Cl₂ is the exclusive formation of the six-membered ring in contrast with the formation of the

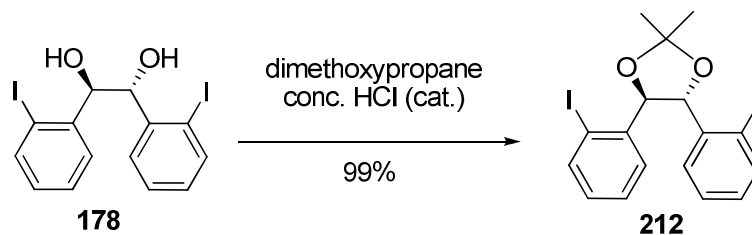
five-membered ring lactone observed upon its reaction with CO₂. It can be presumed that the tetraanion reacts with SiMe₂Cl₂ at either the carbon centre to give intermediate **209**, or at the oxygen centre to give intermediate **210** (Scheme 42). The second addition of the free alkoxide or the free phenyl carbanion into the silicon centre presumably happens quickly and thus leads to the six-membered ring. As the other alkoxide/carbanion is tied up in the lithium ate complex, it is not available to react internally with the silicon centre thus preventing the formation of a five-membered ring.



Scheme 42. Formation of Six-membered Ring in Reaction of Tetraanion with SiMe₂Cl₂

As our impetus for exploring the reactivity of hydrobenzoin was to access the chiral borinic acid **139** (Scheme 22), a potential catalyst for enantioselective Mukaiyama aldol reactions (*vide supra*), we decided to first protect the diol function in the diiodohydrobenzoin **178** as an acetonide to reduce side reactions and introduce the boron following lithium-iodine exchange or Grignard formation.

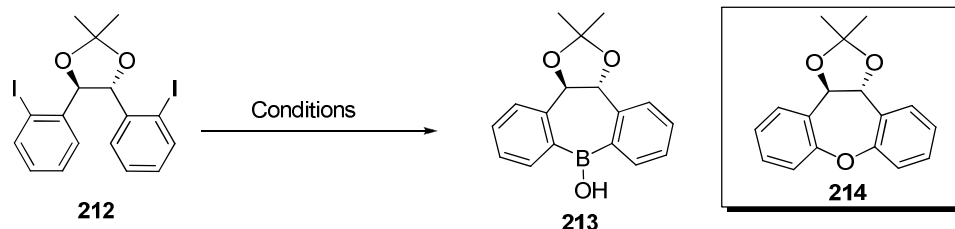
The acetonide **212** was synthesized in 99% yield through the treatment of a solution of diiodo hydrobenzoin **178** in dimethoxypropane with a catalytic amount of concentrated hydrochloric acid (Scheme 43).

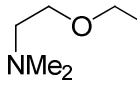


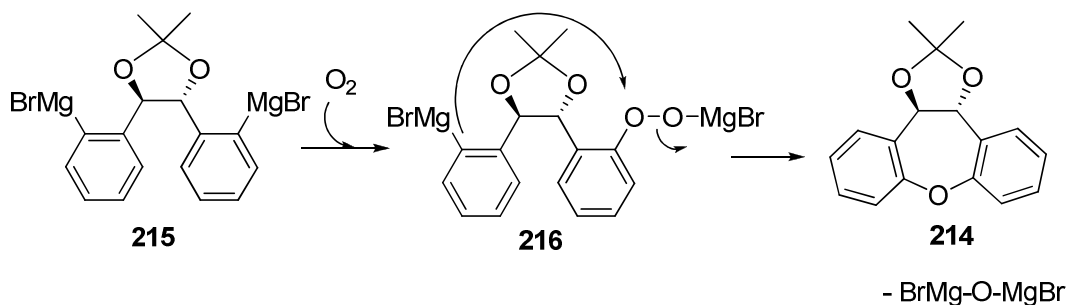
Scheme 43. Protection of Diiodo Hydrobenzoin Derivative **178**

Lithium-halogen exchange of **212** followed by addition of $B(OMe)_3$ gave a complex mixture of products (Table 10, entry 1). Therefore, we endeavoured to affect the formation of a Grignard reagent that would presumably be less reactive than the corresponding organolithium.⁶⁰ However, this strategy also failed to afford the desired boronic acid (entry 2), even in the presence of additives (entry 3). Interestingly, the formation of a Grignard reagent from **212** by addition of $iPrMgCl$ and subsequent reaction with $B(OMe)_3$ resulted in the production of the oxygen bridged compound **214** in 12% yield. The formation of a bridged oxygen compound was verified by mass spectrometry and it is likely that this product arises from reaction with exogenous dioxygen after formation of the digrignard **215** (Scheme 44). Thus, dioxygen would react rapidly with **215** to form the peroxyanion **216**, which undergoes an intramolecular reaction with the remaining phenyl Grignard to form the bridged ether **214**.

Table 10. Attempts to Incorporate Boron *via* the Acetonide Protected Diiodo Hydrobenzoin Derivative **212**



entry	conditions	results
1	1) <i>n</i> -BuLi, 2) B(OMe) ₃	complex mixture
2	1) <i>i</i> -PrMgCl, B(OMe) ₃	214 (12%)
3	1) <i>i</i> -PrMgCl,  , 2) B(OMe) ₃	complex mixture

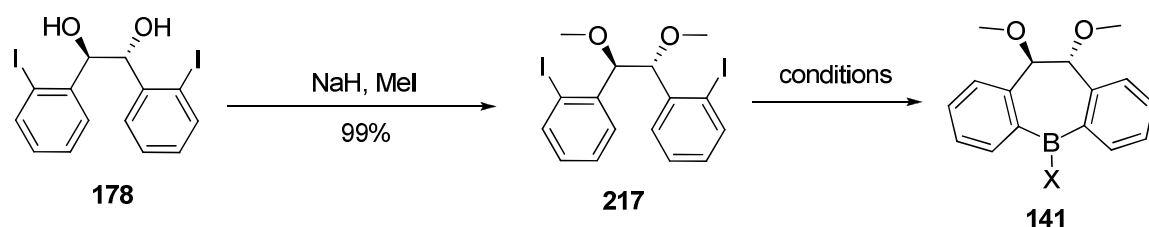


Scheme 44. Reaction of Digrignard **215** with Exogenous Oxygen

As the reactions of the acetonide **212** had been unsuccessful, we sought to improve the conformational flexibility of the system, which should help in forming the boron-bridged tricyclic **139**. Thus, the dimethyl ether of the diiodo derivative **217**⁶¹ was synthesized in near quantitative yield following deprotonation of the alcohol function in **178** with NaH and addition of MeI. Our efforts to incorporate boron into the dimethoxy diiodo derivative **217** are highlighted in Table 12. Again, our initial efforts focused on a lithium-halogen

exchange followed by reaction with $\text{B}(\text{OMe})_3$. Unfortunately, this process afforded a complex mixture of products (entry 1). The reaction of the dimethyl ether **217** with magnesium also failed to afford the Grignard reagent and attempts to improve on this result by heating and/or sonicating the reaction mixture, or cleaning the magnesium (iodine crystal, bromine) failed. However, after a screen of boron sources (entries 4-6) we were gratified to finally see that lithium-halogen exchange followed by addition of $\text{BF}_3 \cdot \text{OEt}_2$ gave a product whose spectral data was consistent with that expected for **141**.

Table 11. Attempted Syntheses of Dimethoxy Boronic Acid **141**



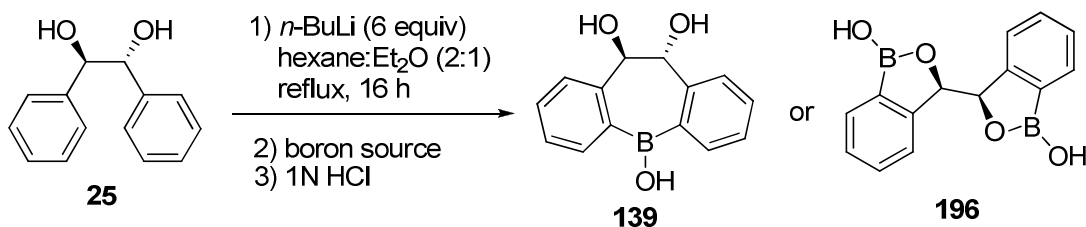
entry	conditions	X	results
1	1) <i>n</i> -BuLi, 2) $\text{B}(\text{OMe})_3$	-OH	complex mixture
2	1) Mg, heat, 2) $\text{B}(\text{OMe})_3$	-OH	starting material
3	2) <i>n</i> -BuLi, 2) $\text{B}(\text{OMe})_3$, 3) ethanolamine	$-\text{OCH}_2\text{CH}_2\text{NH}_2$	complex mixture
4	1) <i>n</i> -BuLi, 2) BBr_3	-OH	complex mixture
5	1) <i>n</i> -BuLi, 2) BCl_3	-OH	complex mixture
6	1) <i>n</i> -BuLi, 2) $\text{BF}_3 \cdot \text{OEt}_2$	-OH	11%

Building on this apparent success and our knowledge of both the spectral and chromatographic behaviour of compounds such as **141**, we reinvestigated the incorporation of boron directly into tetraanion **142**. As outlined in Table 12,

using $\text{BF}_3 \cdot \text{OEt}_2$ we were able to produce a small amount of the presumed borinic acid (7%). Fortunately, changing the boron source to $\text{B}(\text{OMe})_3$ led to increased boron incorporation and an isolated yield of 42% (entry 2). Through careful optimization of this reaction, a number of factors were found to be of critical importance:

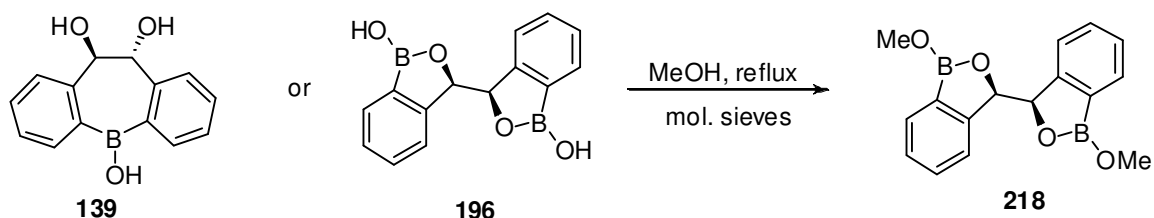
- 1) The amount of product (by analysis of crude ^1H NMR spectra) was highest when work-up conditions were neutral. Consequently, after the addition of 1N HCl to quench reaction mixture, 2N NaOH was added until the pH reached 7.
- 2) Slow addition of the electrophile (diluted in ether) led to increased yields.
- 3) Addition of the boron source at 0 °C gave a higher yield than at -78 °C.

Table 12. Direct Functionalization of Hydrobenzoin with Boron



entry	boron source	yield
1	$\text{BF}_3 \cdot \text{OEt}_2$ in ether	< 7%
2	$\text{B}(\text{OMe})_3$ in ether	42%

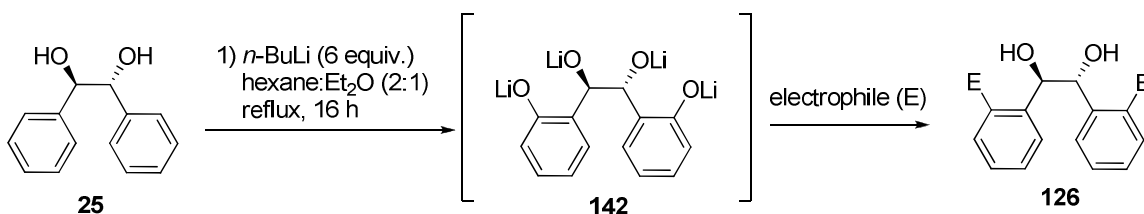
It was also discovered that the product of this reaction forms anhydrides in CDCl_3 which led to complications in our initial attempts to characterize this material by ^1H NMR spectroscopy. Fortunately, it was eventually found that the product is stable in CD_3OD , allowing for characterization by NMR spectroscopy. The formation of anhydrides and/or dimers also posed problems during purification by flash-chromatography, where the high conversion seen in the crude ^1H NMR spectra could not be translated to isolated yields. Crystallization and mass spectroscopy also proved difficult (see experimental) due to formation of dimers, polymers, and/or anhydrides and we were unable to obtain a crystal structure or obtain a parent ion for the product after repeated efforts. It is important to point out that the inability to obtain a parent ion or crystal also prevented us from distinguishing between two possible candidate structures of this product: the borinic acid **139** or the *bis*-benzoxaborol **196** that would come from the *bis*-boronation of hydrobenzoin (Scheme 45). To distinguish between these two entities, the boron-incorporated hydrobenzoin product was heated (65°C) in methanol in the presence of molecular sieves. As shown in Scheme 45, integration of the OCH_3 resonances (δ 3.81 ppm) in ^1H NMR spectrum confirmed the presence of two OCH_3 groups (e.g., **218**).



Scheme 45. Distinguishing Between the Borinic Acid **139** and the *bis*-Benzoxaborol **196**

Although disappointed that we were unable to synthesize the borinic acid **139** and had instead constructed the *bis*-benzoxaborol **196**, we realized the synthetic utility of this *bis*-benzoxaborol as a coupling partner for Suzuki-type cross-coupling reactions (*vide infra*). Thus, in one step from optically pure hydrobenzoin, the *bis*-benzoxaborol should prove a useful synthetic intermediate for auxiliary/ligand syntheses.

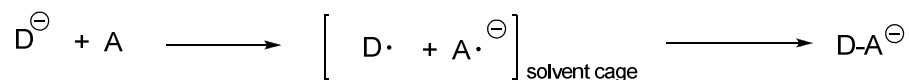
While C-C bond formation from the tetraanion would be an attractive route to functionalized hydrobenzoin, only CO₂ and CH₃I were found to be suitable carbon electrophiles (Table 8, entry 1 and 4). This result was surprising since the reaction of benzyl alcohol with *n*-BuLi followed by carbon electrophiles is reported to result in the production of *ortho*-functionalized benzyl alcohols in high yields (*vide supra*).⁴⁶ Former members of the Britton group found that acetone, acetaldehyde, diethylcarbonate, valeraldehyde, cyclohexanal, allyl bromide, allyl iodide and crotonaldehyde all coupled with the tetraanion in very low yields (< 10%) and/or provided an intractable mixture of products. In the present study, it was found that DMF, paraformaldehyde, and benzaldehyde, (Table 13, entries 1-3) also failed to give the expected product in synthetically useful yields. The crude ¹H NMR revealed that the reaction of the tetraanion with benzaldehyde (entry 3) afforded a mixture of all possible diastereomers.

Table 13. Addition of Carbon Electrophiles to the Tetraanion

entry	electrophile	expected product	result
1	DMF	219	complex mixture
2	(CH ₂ O) _n	220	complex mixture
3	benzaldehyde	221	complex mixture
4	benzyl chloride	222	 starting material
5	benzyl bromide	222	starting material

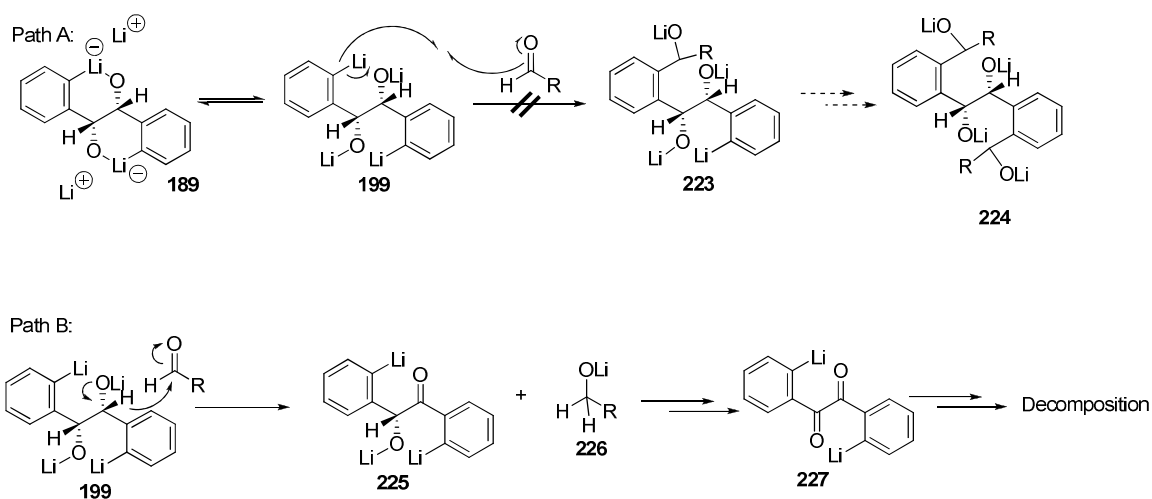
A potential rationale for the failures highlighted in Table 13 involves the fragmentation of the C-C bond of the dilithium alkoxide intermediate via a radical process. It is well established that the reaction of organometallic reagents and carbonyl compounds can occur *via* electron-transfer mechanisms (Scheme 46)⁶²

and in our case, such a process may lead to degradation of the tetraanion as outlined below.



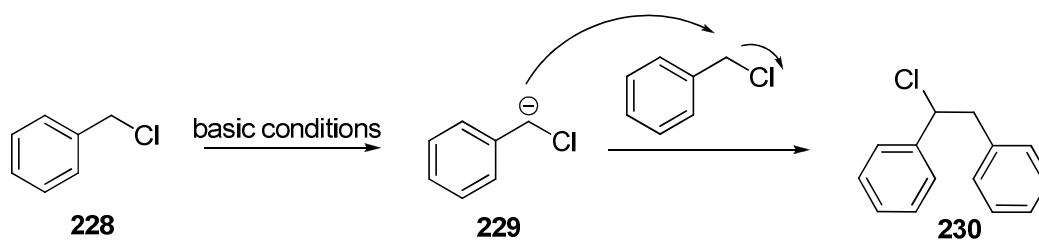
Scheme 46. Addition of Carbanions to Carbonyls by Electron-transfer Mechanism (D = donor, A = acceptor)

The tetraanion **142** may serve as a good reducing agent (*vide supra*) and deliver one electron to the carbonyl function of the added electrophiles. However, the formation of the intermediate **199** from the tetraanion would lead to the competitive degradation of this intermediate via pathway B (Scheme 47), which involves the migration of a hydride to an aldehyde to generate **225** and **226**. Both of these compounds are inherently reactive under the reaction conditions and would likely decompose further.



Scheme 47. Reaction of Tetraanion with Carbonyl Compounds

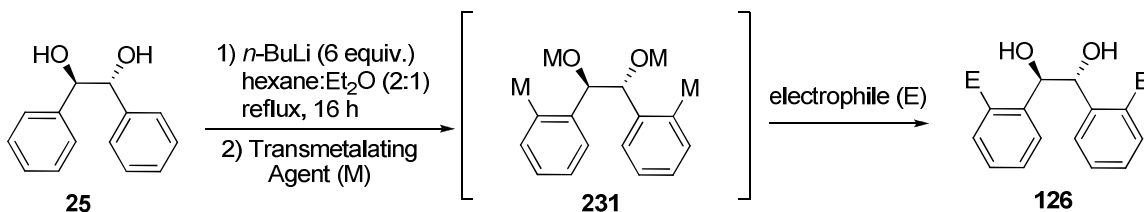
In an attempt to incorporate a benzyl function in the *ortho* position of hydrobenzoin, benzyl bromide was also added to the tetraanion **142** (entry 5). Unfortunately, following work-up, only starting material was recovered. Addition of benzyl chloride was also explored (entry 4), however, deprotonation of benzyl chloride by the excess *n*-BuLi or the tetraanion followed by reaction with a second equivalent of benzyl chloride led exclusively to the compound **230** (Scheme 48).

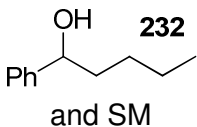
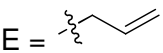
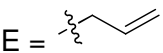


Scheme 48. Reaction of Benzyl Chloride with Itself under Basic Conditions

It was apparent from these results that the basic nature of the tetraanion gave way to side products when reacted with carbon electrophiles. Thus, we attempted to attenuate the reactivity by drawing on the rich history of zinc (Reformatsky)⁶³ and magnesium (Grignard)⁶⁴ carbanions for carbon-carbon bond formations. While we expected that transmetalation of the tetraanion followed by treatment with various electrophiles would lead to improved results, as indicated in Table 14, transmetalation only resulted in recovery of starting material, the addition of *n*-BuLi into the electrophile or a complex mixture of products.

Table 14. Results from Transmetalation of Tetraanion with Zn and Mg

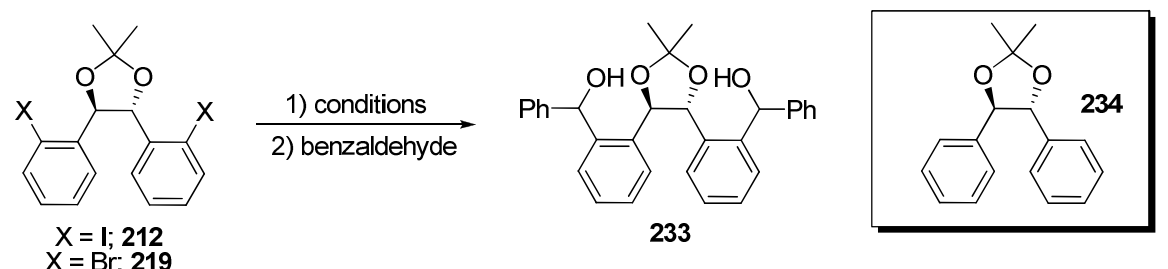


entry	transmetal. agent (conditions) ^a	electrophile (Conditions)	expected product	results
1	ZnCl ₂ (-78 °C → RT) In 1.0 M ether	benzaldehyde (-78 °C → RT)	221	 232 and SM
2	MgBr ₂ (-78 °C → RT)	benzaldehyde (-78 °C → RT)	221	232 and SM
3	MgBr ₂ (-78 °C → RT) In 3 mL THF	benzaldehyde (-78 °C → RT)	221	232 and SM
4	MgBr ₂ (-78 °C → RT) In 30 mL THF	allyl bromide (0 °C → RT)	E = 	SM
5	MgBr ₂ (-78 °C → RT) In 30 mL THF	allyl iodide (0 °C → RT)	E = 	SM
6	MgBr ₂ (-78 °C → RT) In 30 mL THF	benzaldehyde (0 °C → RT)	221	complex mixture
7	MgBr ₂ (-78 °C → RT) In 10 mL THF	DMF (-78 °C → RT)	219	complex mixture

^a Reactions conditions: 0.47 mmol (*R,R*)-hydrobenzoin in mixture of 2:1 hexane-ether ([**25**]=0.1 M). Six equivalents of *n*-BuLi was used.

One of the difficulties that arose during these transmetalation reactions was that there was no easy way to ascertain whether the lithium tetra-anion actually underwent transmetalation. Furthermore, the addition of *n*-BuLi into the aldehydes to afford compound **232**⁶⁵ (e.g., Table 14, entry 1) circumvented the production of the desired product. Despite these obstacles, we continued to probe carbon-carbon bond formation through treatment of the anion derived from the acetonide of diiodohydrobenzoin with benzaldehyde (Table 15). Benzaldehyde was chosen based on its known reactivity with the dianion derived from DoM of benzyl alcohol.⁴⁶

Table 15. Carbon-carbon Bond Formation Reactions with Benzaldehyde



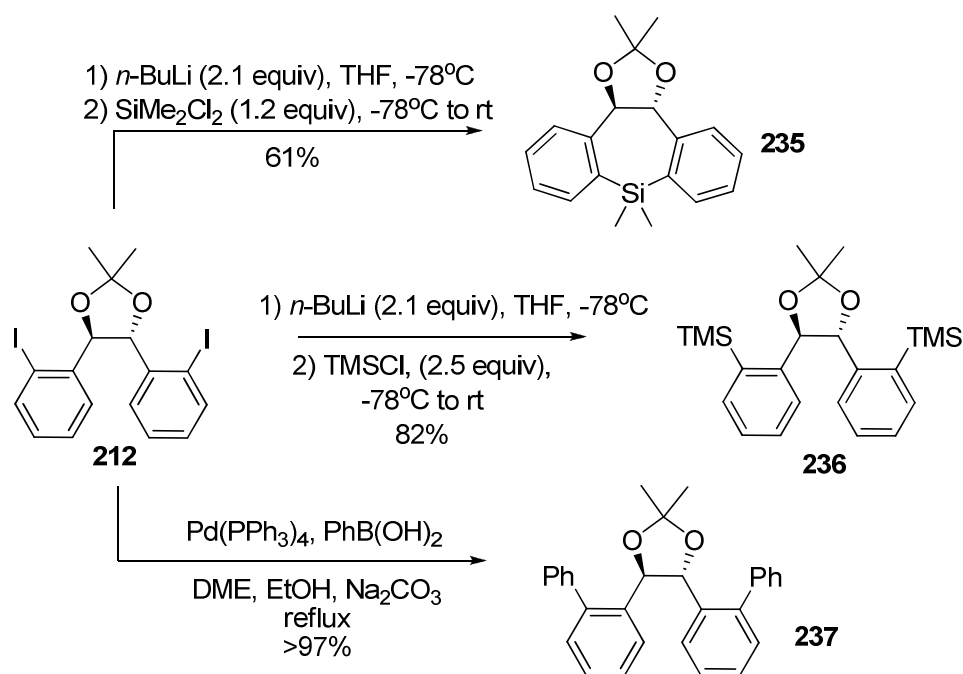
entry	X	conditions	results
1	I	<i>n</i> -BuLi then benzaldehyde	complex mixture, 234
2	I	Benzaldehyde then <i>n</i> -BuLi	complex mixture
3	I	Mg (sonicate, I ₂), then benzaldehyde	SM
4	I	<i>n</i> -BuLi, MgBr ₂ then benzaldehyde	complex mixture
5	Br	Mg (heat for 1 h), then benzaldehyde	SM

On the basis of the disappointing results summarized in Table 15, we decided to move forward and focus on the synthesis of new hydrobenzoin

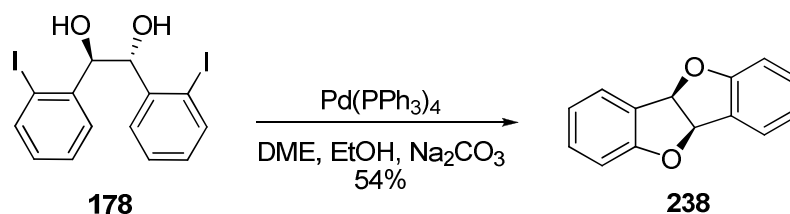
derivatives (Table 8, *vide supra*) that may serve as auxiliaries/ligands in asymmetric synthesis. Although the scope of electrophiles that engaged in useful coupling reactions with the tetraanion **142** were limited, there are distinct advantages of this new method to prepare *ortho*-functionalized hydrobenzoin derivatives when compared to the reported procedures (*vide supra*). As mentioned previously, hydrobenzoin is relatively inexpensive, readily available as either enantiomer or can be synthesized easily on kilogram scale. In addition, formation of the tetraanion is carried out without the need for protecting groups and provides optically pure products.

2.1.7 *Ortho*-Substituted Hydrobenzoin Derivatives from Diiodo **212 and *bis*-Benoxaborol **196**.**

One of the most synthetically useful hydrobenzoin derivatives accessed from our initial screen of electrophiles was the optically pure aryl halide **178**. For example, the dianion derived from the acetonide **212** coupled with electrophiles smoothly (e.g., TMSCl, SiMe₂Cl₂) and also engaged in high yielding palladium catalyzed cross coupling reactions to afford a broader range of *ortho*-substituted hydrobenzoin derivatives (Scheme 49). Unfortunately, the coupling reaction required that the alcohol functions be protected as the corresponding free diol underwent an intramolecular coupling to afford the *cis*-4b, 9b-dihydrobenzofuro[3,2-b]-benzofuran (Scheme 50). The structure of **238** was confirmed by comparison of spectral data (¹H, ¹³C NMR) to those reported in the literature for this substance.⁹⁰



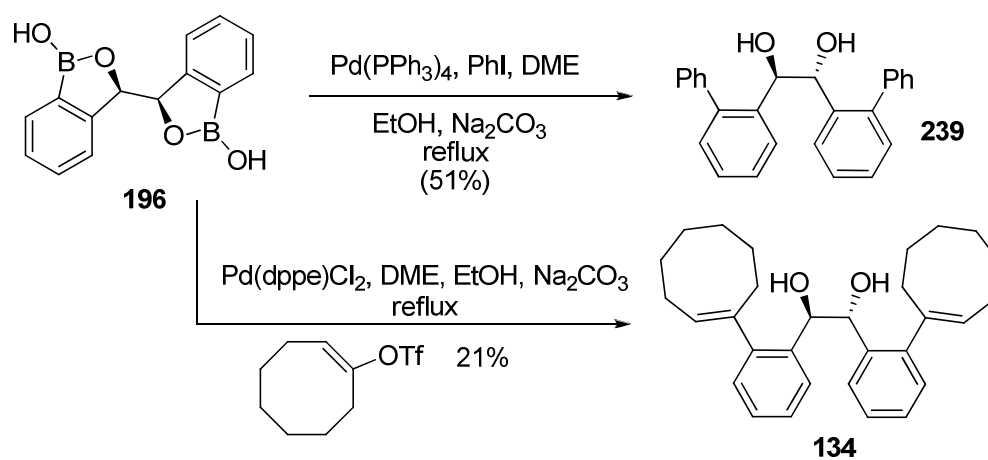
Scheme 49. Synthesis of *ortho*-Substituted Hydrobenzoin Derivatives from Acetone **212**



Scheme 50. *cis*-4b,9b-Dihydrobenzofuro[3,2-*b*]-benzofuran, Product Obtained from Pd(0) Catalyzed Coupling of Diiodo Hydrobenzoin **178**

The *bis*-benzoxaborol **196** also proved to be a versatile intermediate for the synthesis of hydrobenzoin derivatives through cross coupling with aryl halides or vinyl triflates (Scheme 51). This approach complements that described above and avoids the need to protect the diol prior to the coupling step. Thus, in two steps, the optically pure derivatives **239** and **134** could be constructed

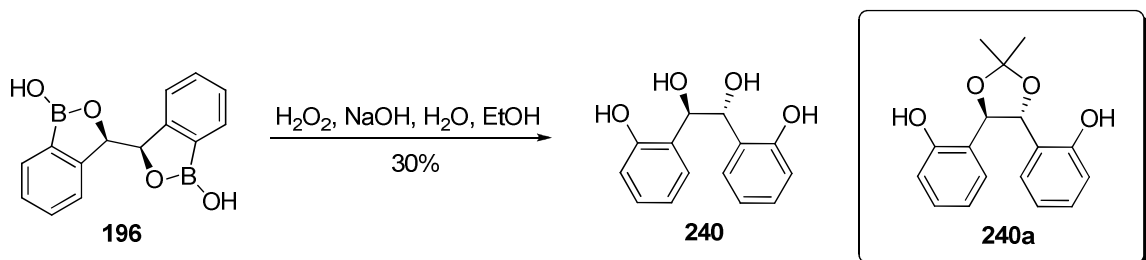
through the intermediacy of **196**. Notably, for the purposes of cross-coupling, the purification of the *bis*-benzoxaborol proved unnecessary. When the crude *bis*-benzoxaborol was used, the overall yield of compound **239** from (*R,R*)-hydrobenzoin is 32% compared to 21% when **196** was purified by flash-chromatography. The *bis*-benzoxaborol also engaged in cross-coupling reactions with vinyl triflates, which allows access to the Vivol precursor **134** in three steps in contrast to the seven steps required in the original preparation of this material by Hall.²²



Scheme 51. Cross Coupling of *bis*-Benzoxaborol with Aryl Halides and Vinyl Triflates

The *bis*-benzoxaborol **196** could also be oxidized to afford the C_2 symmetric *bis*-phenol **240** (Scheme 52). Notably, the acetonide of this *bis*-phenol was reported by others as a BINOL-like ligand for asymmetric synthesis.⁶⁶ It is noteworthy that the published synthesis of the acetonide derived from the *bis*-phenol **240a** (see inset) proceeds in 6% overall yield following a six-step

sequence of reactions that requires two resolutions. That the tetrol **240** is now accessible in a one-pot procedure should allow for further exploration of this ligand/auxiliary in asymmetric synthesis.

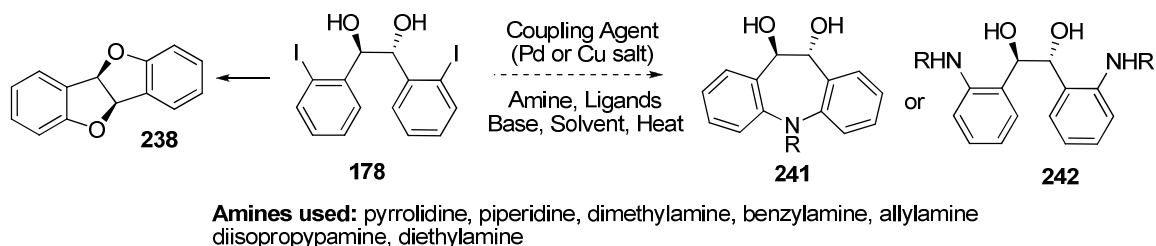


Scheme 52. Oxidation of *bis*-Benzoxaborol to Give *bis*-Phenol **240**

2.1.8 Buchwald-Hartwig Couplings to form Azepines.

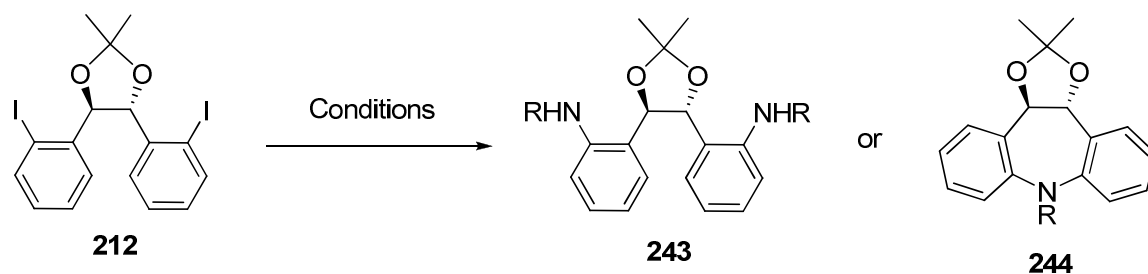
We also wished to exploit the diiodohydrobenzoin derivatives **178** in the synthesis of azepines **241** or diamine **242** using Buchwald-Hartwig type coupling conditions (Scheme 53). Unfortunately, although a large number of reaction conditions and amines were screened, none afforded the desired azepines or diamines due to the competing intramolecular C-O coupling that leads to the *cis*-4b,9b-dihydrobenzofuro[3,2-b]-benzofuran **238**.

In an effort to circumvent this undesired intramolecular C-O coupling reaction, the diol function in **178** was protected as the corresponding acetonide. Unfortunately, again under a variety of conditions, the acetonide **212** also failed to engage in C-N coupling reactions to provide either of the desired products and only starting material was recovered (Table 16).



Scheme 53. Attempted Buchwald-Hartwig Couplings.

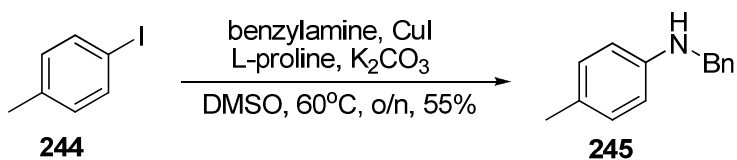
Table 16. Attempted Syntheses of *ortho*-Amino Hydrobenzoin Derivatives



entry	catalyst/co-catalyst	base	amine	solvent	results
1	CuI, L-proline	K ₂ CO ₃	pyrrolidine	DMSO	SM
2	CuI, L-proline	K ₂ CO ₃	allylamine	DMSO	SM
3	CuI, L-proline	K ₂ CO ₃	benzylamine	DMSO	SM
4	Pd(PPh ₃) ₄	K ₃ PO ₄ •H ₂ O	aniline	Toluene	SM

To verify whether these failures were due to the inherent features of acetonide **212** or a consequence of poor laboratory practice, we repeated a known reaction of 4-iodotoluene with benzylamine (Scheme 54).⁶⁷ Although a lower yield was obtained for this coupling than that reported in the literature (55% versus the reported 85%), the success of this reaction and failure of the coupling reaction involving the acetonide **212** indicates that the later substance is simply not a good substrate for this type of coupling reaction. While success in this

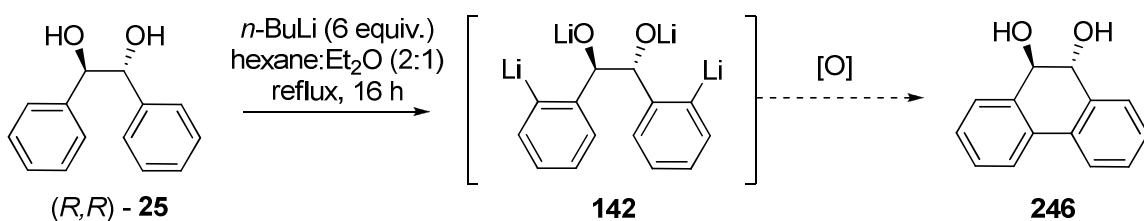
reaction would lead to a variety of useful intermediates, further attempts to optimize this process were abandoned.



Scheme 54. Coupling of 4-Iodotoluene with Benzylamine

2.1.9 Intramolecular Cross-Coupling Reactions

Classes of natural products that include structures similar to the tricyclic phenanthrene diol **246** depicted in Scheme 55 include aporphines such as oliveroline (G2 checkpoint inhibitors)⁶⁸ and pradimicinones.⁶⁹ In addition, phenanthrenediols have also been reported as metabolites in human and rat urine⁷⁰ and have also shown potential utility as molecular switches.⁷¹ It was envisaged that oxidation of the tetraanion may provide rapid access to the carbon skeleton of these compounds and their analogues.



Scheme 55. Proposed Synthesis of Dihydrophenanthrene **246**

While there are many examples of biaryl couplings, including the Ullmann (copper-catalyzed), Stille, and Suzuki reactions (palladium-catalyzed) and the Suzuki reaction (palladium-catalyzed),⁷² our initial efforts focused on identifying a

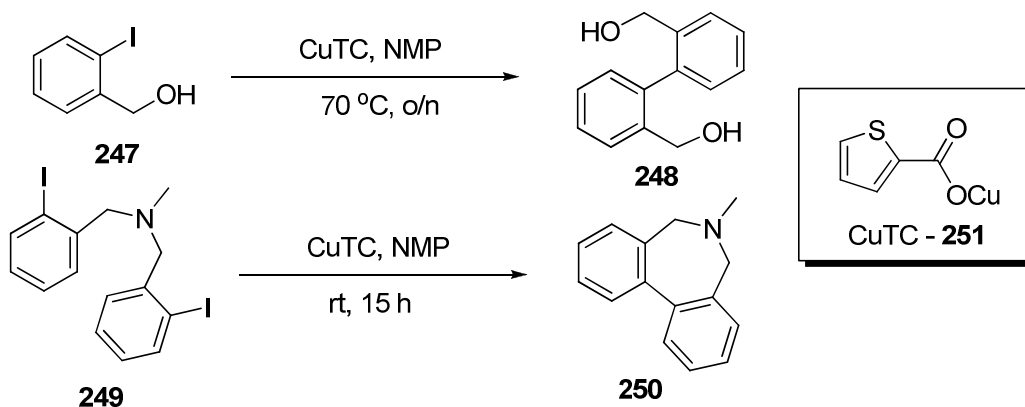
suitable copper reagent that would promote the oxidative coupling of the lithium tetraanion as described in Scheme 55. Also, based on the precedent established by Furstner for the iron-catalyzed cross-coupling of sp^2 hybridized magnesium carbanions,⁷³ and Negishi for the homo-coupling of sp^2 and sp^3 lithium carbanions using stoichiometric palladium, the reported conditions for these couplings were repeated with tetraanion **142** as indicated in Table 17.

Table 17. Results of Oxidative Couplings

entry	coupling reagent (equiv)	solvent added	temperature	results
1	CuI (7)	ether (5 mL)	-78 °C → RT	complex mixture
2	CuBr (7)	ether (5 mL)	-78 °C → RT	complex mixture
3	CuCl ₂ (7) with air	ether (5 mL)	-78 °C → RT	complex mixture
4	CuBr ₂ (7)	ether (5 mL)	-78 °C → RT	complex mixture
5	CuI (7) with air	ether (5 mL)	-78 °C → reflux	complex mixture
6	CuBr ₂ with air	none	-78 °C → reflux	complex mixture
7	Cu(OTf) ₂ (7)	THF (5 mL)	-78 °C → RT	complex mixture
8	FeCl ₃ (7)	THF (5 mL)	-78 °C → RT	complex mixture
9	FeCl ₃ (2% with DCE)	none	-78 °C	SM
10	FeCl ₃ (7)	THF (20 mL)	-78 °C → RT	SM
11	PdCl ₂ (7)	THF (10 mL)	-78 °C → RT	SM
12	PdCl ₂ (6) with PPh ₃	THF (10 mL)	-78 °C → RT	SM
13	FeCl ₃ (7) with TMEDA	THF (10 mL)	-78 °C → RT	complex mixture

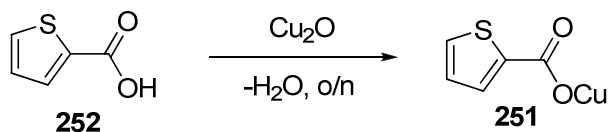
Although none of these reactions were repeated more than three times, the lack of any indication of product formation by ¹H NMR spectroscopy led us to explore the copper system developed by Liebeskind,⁷⁴ who has reported that

copper(I) thiophene-2-carboxylate (CuTC) promoted reductive-Ullmann couplings under mild conditions in *N*-methyl-pyrrolidine (NMP). In Liebskind's work, it was demonstrated that both intramolecular and intermolecular coupling of aryl iodides could be carried out effectively using CuTC (Scheme 56).



Scheme 56. Examples of Reactions Using Copper Thiophene Carboxylate

The synthesis of the CuTC catalyst is straightforward and involves the reaction of thiophene carboxylic acid **252** with copper oxide. (Scheme 57).

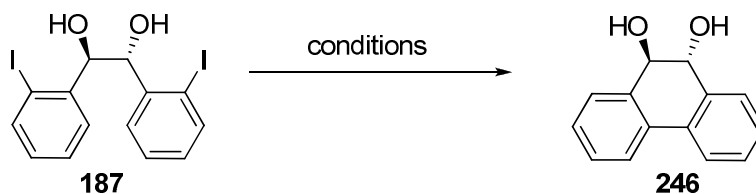


Scheme 57. Synthesis of Copper Thiophene Carboxylate

Starting with the diiodohydrobenzoin **178**, several different conditions were explored in an effort to affect the intramolecular CuTC promoted coupling (Table 19), however, none afforded the desired phenanthrenediol.

Table 18. Synthesis of Diiodohydrobenzoin Derivative **187** with Copper

Thiophene Carboxylate

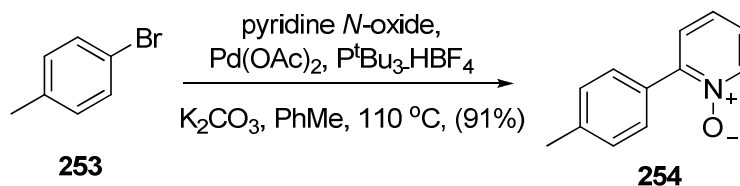


entry	concentration [M]	temp	time	results
1	0.25	rt	3 days	dimerization
2 ^a	0.05	rt	1 day	SM
3	0.05	rt	1 day	complex mixture
4 ^b	0.05	70 °C	1 day	complex mixture

^a Solution of diiodo hydrobenzoin **187** in *N*-methylpyrrolidine was added slowly via syringe pump over several hours. ^b Solution of diiodo hydrobenzoin **187** in *N*-methylpyrrolidine was added slowly via syringe pump over several hours before heating.

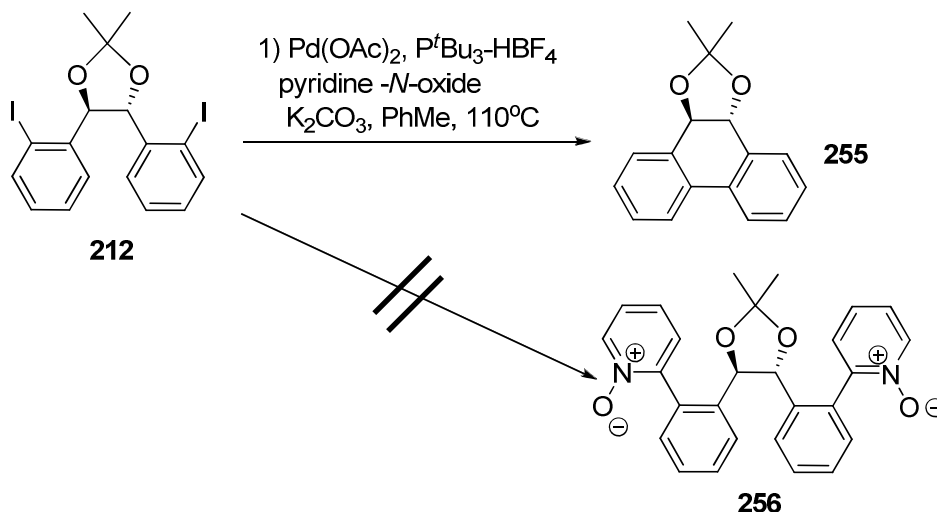
2.1.10 *ortho*-Pyridine Substituted Hydrobenzoin

Based on the disappointing results summarized in Table 18 we set aside the synthesis of the dihydrophenanthrene diol **246** and turned our attention towards the synthesis of the *ortho*-pyridine substituted hydrobenzoin as potential Lewis acid-base catalysts. In this regard, Fagnou⁷⁵ has reported the coupling of aryl halides with pyridine *N*-oxide, which served as an air-stable surrogate for 2-bromopyridines. As shown in Scheme 58, arylbromide **253** undergoes coupling with pyridine *N*-oxide in high yield (91%) to afford the coupled product **254** that was subsequently reduced to afford the 2-pyridyl substituted product (not shown).



Scheme 58. Example of Coupling of Aryl Halide with Pyridine *N*-Oxide

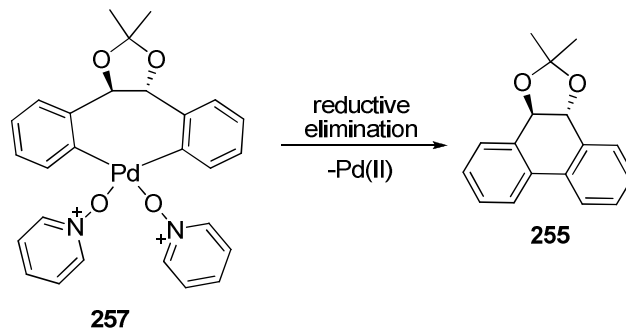
Using the same conditions, we attempted to couple acetone **212** (Scheme 59) with pyridine *N*-oxide to give *bis*-pyridine oxide **256**. Remarkably, while we had failed in our efforts to synthesize the dihydrophenanthrenediols (*vide supra*), the conditions outlined in Scheme 59 led to the formation of the acetone of the dihydrophenanthrenediol product **255** in approximately 35% by crude NMR.



Scheme 59. Serendipitous Reductive Cyclization Using Pyridine *N*-Oxide and Palladium

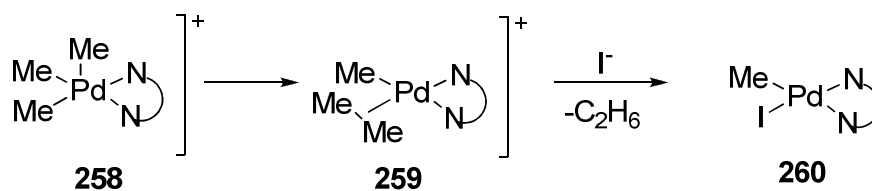
The exact role played by the pyridine *N*-oxide in this process is not clear, however, it can be assumed that it facilitates the formation of a Pd(II) complex that can reductively eliminate to afford the coupled product (Scheme 60).

Analogously, palladium (IV) complexes stabilized by bipyridine ligands have been shown to undergo a C-C coupling with MeI under certain conditions (Scheme 61).⁷⁶ Thus, it appears that the role of the donor ligands is important in this coupling reaction. Indeed, without the addition of pyridine *N*-oxide, the coupled product **255** is not observed and only starting material is recovered. Although the presence of the dihydrophenanthrenediol **255** was observed by crude NMR, purification of this material from other products obtained from the reaction proved difficult – owing to the instability of **255**.



Scheme 60. Reductive Elimination of Pd(II) Species to Give Coupled Product

255



Scheme 61. Reductive Elimination of Ethane via Pd(IV) Species with Bipyridine

Ligand.

2.2 Conclusion

While the benzyl alcohol group has not been exploited as a DMG owing to its reputation as a weak directing group, we have taken advantage of its ability to direct metalations in the synthesis of *ortho*-substituted hydrobenzoin derivatives via the intermediacy of a presumed novel tetraanion. Reaction conditions were optimized using deuterium quench experiments and it was found that heating a solution of hydrobenzoin in a mixture of hexane-ether (2:1) for 16 hours along with six equivalents of *n*-BuLi, followed by treatment with D₂O led to 92% of the expected deuterium incorporation. During the course of these studies it was also found that the second aryl deprotonation is faster than the initial aryl deprotonation. The formation of the tetraanion was found to proceed with no epimerization at the stereogenic centers allowing for the synthesis of a large range of optically pure *ortho*-substituted hydrobenzoin derivatives.

A large variety of electrophiles that engaged in useful reactions with the tetraanion **142** led to efficient syntheses of dimethyl-(**194**), dibromo-(**83**), diiodo-(**178**) hydrobenzoin derivatives as well as the synthesis of heterocyclic rings when the tetraanion was reacted with B(OMe)₃ (**196**), SiMe₂Cl₂ (**197**) and CO₂ (**195**) in moderate yield. Unfortunately, it proved difficult to carry out carbon-carbon bond formation reactions with the tetraanion.

Although the scope of derivatives that could be synthesized directly from tetraanion **142** was limited, lithium-iodine exchange or palladium coupling of the acetone of the diiodohydrobenzoin **178** further enhanced the scope of this methodology. From this intermediate, bridged compounds (i.e., **235**), and di-

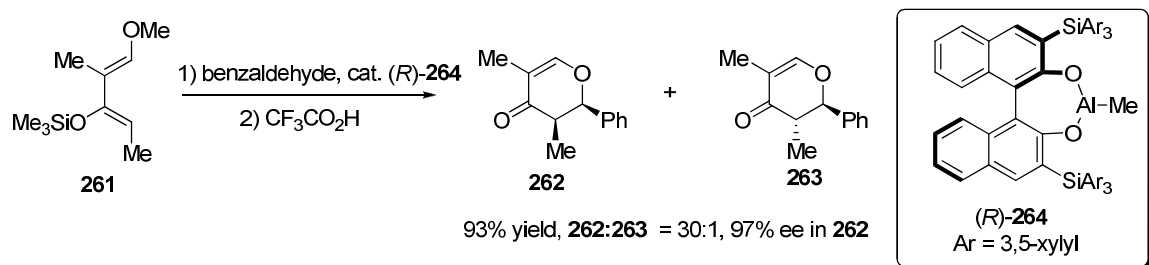
substituted compounds (e.g., **236-237**) could be prepared in excellent yield. In addition, we were able to exploit the *bis*-benzoxaborol **196** in cross-coupling reactions with aryl halides and vinyl triflates, complementing the process described above. Furthermore, oxidation of this *bis*-benzoxaborol gave access to the BINOL-like tetrol **240** in one step in 17% yield which greatly improves upon the literature synthesis of this substance.

3: FUTURE DIRECTION

Further development of the Pd-coupling of diiodo hydrobenzoin derivative **212** with a library of boronic acids should provide access to a wide variety of new chiral ligands/auxiliaries suitable for use in asymmetric synthesis. Similarly, optimization of the palladium-coupling of the *bis*-benzoxaborol derivative **196** with various aryl halides may allow for rapid synthesis of ligand libraries.

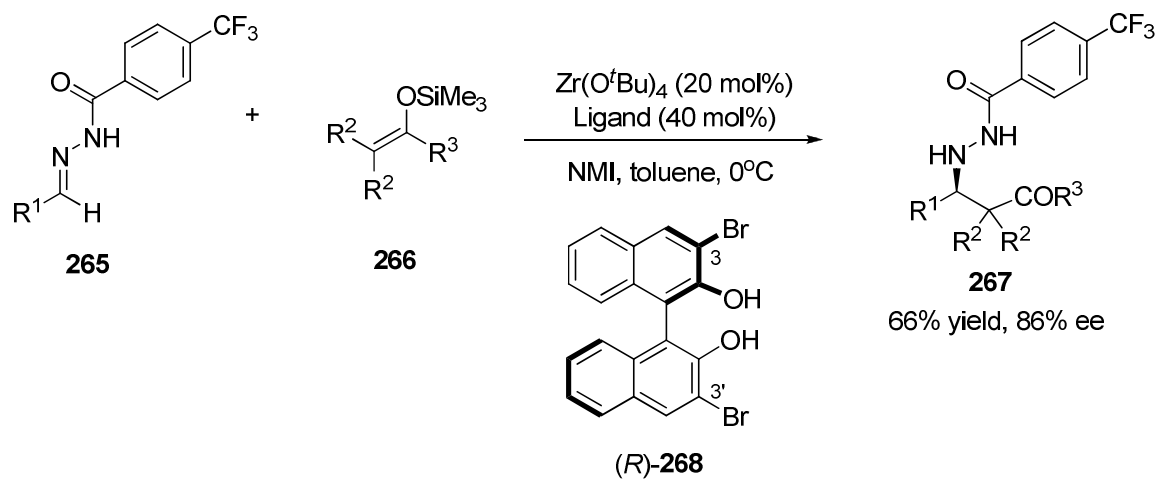
Although the mechanism of this reaction was briefly investigated, further studies regarding the rate of this process and stoichiometry of the transition state should be initiated. Kinetic studies as well as a crystal structure of this novel tetraanion would enhance our understanding of this reaction and possibly allow further optimization of this methodology.

Application of these hydrobenzoin derivatives in catalytic asymmetric synthesis is an obvious and essential goal. An asymmetric hetero-Diels Alder reaction was recently reported using a C_2 -symmetric BINOL catalyst (Scheme 60).⁷⁷ Chiral aluminium complex **264** has been shown to impart good enantioselectivity in these syntheses of dihydropyrones (97% ee) as well as in ene reactions (up to 88% ee) and asymmetric Claisen rearrangements (up to 93% ee). Extension of our *ortho*-functionalized hydrobenzoin derivatives to this reaction may provide a more selective and economical route to this class of molecules.



Scheme 62. Hetero-Diels-Alder Reaction Using *ortho*-Silylated Derivative (*R*)-**264**

3,3'-Substituted BINOLs have also been used to promote the asymmetric addition of silyl enol ethers to imines in asymmetric Mannich reactions (Scheme 63). The addition of silyl enol ether **266** to hydrazone **265** occurred in 66% yield and 86% ee.⁷⁸ Akin to the Diels-Alder reaction described above, a screen of hydrobenzoin derivatives could lead to results that improve upon this enantioselectivity and lead to an efficient and economical route to β -aminocarbonyls. Thus, building on considerable precedent related to the use of 3,3'-substituted BINOL as an asymmetric catalyst, chiral hydrobenzoin derivatives could be screened in these reactions to see if there is a similar increase in enantioselectivity.



Scheme 63. Asymmetric Mannich Reaction using BINOL

4: GENERAL CONCLUSION

Chapter 1 described the need for new auxiliaries and catalysts in asymmetric synthesis, as well as the definition of these terms and classic examples of their use in synthesis. A survey of literature also revealed the synthetic utility of hydrobenzoin as both an auxiliary and catalyst in asymmetric aldol reactions, Diels-Alder reactions and Evans-Tischenko reactions amongst others. We initially set out to synthesize chiral borinic acid **139** in hope of imparting enantioselectivity in a Mukaiyama aldol reaction in water. However, during the course of our investigation, it was discovered that refluxing hydrobenzoin with *n*-BuLi afforded the product **126** from a bidirectional metalation without the need for protecting groups on the diol function. Moreover, this reaction intermediate was found to maintain its optical purity during the course of the reaction.

In Chapter 2 is described our efforts to exploit this new and efficient route to *ortho*-functionalized hydrobenzoin derivatives via the tetraanion **142** in the synthesis of new classes of ligands/catalysts. Optimization of this bidirectional metalation reaction involved reacting the tetraanion with D₂O under various conditions. A 2:1 solvent mixture of hexane-ether, 16 hours of reflux and 6 equivalents of *n*-BuLi provided 92% of the expected deuterium incorporation (Table 6, entry 7) and thus these conditions were used in subsequent studies. Gas evolution and deuterium monitoring studies revealed the rapid deprotonation

of the alcohol functions (20 mins) is followed by a slower deprotonation of the *ortho* protons on the aromatic rings. Surprisingly, deprotonation of the second aromatic ring was discovered to be faster than the initial aromatic deprotonation. Although mechanistic insights into this reaction would require further studies on rate and stoichiometry, we postulated that the “tetraanion” could form a *bis*-indane structure of type **188**, which could equilibrate to a *cis*-decalin like structure of type **189**. Formation of a ring-like structure could explain the increased rate for the second deprotonation as the second aromatic ring may be positioned in closer proximity to an alkyllithium-lithium alkoxide complex. Whether this reaction proceeds via a CIPE mechanism, KEM mechanism, an inductive mechanism or an alternative mechanism remains difficult to ascertain without further investigation.

One of our goals was to exploit this tetraanion as a reactive intermediate for synthetic purposes. As shown in Table 8, in one step from chiral hydrobenzoin, we were able to functionalize both *ortho*-positions directly with CH₃ (**194**), iodine (**178**), bromine (**87**), silicon (**197**), CO₂ (**195**), and boron (**196**) in yields ranging from 33-53%.

Although the C-C bond formation reaction of tetraanion **142** would be valuable, we were not able to exploit this process even after screening a large range of carbon electrophiles. Attempts to improve upon this result by transmetalation with magnesium or zinc also afforded complex mixtures, starting material or reduction products. Due to these disappointing results we focused our attention to further diversifying the range of *ortho*-substituted hydrobenzoin

derivatives using the acetonide of diiodohydrobenzoin **212**. Although less concise than direct functionalization via the tetraanion, we were able to synthesize bridged compounds (e.g., **235**), couple sterically bulky groups (e.g., TMSCl), and synthesize boronic acids via lithium-iodine exchange and palladium coupling in high yield.

The disappointment in our inability to synthesize the boronic acid **139** was somewhat offset by the production of the *bis*-benzoxaborol compound **196**, which proved to be a useful intermediate in couplings with aryl halides (e.g., **239**) or vinyl triflates (e.g., Vivol precursor **134**). In contrast to couplings with the diiodo derivative **212**, couplings with the *bis*-benzoxaborol derivative **196** do not require additional protection steps and this material could be used directly in coupling reactions without the need for purification. Thus, through the ready availability of these aryl halides and boronic acids, the range of *ortho*-substituted hydrobenzoin that can now be accessed is numerous.

We also sought to exploit the tetraanion in the synthesis of azepines **241** or diamine ligands **242**. A large array of Buchwald-Hartwig type coupling conditions failed to provide the desired product even after protection of the diol functionality as an acetonide or dimethyl ether. Consequently, we turned our attention to the synthesis of dihydrophenanthrenediol **246** using palladium, iron and copper (including copper thiophene carboxylate) catalysts to impart either an oxidative coupling via the tetraanion **142** or a reductive coupling via the diiodo compound **212**. All our efforts using these well-documented literature procedures failed to yield **246**. However, during our investigations into the coupling of

pyridine *N*-oxide to the diiodo derivative **212** via palladium coupling, we discovered, serendipitously, that these conditions afforded the desired dihydrophenanthrenediol **246**. Indeed, when the reaction was conducted in the absence of pyridine *N*-oxide, no coupled product was observed.

In conclusion, we have exploited the novel tetraanion **142** to synthesize a broad array of new *ortho*-substituted hydrobenzoin derivatives. Figure 13 summarizes the range of new ligands available using this bidirectional metalation of hydrobenzoin.

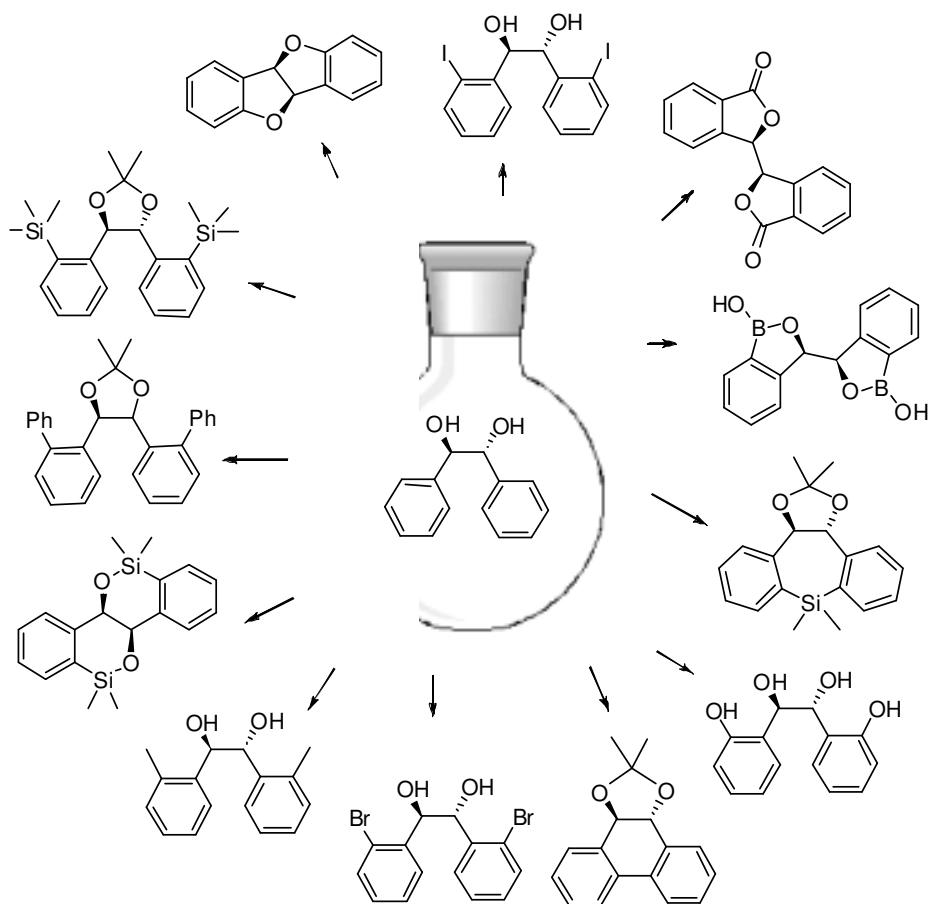


Figure 13. Summary of *ortho*-substituted hydrobenzoin derivatives synthesized.

5: EXPERIMENTAL

5.1 General

All reactions described were performed under an atmosphere of dry argon using oven-dried or flame-dried glassware. THF, Et₂O, and hexanes were used directly from an MBraun Solvent Purifier System (MB-SP Series) or purchased in Dri-solv bottles (EMD). Cold temperatures were maintained by using the following reaction baths: 0 °C, ice water; -78 °C, dry-ice-acetone. Flash chromatography was carried out with 230-400-mesh silica gel (E.Merck, Silica Gel 60) following the technique described by Still.⁷⁹ Concentration of solvents was accomplished with a Buchi rotary evaporator using acetone-dry-ice condenser and removal of trace solvent was accomplished with a Welch vacuum pump.

NMR spectra were recorded using deuteriochloroform (CDCl₃) or deuteriomethanol (CD₃OD) as the solvent. Signal positions are given in parts per million (ppm) from tetramethylsilane (δ 0) and were measured relative to the signal of the solvent (CDCl₃: δ 7.26, ¹H NMR; δ 77.16, ¹³C NMR; CD₃OD: δ 3.31, ¹H NMR; δ 49.0, ¹³C NMR).⁸⁰ Coupling constants (*J* values) are given in Hertz (Hz) and are reported to the nearest 0.1 Hz. ¹H NMR spectral data are tabulated in the order: multiplicity (s, singlet; d, doublet; t, triplet; m, multiplet), number of protons, coupling constant(s). Proton nuclear magnetic resonance (¹H NMR) and carbon nuclear magnetic resonance (¹³C NMR) spectra were recorded on a

Bruker 600 (^1H , 600 MHz; ^{13}C , 150 MHz), Varian Inova 500 (^1H , 500 MHz; ^{13}C , 125 MHz), or Varian Inova 400 (^1H , 400 MHz; ^{13}C , 100 MHz) as indicated.

Infrared (IR) spectra were recorded on MB-series Bomem/Hartman & Braun Fourier transform spectrophotometer with internal calibration as KBr pellets or NaCl plates. Only selected, characteristic absorption data are provided for each compound.

n-BuLi was purchased from Aldrich chemical company, stored at 4 °C, and titrated using menthol in THF containing 2,2'-bipyridyl as an indicator.⁸¹

Mass Spectrometry was recorded by the Simon Fraser University and University of Notre Dame Mass Spectrometry Services Laboratory using either electron impact (EI), electrospray (ESI) or fast atom bombardment (FAB). Optical rotations were measured on a Perkin Elmer Polarimeter 341.

Gas Chromatograph (GC) analysis was performed on a Hewlett Packard model 5890 gas chromatograph, equipped with flame ionization detector and a Cyclosil-B chiral column (30m length, 0.320 mm ID, 0.25 μm film).

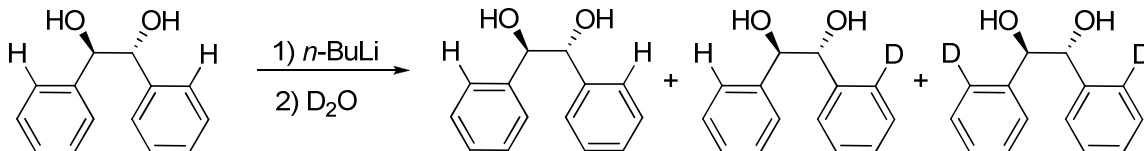
5.2 Verification of Optical Purity (GC) of Tetraanion after treatment with H₂O.

To a stirred suspension of (*R,R*)-(+)-hydrobenzoin (100 mg, 0.470 mmol) in a mixture of hexane (2.5 mL) and ether (1.8 mL) was added *n*-BuLi (1.1 mL, 2.8 mmol, 2.5 M solution in hexanes) (CAUTION: Pyrophoric)⁸² dropwise at room temperature. The yellow reaction mixture was heated at reflux for 16 hours, resulting in the formation of a deep orange/red solution. The reaction mixture was then treated with water and extracted with ethyl acetate (3 x 20 mL). The combined organic layers were dried (MgSO₄), filtered and concentrated, providing a crude residue that was subjected to GC analysis (temperature program: 90 °C held for 1 minute then increased by 5 °C per minute until 200 °C). Only (*R,R*)-hydrobenzoin was detected. Retention time for (*S,S*)-hydrobenzoin = 39.9 min; retention time for (*R,R*)-hydrobenzoin = 40.8 min.

5.3 Butane Gas Evolution Studies

To a stirred suspension of (*R,R*)-(+)-hydrobenzoin (100 mg, 0.470 mmol) in a mixture of hexane (2.5 mL) and ether (1.8 mL) was added *n*-BuLi (1.1 mL, 2.8 mmol, 2.5 M solution in hexanes) (CAUTION: Pyrophoric)⁸² dropwise at room temperature. The yellow reaction mixture was heated at reflux for 16 hours, resulting in the formation of a deep orange/red solution. The evolution of butane during this period was monitored by connecting the reaction vessel *via* a flexible metal canula to a graduated cylinder submersed upside down into a beaker containing water that was calibrated to 25 °C. Measurements were taken by millilitres and converted to mmol of gas evolved.

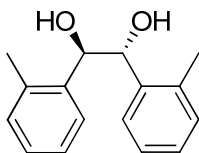
5.4 Procedure for Deuterium Quench



To a stirred suspension of *(R,R)*-(+)-hydrobenzoin (1.0 g, 4.7 mmol) in a mixture of hexane (18 mL) and ether (18 mL) was added *n*-BuLi (11.2 mL, 28.0 mmol, 2.50 M solution in hexanes) (CAUTION: Pyrophoric)⁸² dropwise at room temperature. After the addition was complete, a 0.5 mL aliquot was removed and transferred to a vial containing 1 mL of D_2O (time = 0). The reaction was then heated to reflux and maintained at this temperature while aliquots (0.5 mL) were removed and quenched in D_2O (1 mL) at various time intervals. Throughout the course of the reaction, the color changed as follows: 0.5 hrs: orange; 7 hours: orange-red; 12 hours: deep red. Each aliquot was treated with D_2O and left for 1 hour at room temperature. After this time the aliquot was diluted with ethyl acetate (1 mL), the organic layer was removed, concentrated to dryness and subsequently dissolved in 1 mL of methanol. After 1 hour, the methanol was evaporated and the resulting crude material was analyzed by mass spectrometry and NMR spectroscopy.

5.5 Preparation of Hydrobenzoin Derivatives

5.5.1 Preparation of (1*R*,2*R*)-1,2-di-*o*-tolylethane-1,2-diol (194)²²



To a stirred suspension of (*R,R*)-(+)-hydrobenzoin (100 mg, 0.47 mmol) in a mixture of hexane (2.5 mL) and ether (1.8 mL) was added *n*-BuLi (1.1 mL, 2.80 mmol, 2.5 M solution in hexanes) (CAUTION: Pyrophoric)⁸² dropwise at room temperature. The yellow reaction mixture was heated at reflux for 16 hours resulting in the formation of a deep orange/red solution. After cooling to -78 °C, iodomethane (0.20 mL, 3.26 mmol) was added dropwise and the mixture was stirred for an additional 4 hours while gradually warming to room temperature. The reaction mixture was then treated with water and extracted with ethyl acetate (4 x 20 mL). The combined organic extracts were dried (MgSO₄), filtered and concentrated. Purification of the crude product by flash column chromatography (5:2 hexane:ethyl acetate) afforded the title compound (60 mg, 53%) as a colourless solid.

¹H NMR (600 MHz, CDCl₃) δ: 7.61 (dd, 2H, *J* = 0.9, 7.8 Hz), 7.21 (t, 2H, *J* = 7.8 Hz), 7.12 (dt, 2H, *J* = 1.2, 7.2 Hz), 6.92 (t, 2H, *J* = 7.2 Hz), 4.96 (s, 2H), 3.07 (s, 2H), 1.65 (s, 6H).

¹³C NMR (150 MHz, CDCl₃) δ: 138.1, 135.9, 130.2, 127.7, 127.3, 126.0, 74.7, 18.8

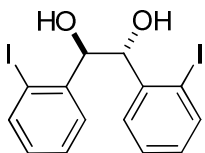
IR: 3405, 3057, 3027, 2925, 1490, 1192, 759 cm^{-1}

Exact mass calcd. for $\text{C}_{16}\text{H}_{18}\text{O}_2\text{Na}$: 265.1204; found: 265.1204

$[\alpha]_{\text{D}}^{25} = +73.0$ ($c = 0.89$, EtOH); literature value for (1*S*,2*S*)-1,2-di-*o*-tolylethane-1,2-diol: $[\alpha]_{\text{D}}^{25} = -64.8$ ($c = 0.83$, EtOH)⁸³

Melting Point: 109 °C (literature value: 108-109 °C)⁸³

5.5.2 Preparation of (1*R*,2*R*)-1,2-bis-(2-iodophenyl)-ethane-1,2-diol (178)²²



To a stirred suspension of (*R,R*)-(+)-hydrobenzoin (1.0 g, 4.7 mmol) in a mixture of hexane (22 mL) and ether (18 mL) was added *n*-BuLi (13.7 mL, 28.0 mmol, 2.04 M solution in hexanes) (CAUTION: Pyrophoric)⁸² dropwise at room temperature. The yellow reaction mixture was heated at reflux for 16 hours resulting in the formation of a deep orange/red solution. After cooling to -78 °C, iodine (8.23 g, 32.7 mmol) was added in one portion and the reaction mixture was warmed to room temperature and allowed to stir for a further 5 hours. This mixture was then treated with a saturated solution of sodium thiosulfate, and extracted with ethyl acetate (4 x 120 mL). The combined organic layers were

dried (MgSO₄), filtered and concentrated. Purification of the crude product by flash column chromatography (7:3 hexane:ethyl acetate) afforded (1*R*,2*R*)-1,2-*bis*-(2-iodophenyl)-ethane-1,2-diol (**178**) (1.13 g, 53%) as a light yellow solid.

¹H NMR (600 MHz, CDCl₃) δ: 7.73 (dt, 2H, *J* = 1.1, 8.0 Hz), 7.69 (dm, 2H, *J* = 7.8), 7.37 (tt, 2H, *J* = 1.2, 7.6 Hz), 6.98 (tm, 2H, *J* = 8.0), 5.15 (s, 2H), 2.95 (m, 2H).

¹³C NMR (150 MHz, CDCl₃) δ: 141.8, 139.7, 130.1, 129.9, 128.5, 99.3, 79.9

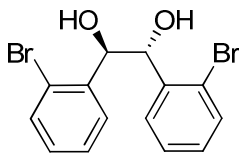
IR: 3391, 3056, 2918, 1560, 1466, 1048, 1009, 756 cm⁻¹

Exact mass calcd. for C₁₄H₁₂O₂I₂Na: 488.8824; found: 488.8829

[α]_D²⁵ = -56.0 (*c* = 0.83, EtOH)

Melting Point: 100 °C

5.5.3 Preparation of (1*R*,2*R*)-1,2-*bis*-(2-bromophenyl)-ethane-1,2-diol (**83**)²²



To a stirred suspension of (*R,R*)-(+)-hydrobenzoin (100 mg, 0.470 mmol) in a mixture of hexane (2.5 mL) and ether (1.8 mL) was added *n*-BuLi (1.10 mL, 2.80 mmol, 2.50 M solution in hexanes) (CAUTION: Pyrophoric)⁸² dropwise at room temperature. The yellow reaction mixture was heated at reflux for 16 hours resulting in the formation of a deep orange/red solution. After cooling to -78 °C, dibromoethane (0.28 mL, 3.22 mmol) was added in one portion and the reaction mixture was warmed to room temperature and left to stir for 5 hours. The reaction mixture was then treated with a saturated solution of sodium thiosulfate (7 mL), and extracted with ethyl acetate (3 x 10 mL). The combined organic layers were dried (MgSO₄), filtered and concentrated. Purification of the crude product by flash column chromatography (7:3 hexane:ethyl acetate) afforded (*1R,2R*)-1,2-*bis*-(2-bromophenyl)-ethane-1,2-diol (**83**) (57 mg, 33%) as a light yellow solid.

¹H NMR (600 MHz, CDCl₃) δ: 7.69 (dd, 2H, *J* = 1.8, 7.8 Hz), 7.45 (dd, 2H, *J* = 1.2, 8.0), 7.34 (dt, 2H, *J* = 1.2, 7.6), 7.14 (tdd, 2H, *J* = 0.6, 7.6, 1.8), 5.32 (dd, 2H, *J* = 1.0, 2.6), 2.78-2.81 (2H, m).

¹³C NMR (150 MHz, CDCl₃) δ: 138.9, 132.9, 129.9, 129.7, 127.6, 123.1

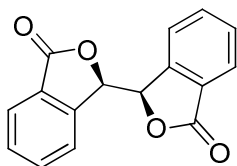
IR: 3423, 3057, 2923, 1563, 1471, 1430, 1049, 1023, 743 cm⁻¹

Anal calcd. for C₁₄H₁₂Br₂O₂: C, 45.20; H, 3.25; found: C, 45.37, H, 3.19

$[\alpha]_{\text{D}}^{25} = -33.0$ ($c = 1.28$, EtOH); literature value: $[\alpha]_{\text{D}}^{25} = -38.3$ ($c = 1.28$, EtOH)⁸⁴

Melting Point: 102-104 °C (literature value: 110-110.5 °C)⁸⁴

5.5.4 Preparation of the *bis*-lactone (**195**)



To a stirred suspension of (*R,R*)-(+)-hydrobenzoin (1.0 g, 4.7 mmol) in a mixture of hexane (20 mL) and ether (18 mL) was added *n*-BuLi (15.8 mL, 28.2 mmol, 1.79 M solution in hexanes) (CAUTION: Pyrophoric)⁸² dropwise at room temperature. The yellow reaction mixture was heated at reflux for 16 hours resulting in the formation of a deep orange/red solution. After cooling to -78 °C, CO₂ gas⁸⁵ (excess) was added, which resulted in the formation of a yellow precipitate, and the reaction mixture was warmed to room temperature. The reaction mixture was then treated with water and concentrated until the organic solvents had been removed. The residual aqueous layer was acidified to pH 2 and the resulting precipitate was filtered and collected. Recrystallization from hot ethanol/water provided **195** as colorless crystals (492 mg, 40%).

¹H NMR (600 MHz, CD₃OD) δ : 7.84 (d, 2H, $J = 7.6$ Hz), 7.80-7.78 (m, 4H), 7.60-7.64 (m, 2H), 6.26 (s, 2H).

^{13}C NMR (150 MHz, CD_3OD) δ : 171.6, 147.5, 135.8, 131.1, 127.4, 126.5, 123.8, 80.6

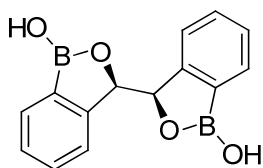
IR (KBr pellet, cm^{-1}): 3062, 2943, 2006, 1770, 1609, 1467, 1350, 1285, 1203, 943, 758

Exact mass calcd. for $\text{C}_{16}\text{H}_{10}\text{O}_4\text{Na}$: 289.0477; found: 289.0476

$[\alpha]_{\text{D}}^{25} = -41.7$ ($c = 0.42$, CHCl_3)

Melting Point: 225 °C

5.5.5 Preparation of *bis*-benzoxaborol (196)



To a stirred suspension of (*R,R*)-(+)-hydrobenzoin (1.0 g, 4.7 mmol) in a mixture of hexane (17 mL) and ether (18 mL) was added *n*-BuLi (19 mL, 28.0 mmol, 1.46 M solution in hexanes) (CAUTION: Pyrophoric)⁸² dropwise at room temperature. The yellow reaction mixture was heated at reflux for 16 hours resulting in the formation of a deep orange/red solution. After cooling to 0 °C, a solution of $\text{B}(\text{OMe})_3$ (3.65 mL, 32.7 mmol) in ether (50 mL) was added dropwise over 90 minutes and the mixture was stirred for an additional 7 hrs at 0 °C. The

reaction mixture was then treated with 1N HCl until the pH reached 2, then neutralized with 2 N NaOH to pH = 7, and extracted with ethyl acetate (4 x 100 mL). The combined organic layers were dried (MgSO₄), filtered and concentrated. Purification of the crude product by flash column chromatography (2.5% MeOH in CH₂Cl₂) afforded the title compound as a pale yellow solid (521 mg, 42%).

¹H NMR (600 MHz, CD₃OD) δ: 7.71 (d, 2H, *J* = 7.4 Hz), 7.51 (dt, 2H, *J* = 1.4, 7.5 Hz), 7.44 (d, 2H, *J* = 7.5 Hz), 7.37 (dt, 2H, *J* = 1.2, 7.4 Hz), 5.23 (s, 2H)⁸⁶

¹³C NMR (150 MHz, CD₃OD) δ: 145.7, 133.7, 132.7, 129.3, 128.4, 74.8

IR (KBr pellet): 3420, 1602, 1371, 1347, 1288, 1239 cm⁻¹

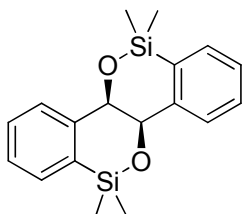
[α]_D²⁵ = +75.8 (*c* = 0.33, CH₃OH)

Melting Point: 63-85 °C

As repeated efforts⁸⁷ to obtain an accurate mass for this compound failed, the following experiment confirmed the presence of two OCH₃ groups and is in agreement with the assigned structure of **196** as a *bis*-benzoxaborol (not a bridged borinic acid). These compounds would be indistinguishable by NMR spectroscopic analysis in CD₃OD. The purified product of this reaction was

dissolved in methanol and heated at reflux for 4 hours in the presence of 4Å molecular sieves. The reaction mixture was then cooled, filtered and concentrated to dryness to provide the corresponding *bis*-methyl ester. The integration of the OCH₃ resonance (δ : 3.81 ppm) in the ¹H NMR spectrum of this substance confirmed the presence of two methoxy groups and supports the formation of a *bis*-benzoxaborol. ¹H NMR (600.3 MHz, CDCl₃) δ : 7.87 (d, 2H, *J* = 6.1 Hz), 7.61-7.43 (m, 6H), 5.32 (s, 2H), 3.81 (s, 6H). In addition, the *bis*-benzoxaborol **196** may possess two five- or six-membered oxaborine rings. On the basis of the observation of two bands at 1346 and 1371 cm⁻¹ in the IR spectrum of this compound, which are consistent with those reported at 1345 cm⁻¹ and 1365 cm⁻¹ for the B-O stretching modes in 3-methyl-1,2-benzoxaborol, we have tentatively assigned the structure for **196** as shown.⁸⁸

5.5.6 Preparation of the *bis*-siloxane (**197**)



To a stirred suspension of (*R,R*)-(+)-hydrobenzoin (200 mg, 0.930 mmol) in a mixture of hexane (4.6 mL) and ether (3.6 mL) was added *n*-BuLi (2.54 mL, 5.58 mmol, 2.20 M solution in hexanes) (CAUTION: Pyrophoric)⁸² dropwise at room temperature. The yellow reaction mixture was heated at reflux for 16 hours resulting in the formation of a deep orange/red solution. After cooling to -78 °C, a solution of dichlorodimethylsilane (0.79 mL, 6.51 mmol) in ether (10 mL) was

added in over 30 minutes and the reaction mixture was then warmed to room temperature and left to stir overnight. The resulting mixture was then treated with a saturated solution of sodium thiosulfate, and extracted with ethyl acetate (4 x 30 mL). The combined organic layers were dried (MgSO₄), filtered and concentrated. Purification of the crude product by flash column chromatography (10:1 hexane:ethyl acetate) afforded the *bis*-siloxane **197** (109 mg, 36%) as a colorless solid.

¹H NMR (600 MHz, CDCl₃) δ: 7.51 (dd, 2H, *J* = 1.3, 7.0 Hz), 7.42 (dt, 2H, *J* = 1.3, 7.5 Hz), 7.39 (dt, 2H, *J* = 1.0, 7.0 Hz), 7.30 (dd, 2H, *J* = 7.5, 1.0 Hz), 4.96 (s, 2H), 0.42 (s, 6H), 0.41 (s, 6H).

¹³C NMR (150 MHz, CD₃OD) δ: 146.6, 134.1, 133.3, 130.2, 128.7, 128.4, 75.1, 1.1, -0.1.

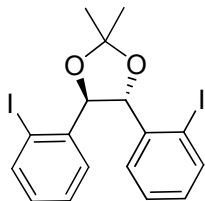
IR (KBr pellet):: 3057, 2951, 1594, 1253, 1137, 1079, 1045, 1026, 869, 828, 789, 743 cm⁻¹.

Exact mass calcd. for C₁₈H₂₂O₂Si₂Na: 326.1158; found: 327.1240

[α]_D²⁵ = +88.3 (c = 0.58, CHCl₃)

Melting Point: 81-83 °C

5.5.7 Preparation of (4*R*, 5*R*)-4,5-bis-(2-iodophenyl)-2,2-dimethyl-1,3-dioxolane (212)



To (1*R*,2*R*)-1,2-bis-(2-iodophenyl)-ethane-1,2-diol **178** (200 mg, 0.430 mmol), in dimethoxypropane (0.53 mL, 4.3 mmol) was added a catalytic amount of concentrated HCl. The reaction mixture was allowed to stir at room temperature for 3 hours after which time a drop of NEt₃ (approximately 10 μ L) was added. Concentration of the mixture provided a yellow oil that was dissolved in dichloromethane and filtered through short plug of neutral alumina. Concentration of the filtrate afforded the title compound as colorless crystals (215 mg, 99%).

¹H NMR (600 MHz, CDCl₃) δ : 7.72 (dd, 2H, J = 1.2, 7.8 Hz), 7.70 (dd, 2H, J = 1.8, 7.8 Hz), 7.43 (dt, 2H, J = 1.2 Hz, 7.8 Hz), 7.00 (dt, 2H, J = 1.8 Hz, 7.8 Hz), 5.04 (s, 2H), 1.75 (s, 6H).

¹³C NMR (150 MHz, CDCl₃) δ : 139.8, 138.4, 130.1, 128.9, 128.7, 109.6, 98.4, 87.9, 27.4.

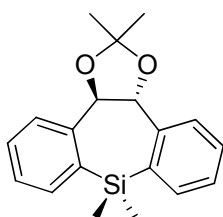
IR (KBr pellet):: 3067, 2982, 2901, 1965, 1566, 1468, 1436, 1372, 1233, 1065, 758 cm⁻¹

Exact mass calcd. for C₁₇H₁₇O₂I₂: 506.9318; found: 506.9314

[α]_D²⁵: -1.50 (*c* = 1.00, CHCl₃)

Melting Point: 126 °C

5.5.8 Preparation of silepine (235)



To a stirred solution of (4*R*,5*R*)-4,5-*bis*-(2-iodophenyl)-2,2-dimethyl-1,3-dioxolane **212** (150 mg, 0.300 mmol) in ether (6 mL) at -78 °C was added *n*-BuLi (0.26 mL, 0.63 mmol, 2.5 M in hexanes) dropwise. The resulting slightly yellow solution was allowed to stir for 10 minutes and then dichlorodimethylsilane (44 μ L, 0.36 mmol) was added dropwise. After 3 hours at -78 °C the reaction mixture was treated with a saturated solution of NH₄Cl and extracted with ether (3 x 15 mL). The combined organic layers were washed with brine, dried (MgSO₄), and concentrated. Purification of the crude product by flash column chromatography (20:1 hexane: ethyl acetate) afforded **235** as a colorless oil (57 mg, 61%).

¹H NMR (500 MHz, CDCl₃) δ : 7.76 (d, 2H, *J* = 7.5 Hz), 7.65 (d, 2H, *J* = 7.5 Hz), 7.46 (t, 2H, *J* = 7.5 Hz), 7.35 (t, 2H, *J* = 7.5 Hz), 5.22 (s, 2H), 1.61 (s, 6H), 0.53 (s, 6H)

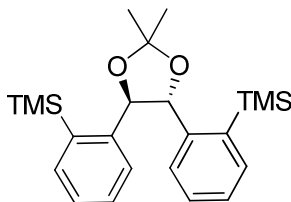
^{13}C NMR (125 MHz, CDCl_3) δ : 146.9, 134.4, 134.2, 129.6, 126.7, 123.9, 109.7, 83.1, 26.8, 0.5

IR (NaCl plates): 3056, 2986, 1692, 1410, 1249, 814, 761.

Exact mass calcd. for $\text{C}_{19}\text{H}_{23}\text{O}_2\text{Si}$: 311.1467; found: 311.1451

$[\alpha]_{\text{D}}^{25} = +99.0$ ($c = 0.30$, CHCl_3)

5.5.9 Preparation of (4*R*,5*R*)-4,5-bis-(2-trimethylsilylphenyl)-2,2-dimethyl-1,3-dioxolane (**236**)²²



To a stirred solution of (4*R*,5*R*)-4,5-bis-(2-iodophenyl)-2,2-dimethyl-1,3-dioxolane **212** (150 mg, 0.30 mmol) in ether (3 mL) at -78 °C was added *n*-BuLi (0.28 mL, 0.63 mmol, 2.25 M solution in hexanes) dropwise. After the reaction mixture had stirred for 15 minutes at -78 °C, chlorotrimethylsilane (95 μL , 0.75 mmol) was added and the resulting mixture was allowed to warm to room temperature overnight. The reaction mixture was then treated with water and the aqueous layer was removed and extracted with ethyl acetate (3 x 20 mL). The combined organic layers were dried (MgSO_4), filtered and concentrated.

Purification of the crude product by flash column chromatography (20:1 hexane:ethyl acetate) afforded the title compound as a white solid (97 mg, 82%).

^1H NMR (600 MHz, CDCl_3) δ : 7.69 (dd, 2H, $J = 1.2, 8.4$ Hz), 7.45-7.41 (m, 4H), 7.26 (dt, 2H, $J = 1.2, 7.8$ Hz), 5.29 (s, 2H), 1.69 (s, 6H), 0.06 (s, 18H)

^{13}C NMR (150 MHz, CDCl_3) δ : 141.9, 140.3, 134.9, 129.6, 128.3, 127.9, 109.2, 84.2, 27.8, 0.7

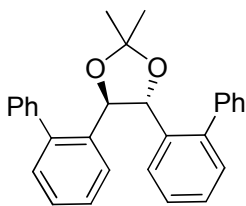
IR (KBr pellet):: 3058, 2979, 1591, 1377, 1251, 1234, 766, 754 cm^{-1}

Exact mass calcd. for $\text{C}_{23}\text{H}_{34}\text{O}_2\text{Si}_2\text{Na}$: 421.1995; found: 421.2009

$[\alpha]_{\text{D}}^{25} = +51.1$ ($c = 1.32$, CHCl_3); literature value: $[\alpha]_{\text{D}}^{25} = +44.73$ ($c = 1.24$, CHCl_3)²²

Melting Point: 81 °C

5.5.10 Preparation of 4,5-bis-biphenyl-2-yl-2,2-dimethyl-[1,3]-dioxolane (237)^{89,90}



To a stirred suspension of Pd(PPh₃)₄ (12 mg, 0.01 mmol) in dimethoxyethane (1.6 mL) was added (*4R,5R*)-4,5-*bis*-(2-iodophenyl)-2,2-dimethyl-1,3-dioxolane **212** (80 mg, 0.16 mmol). The reaction mixture was stirred for 10 minutes, then a solution of phenyl boronic acid in ethanol (58 mg, 0.47 mmol dissolved in minimal ethanol) and a solution of Na₂CO₃ (0.32 mL, 0.64 mmol, 2M solution in deionized water) were added sequentially. The resulting mixture was heated at reflux overnight and then cooled to room temperature, filtered through celite and washed with diethyl ether. The filtrate was concentrated to afford a yellow residue that was diluted with diethyl ether and washed with brine. The organic layer was dried (MgSO₄), filtered and concentrated to afford a white powder. Purification of the crude product by flash column chromatography (basic alumina, 9:1 hexane:ether) afforded the title compound as a white powder (65 mg, 100%).

¹H NMR (600 MHz, CDCl₃) δ: 7.31-7.27 (m, 4H), 7.23 (dt, 2H, *J* = 1.4, 7.5 Hz), 7.20 (tt, 2H, *J* = 1.2, 7.4Hz), 7.09 (br m, 6H), 6.58 (br s, 4H), 4.91 (s, 2H), 1.51 (s, 6H)

¹³C NMR (150 MHz, CDCl₃) δ: 142.6, 140.3, 133.1, 129.9, 129.1, 128.0, 127.8, 127.7, 127.5, 126.6, 108.8, 81.7, 27.4

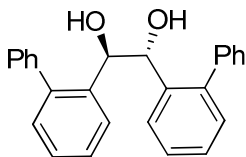
IR (KBr pellet):: 3058, 2924, 1480, 1378, 1370, 1234, 1048, 762, 698 cm⁻¹

Exact mass calcd. for $C_{29}H_{26}O_2Na$: 429.1830; found: 429.1824

$[\alpha]_D^{25} = +78.6$ ($c = 0.35$, $CHCl_3$)

Melting Point: 122 °C

5.5.11 Preparation of (1*R*,2*R*)-1,2-di(biphenyl-2-yl)ethane-1,2-diol (239)²²



To a solution of iodobenzene (140 μ L, 1.26 mmol) in dimethoxyethane (2 mL) was added the *bis*-benzoxaborol acid **196** (50mg, 0.21 mmol) dissolved in a minimal amount of ethanol (0.3 mL), followed by a solution of Na_2CO_3 (0.84 mL, 1.7 mmol, 2.0 M solution in deionized water). $Pd(PPh_3)_4$ (56 mg, 0.12 mmol) was then added and the reaction was heated at reflux overnight. The reaction mixture was then cooled to room temperature and filtered through celite. The filtrate was concentrated and the residue was diluted in ether and washed with brine, dried ($MgSO_4$), filtered and concentrated. Purification of the crude product by flash column chromatography (7:3 hexane:ethyl acetate) afforded the title compound as a pale yellow solid (39 mg, 51%).

1H NMR (600 MHz, $CDCl_3$) δ : 7.30 (tt, 2H, $J = 1.3, 7.3$ Hz), 7.28-7.24 (m, 4H), 7.19, (dt, 2H, $J = 1.4, 7.3$), 7.07 (dt, 2H, $J = 1.3, 7.6$ Hz), 7.03 (dd, 2H, $J = 1.4,$

8.0 Hz), 6.99, (dd, 2H, $J = 1.2, 7.6$ Hz), 6.76, (br s, 4H), 4.93 (s, 2H), 2.70 (t, 2H, $J = 1.4$ Hz)

^{13}C NMR (150.0 MHz, CDCl_3) δ : 142.12, 140.75, 136.79, 129.84, 129.36, 128.09, 127.87, 127.56, 127.53, 126.88, 74.60

IR: 3347, 3073, 2939, 1594, 1479, 1384, 1191, 1048, 997, 762, 745, 708 cm^{-1}

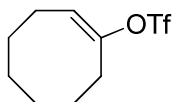
Exact mass calcd. for $\text{C}_{26}\text{H}_{22}\text{O}_2\text{Na}$: 389.1517; found: 389.1515

$[\alpha]_{\text{D}}^{25} = +91.7$ ($c = 0.35$, CHCl_3); literature value: $[\alpha]_{\text{D}}^{25} = +88.68$ ($c = 0.98$, CHCl_3)²²

Melting Point: 148 °C

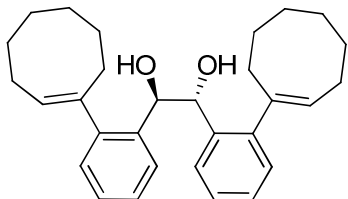
5.5.12 Preparation of (1*R*,2*R*)-1,2-bis(2-(*E*)-cyclooctenylphenyl)ethane-1,2-diol – Vivol precursor (134)

5.5.12.1 Preparation of (*E*)-cyclooctenyl trifluoromethanesulfonate



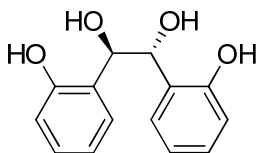
The title compound was prepared by the procedure described by Stang and Treptow.⁹¹ Purification by flash column chromatography (30:1 hexane:ether) afforded the title compound with identical spectral properties as that of literature.⁹²

5.5.12.2 Preparation of (1*R*,2*R*)-1,2-bis(2-(*E*-cyclooctenyl)phenyl)ethane-1,2-diol (134)



To a solution of (*E*)-cyclooctenyl trifluoromethanesulfonate (150 mg, 0.580 mmol) in dimethoxyethane (1.5 mL) was added Pd(dppf)Cl₂ (11 mg, 10% mol equiv). After stirring for 10 minutes, *bis*-benzoxaborol **196** (35 mg, 0.13 mmol) dissolved in a minimal amount of ethanol (0.3 mL) was added followed by a solution of Na₂CO₃ (0.3 mL, 0.60 mmol, 2 M solution in deionized water). After refluxing for 2 days, the reaction mixture was cooled to room temperature and filtered through celite. The filtrate was concentrated and the residue was diluted in ether and washed with brine, dried (MgSO₄), filtered and concentrated. Purification of the crude product by flash column chromatography (20:1 → 7:3 hexane:ethyl acetate) afforded the title compound with identical spectral properties as that of literature (12 mg, 21%).²²

5.5.13 Preparation of (1*R*,2*R*)-1,2-bis(2-hydroxyphenyl)ethane-1,2-diol (240)⁹³⁻⁹⁴



To a suspension of the *bis*-benzoxaborol **196** (60 mg, 0.23 mmol) in water (5 mL) was added H₂O₂ (0.32 mL, 4.0 mmol, 30% solution in water) and 5N NaOH (1.2 mL, 6.0 mmol). After 15 minutes at room temperature, the resulting

yellow solution was extracted with ether (3 x 15 mL) and dichloromethane (4 x 20 mL) and the combined organic layers were dried (MgSO₄), filtered and concentrated. Purification of the crude product by flash column chromatography (7:3 hexane:ethyl acetate) afforded the title compound as a white solid (17 mg, 30%).

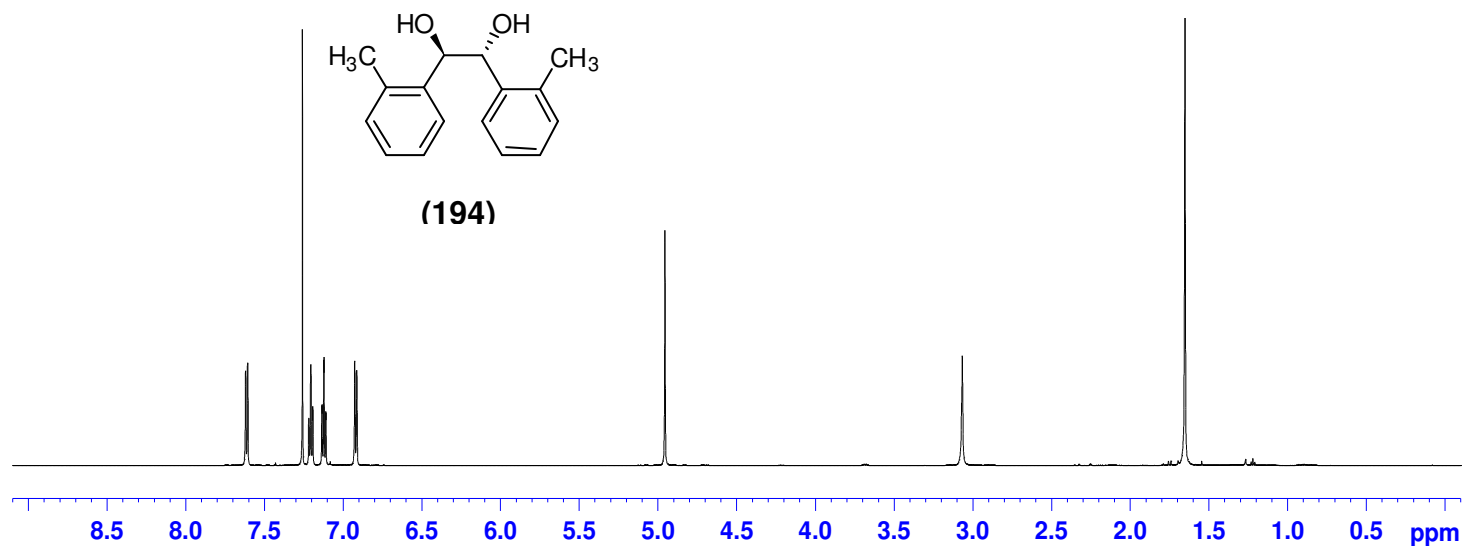
¹H NMR (600.3 MHz, CDCl₃) δ: 7.64 (s, 2H), 7.14 (dt, 2H, *J* = 1.8, 8.4 Hz), 6.87 (dd, 2H, *J* = 1.2, 8.4 Hz), 6.62 (dt, 2H, *J* = 1.2, 7.2 Hz), 6.46 (dd, 2H, *J* = 1.2, 7.2 Hz), 5.03 (s, 2H), 3.59 (s, 2H).

¹³C NMR (151.0 MHz, CDCl₃) δ: 155.5, 129.9, 129.4, 122.6, 120.1, 117.3, 73.6.

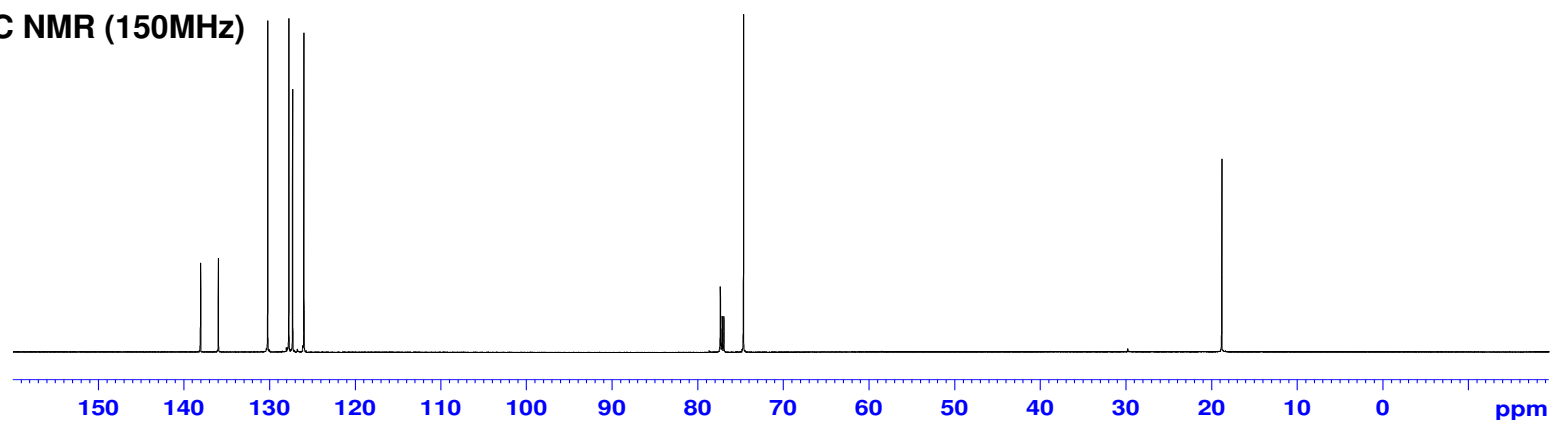
$[\alpha]_D^{25} = +97.9$ (c = 0.58, CHCl₃)

5.6 Selected ^1H and ^{13}C NMR Spectra

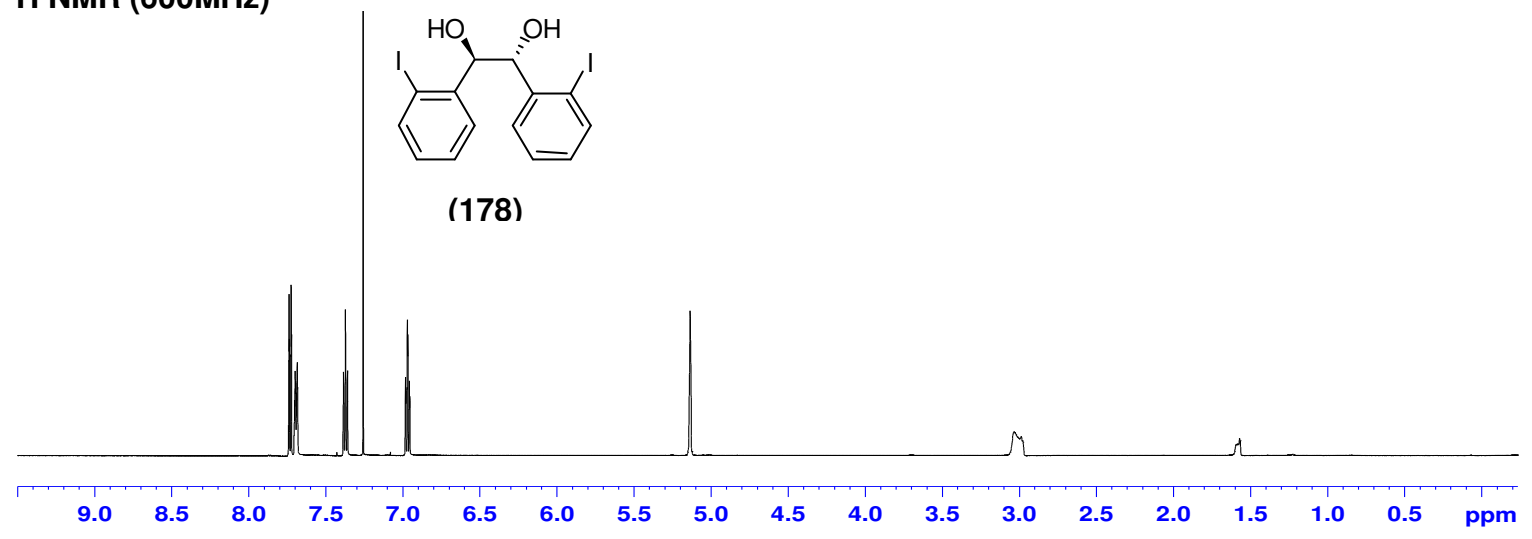
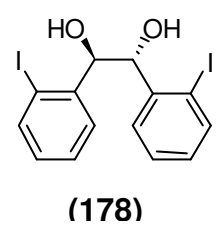
^1H NMR (600MHz)



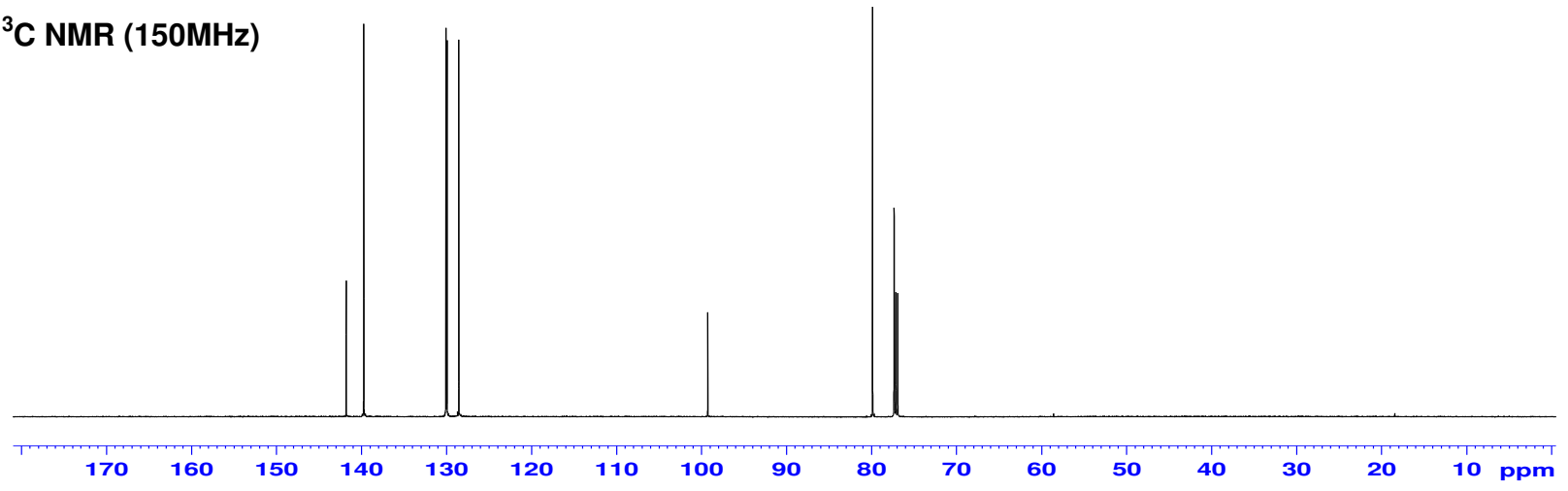
^{13}C NMR (150MHz)



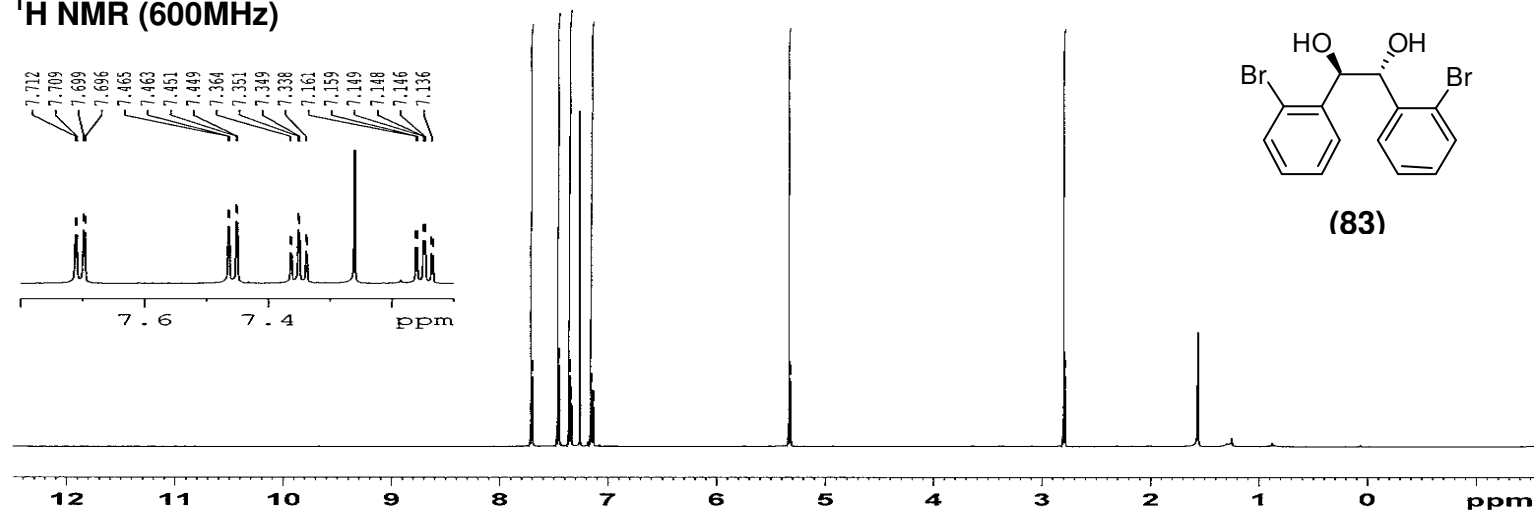
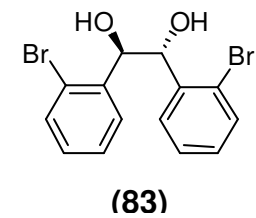
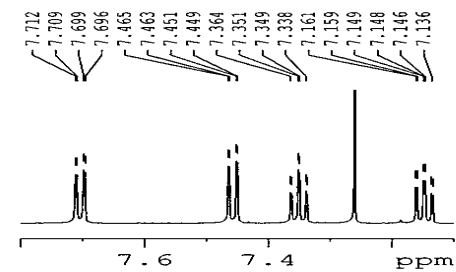
¹H NMR (600MHz)



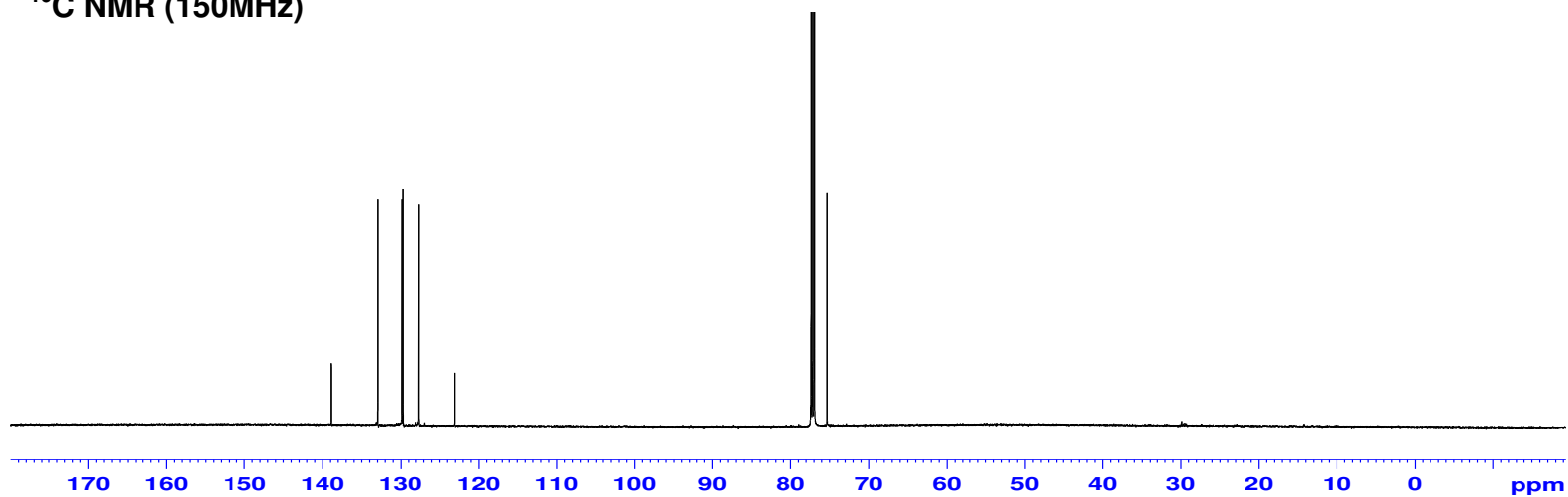
¹³C NMR (150MHz)



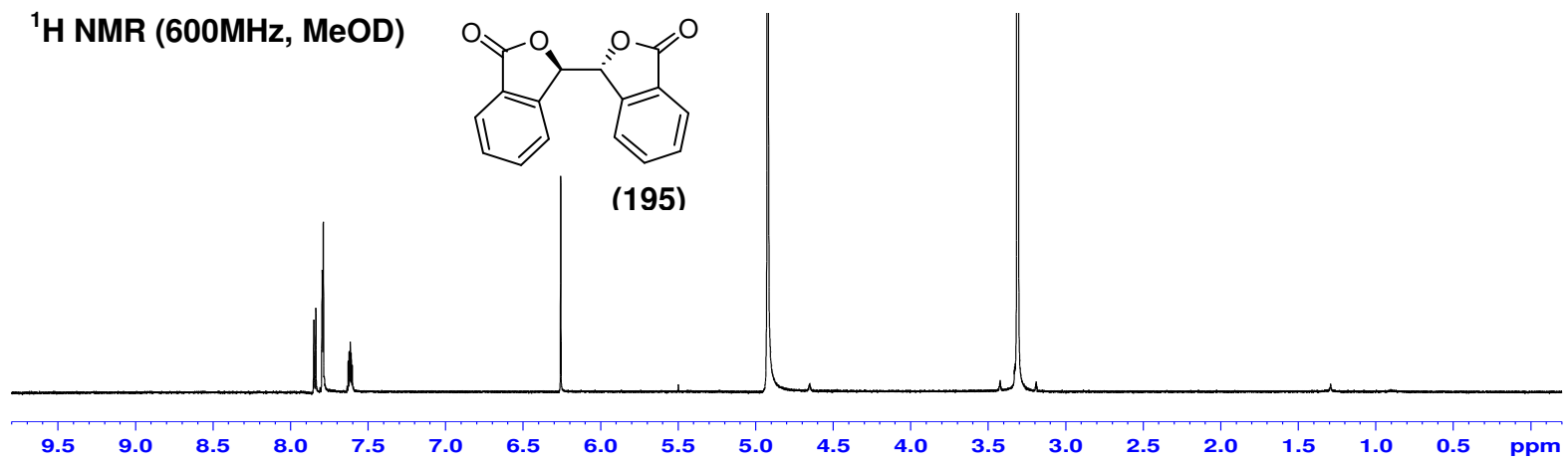
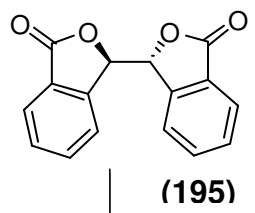
¹H NMR (600MHz)



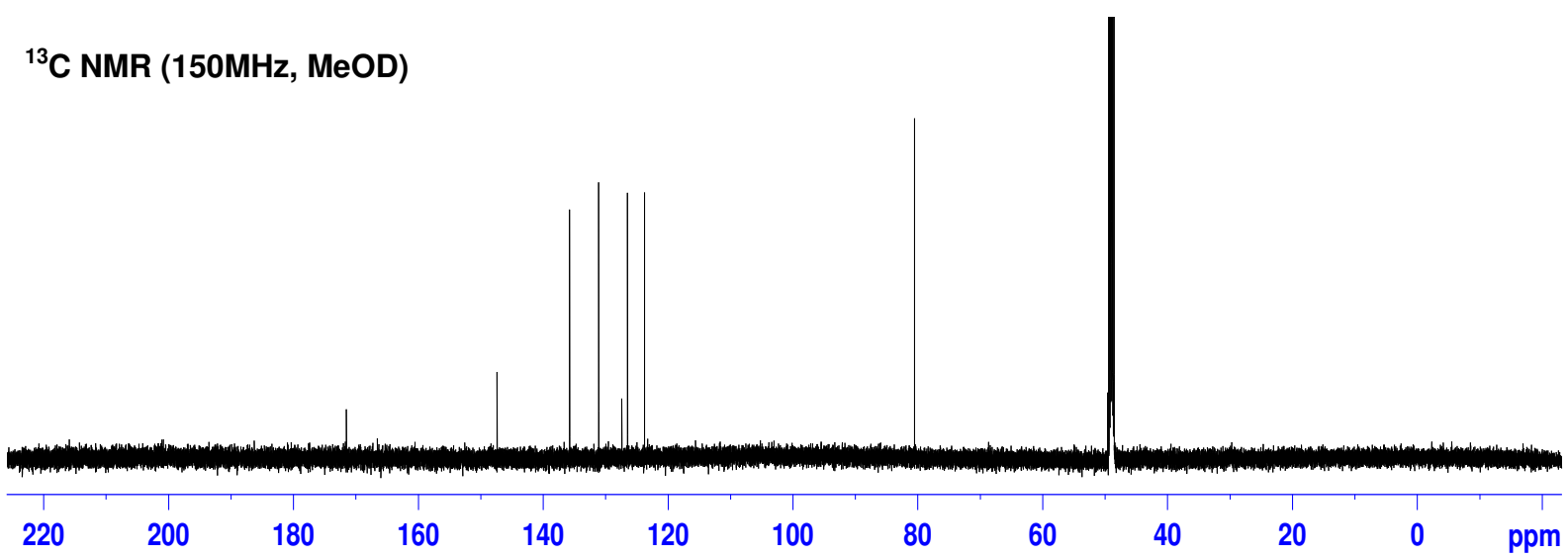
¹³C NMR (150MHz)



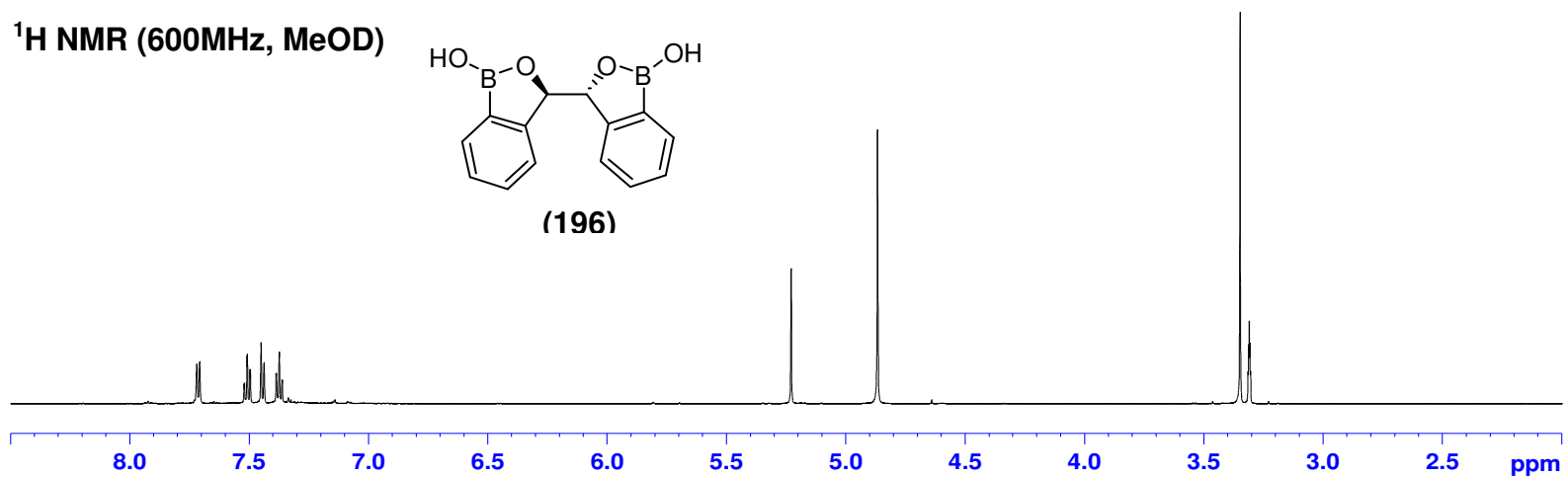
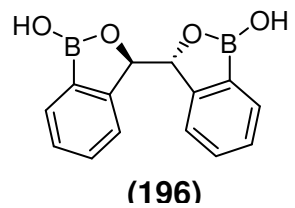
¹H NMR (600MHz, MeOD)



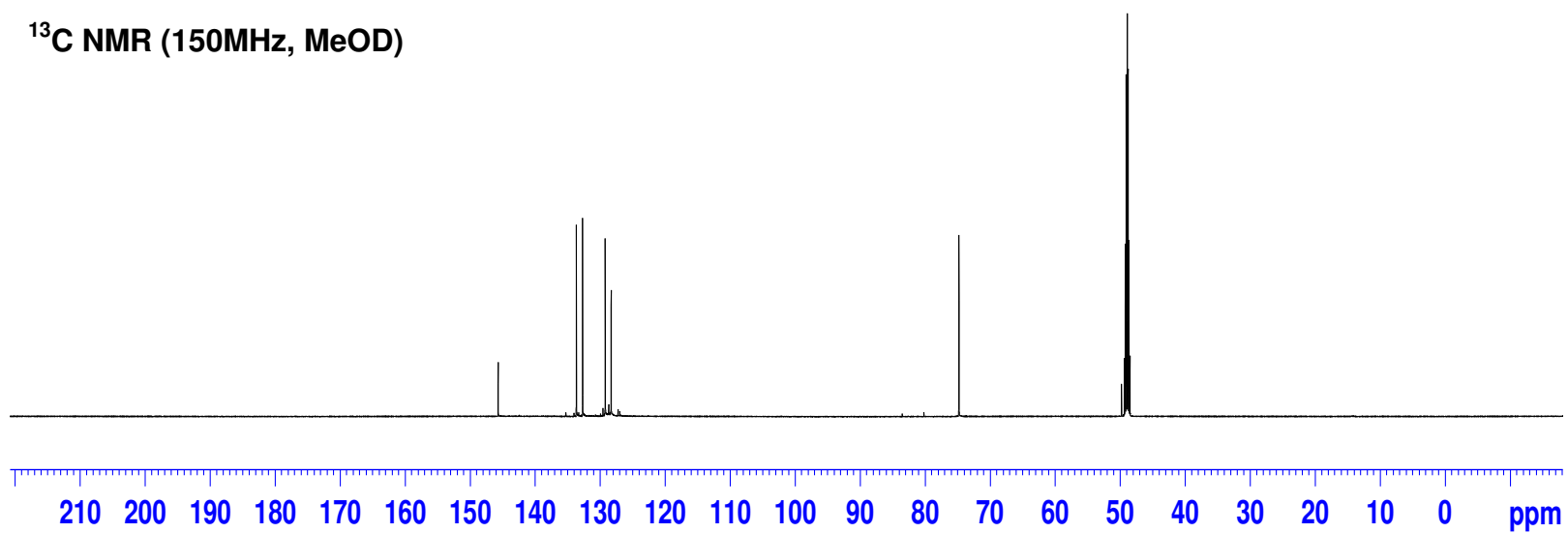
¹³C NMR (150MHz, MeOD)



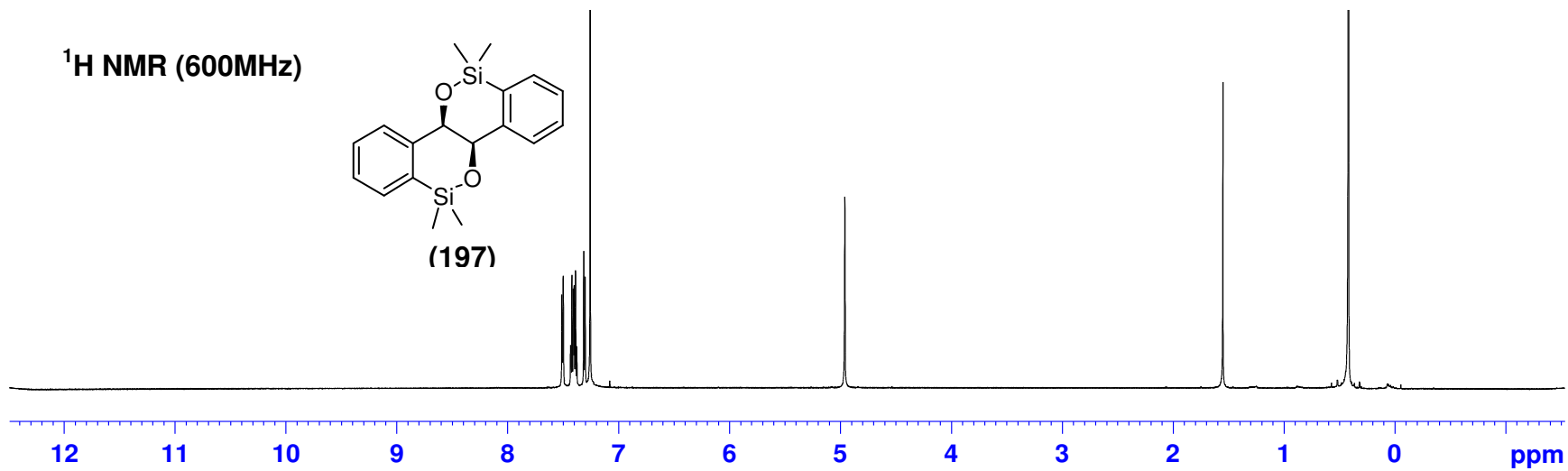
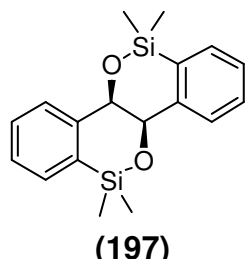
¹H NMR (600MHz, MeOD)



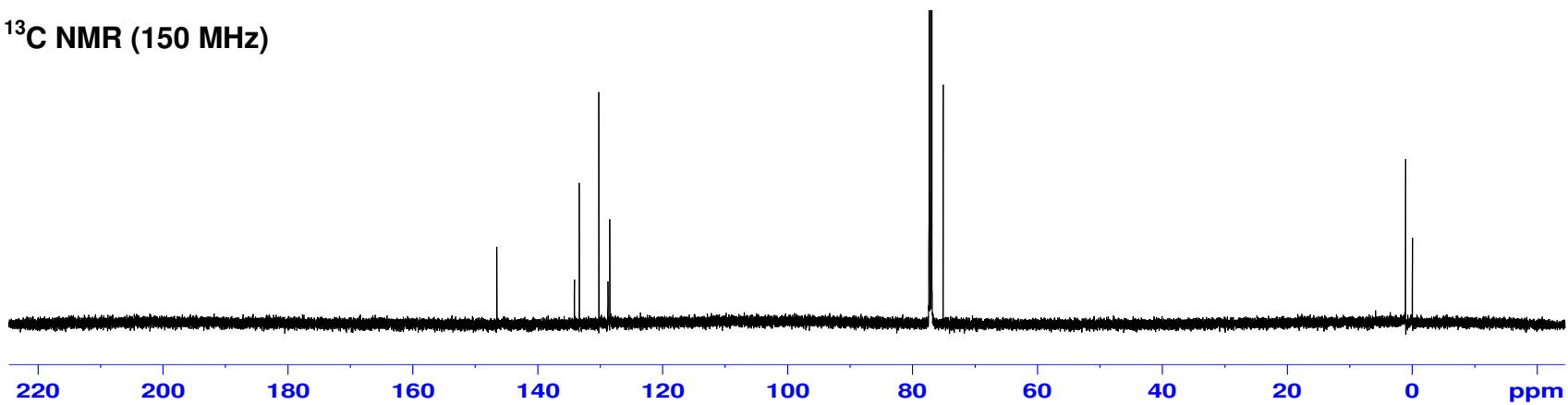
¹³C NMR (150MHz, MeOD)



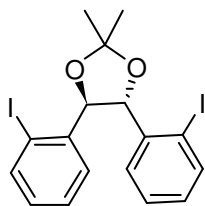
¹H NMR (600MHz)



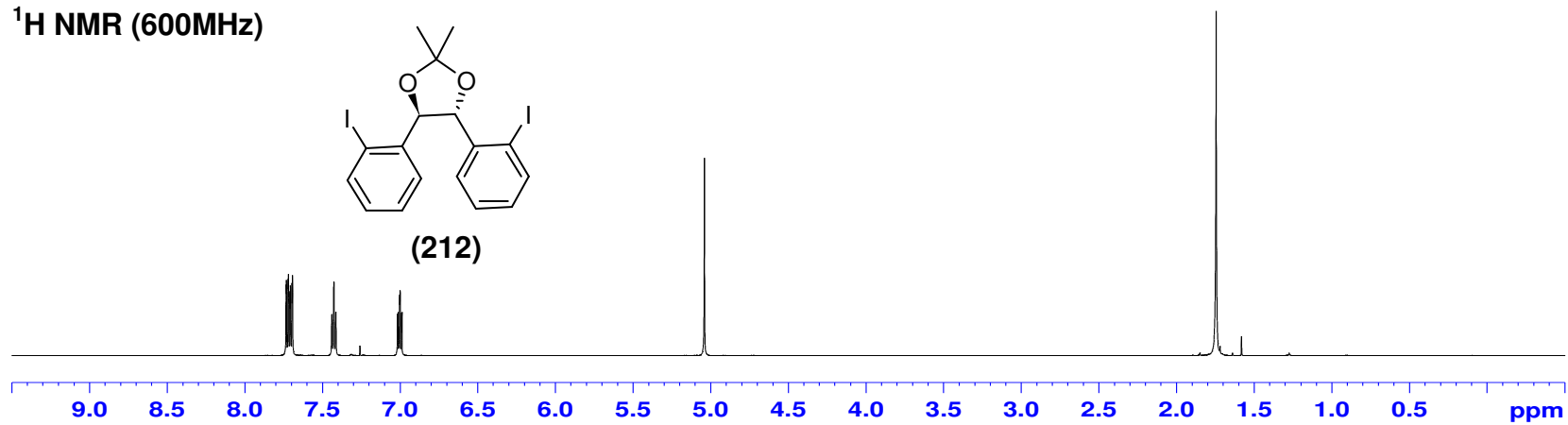
¹³C NMR (150 MHz)



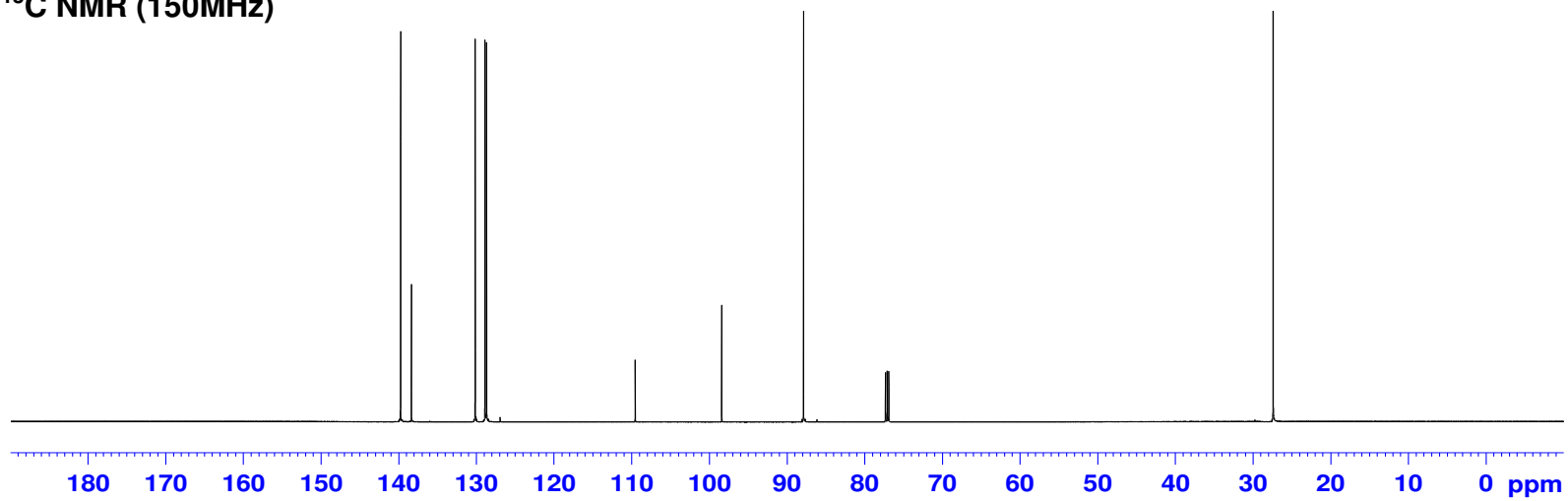
¹H NMR (600MHz)



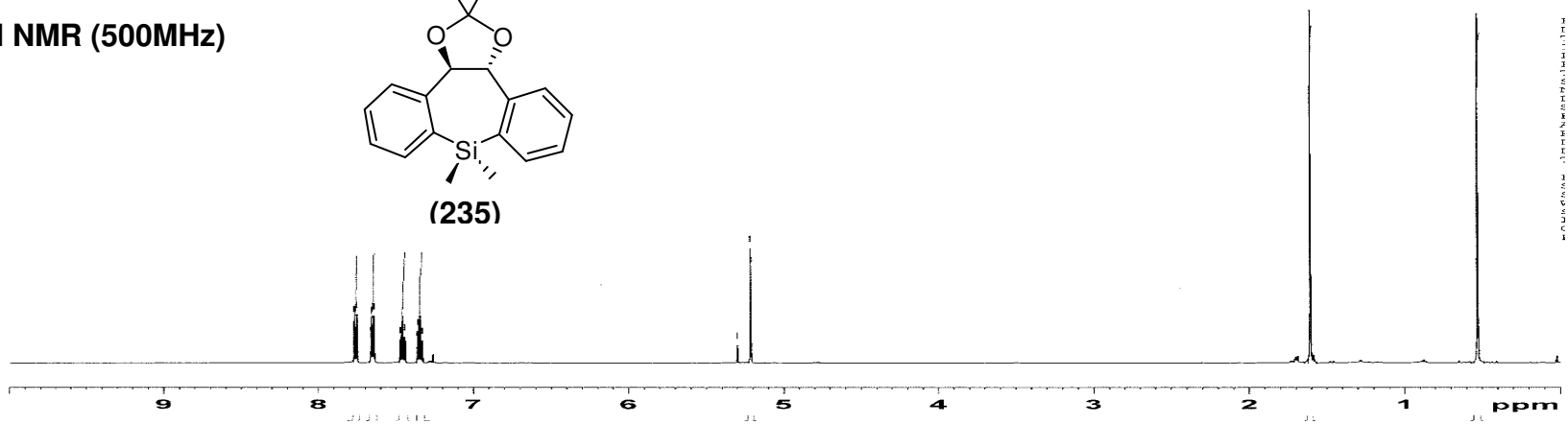
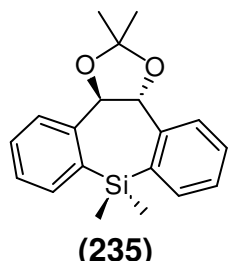
(212)



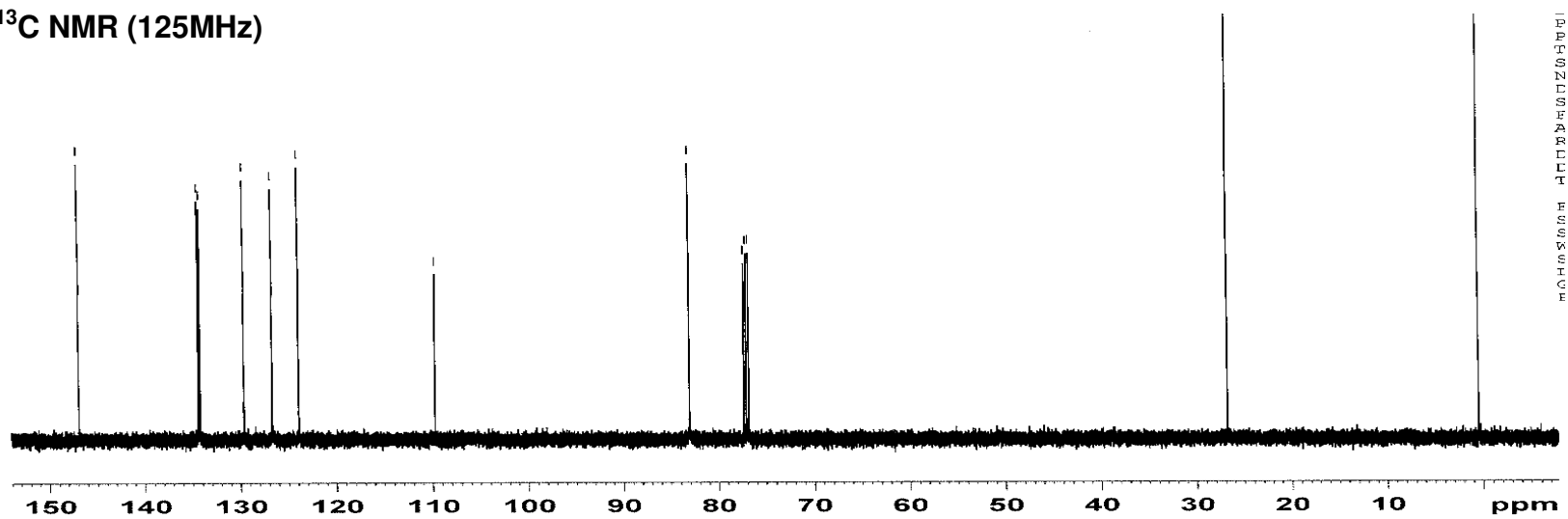
¹³C NMR (150MHz)



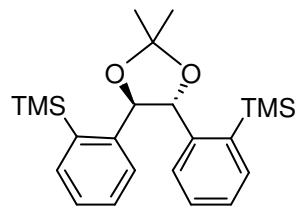
¹H NMR (500MHz)



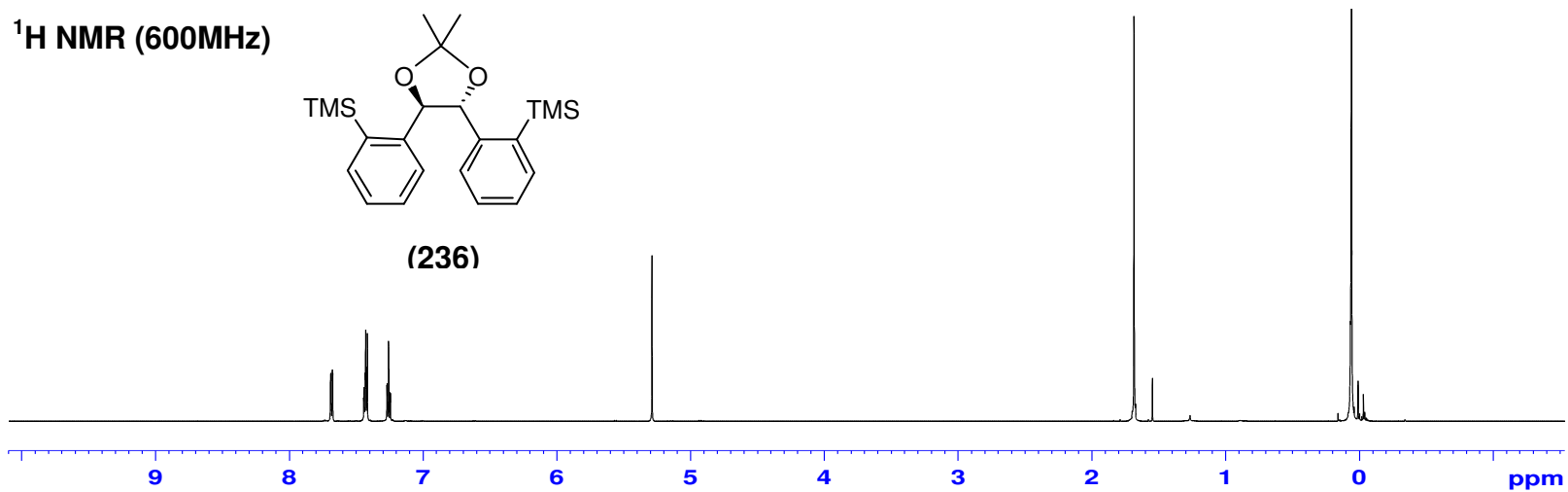
¹³C NMR (125MHz)



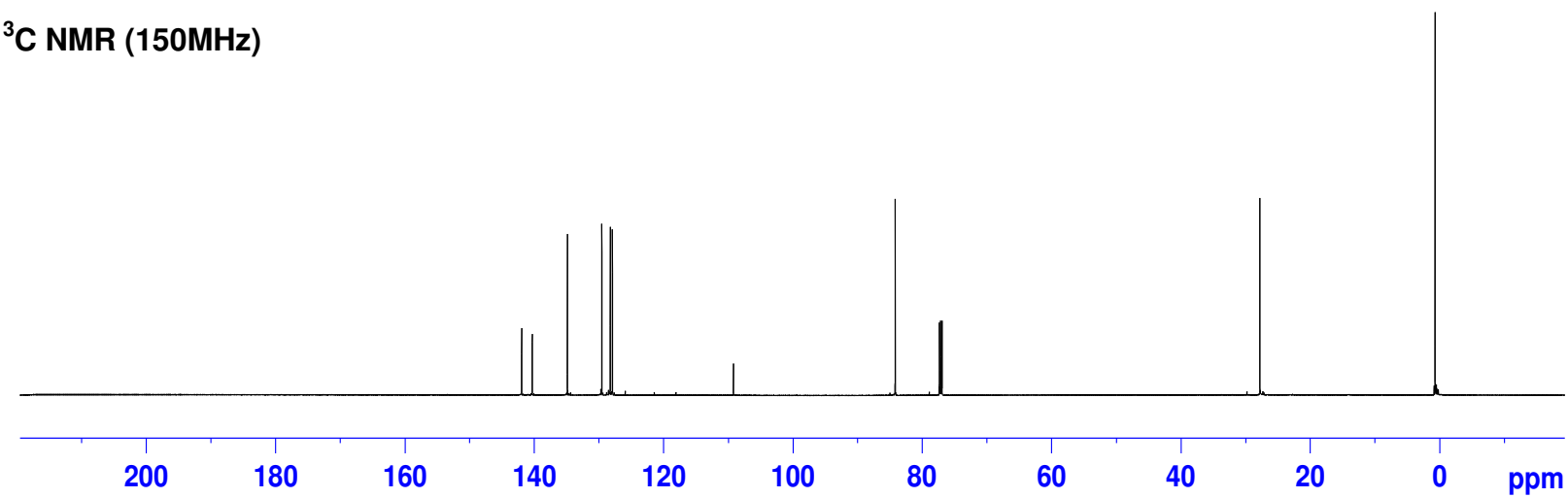
¹H NMR (600MHz)



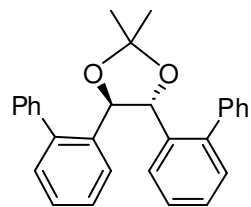
(236)



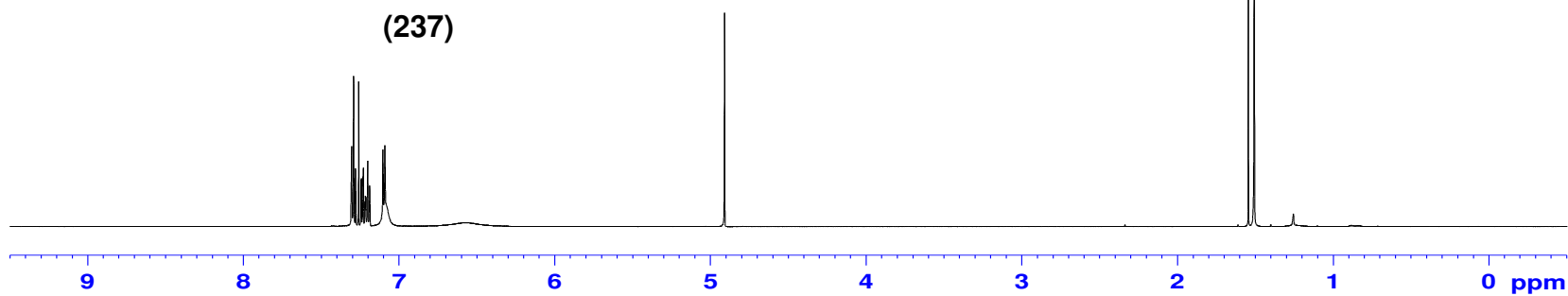
¹³C NMR (150MHz)



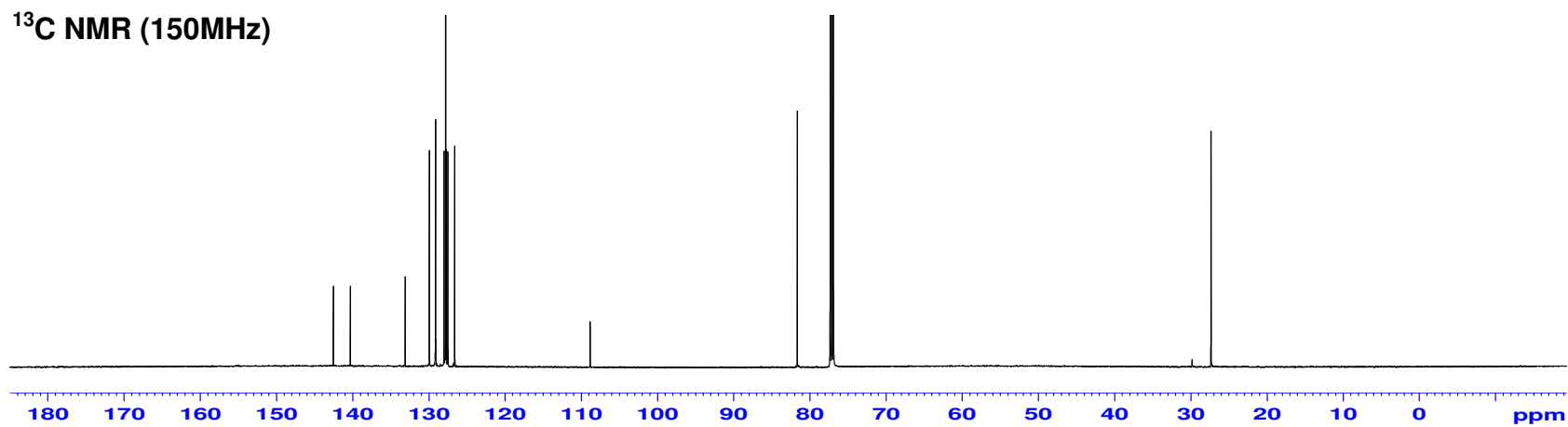
¹H NMR (600MHz)



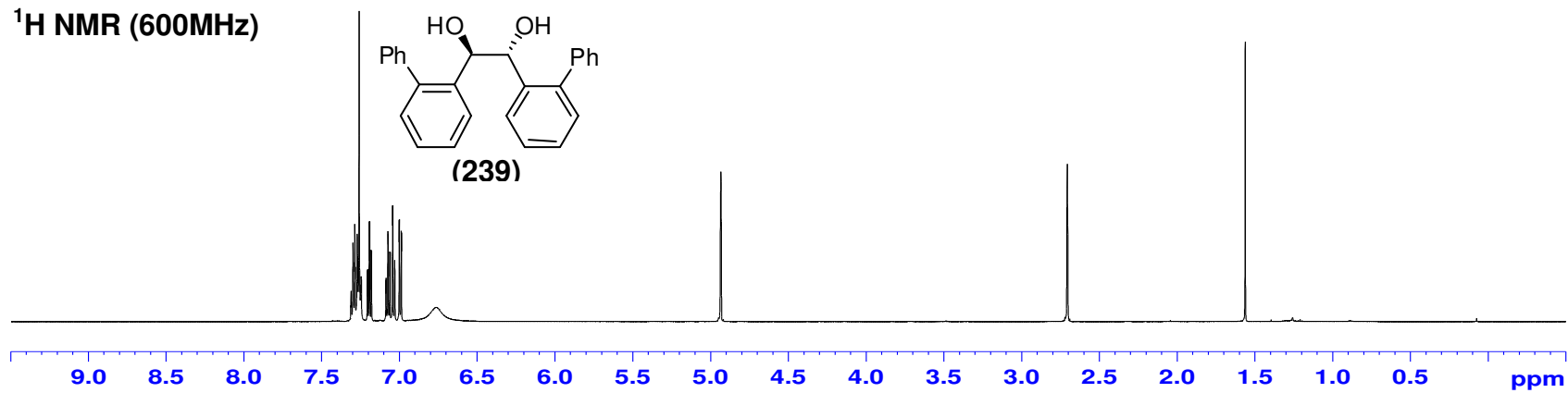
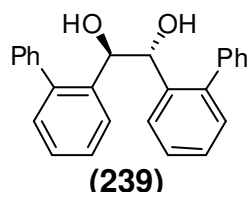
(237)



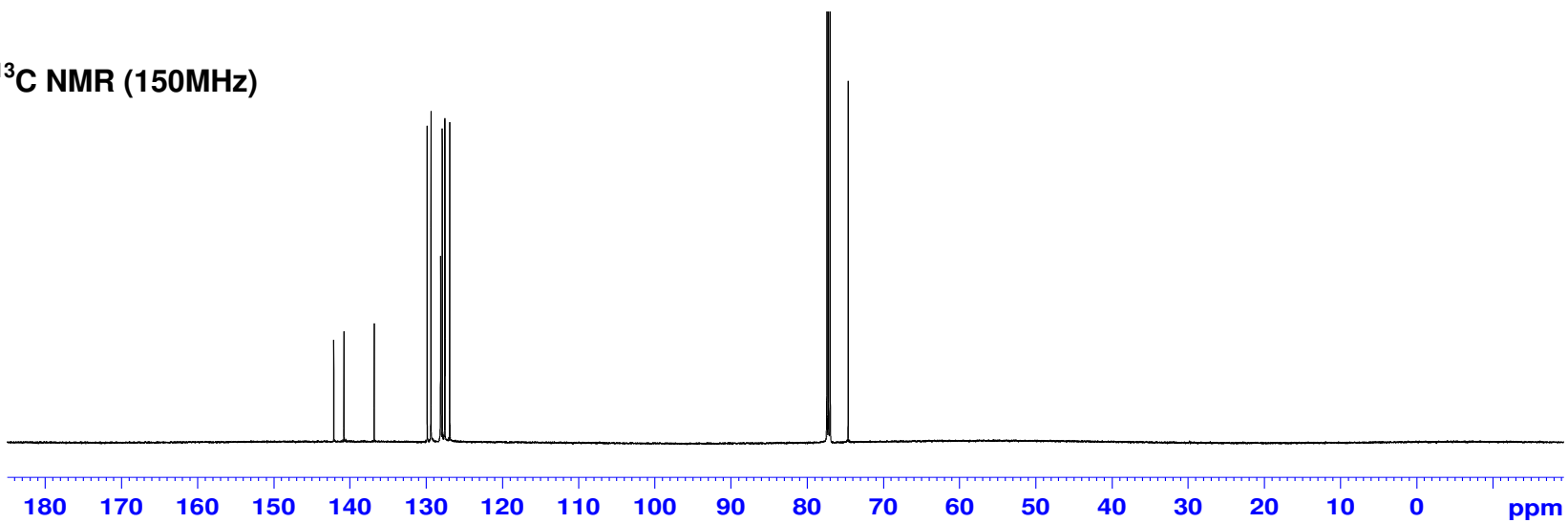
¹³C NMR (150MHz)



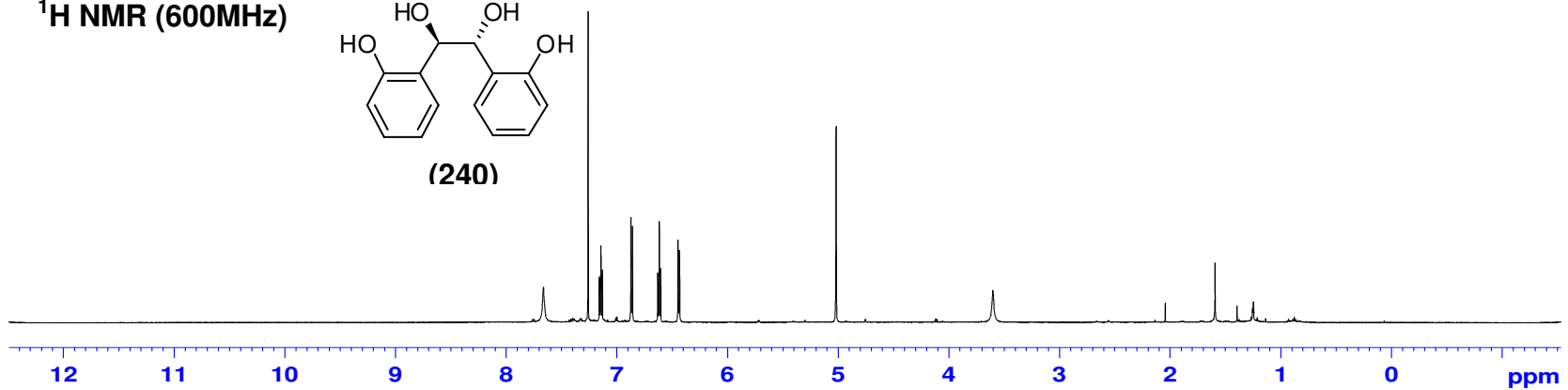
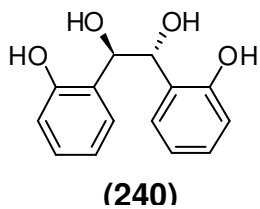
¹H NMR (600MHz)



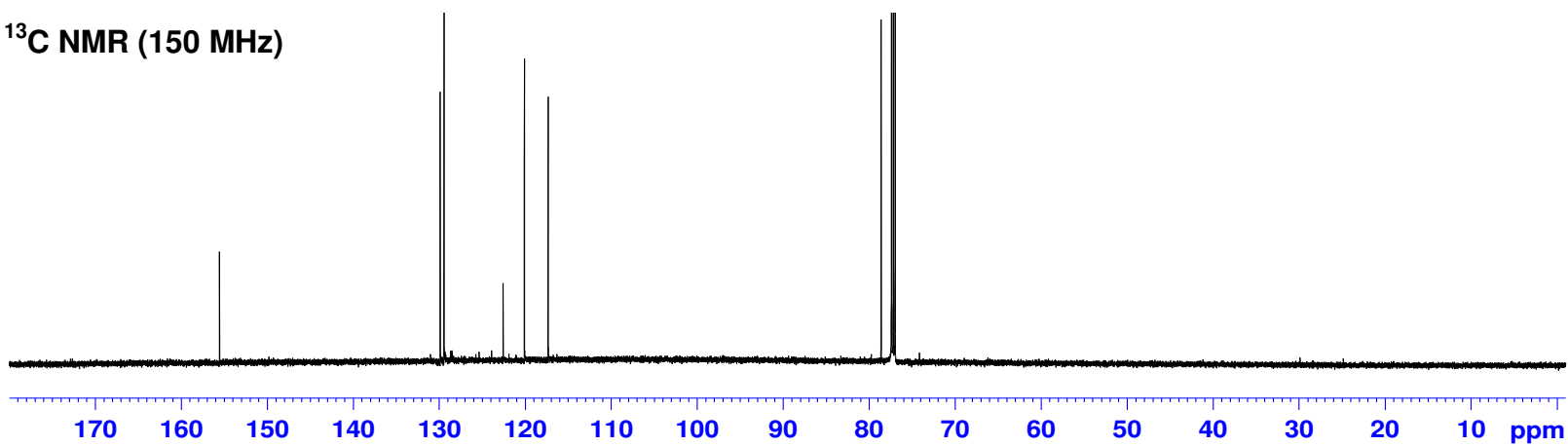
¹³C NMR (150MHz)



¹H NMR (600MHz)



¹³C NMR (150 MHz)



5.7 Crystal Structure Data for Compound 197

A clear colourless Plate-like specimen of $C_{18}H_{22}O_2Si_2$, approximate dimensions 0.03 mm x 0.25 mm x 0.46 mm, was used for the X-ray crystallographic analysis.

The X-ray intensity data were measured.

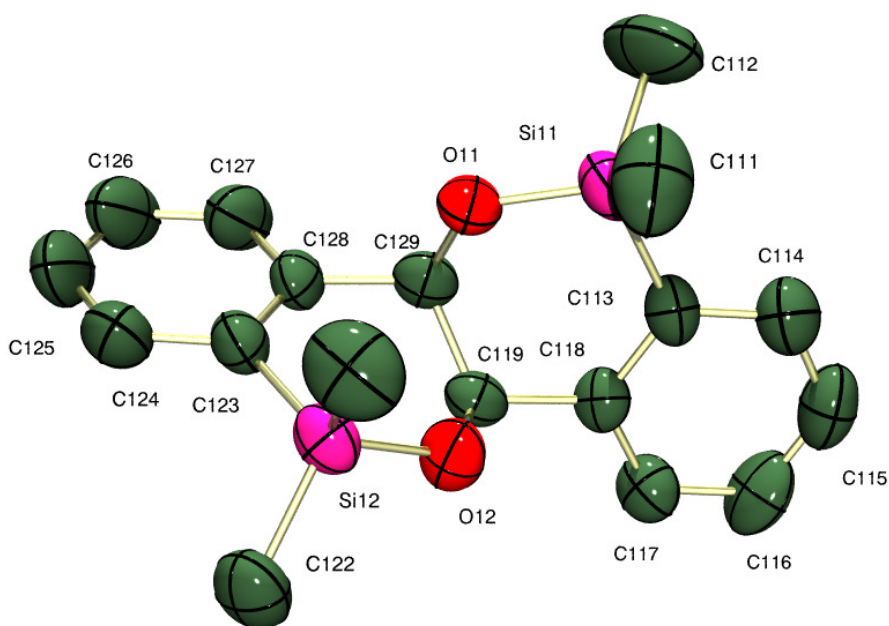
Data collection details for compound 197.

Axis	dx/mm	2 θ /°	ω /°	ϕ /°	χ /°	Width/°	Frames	Time/s
Omega	60.291	-28.00	-28.00	0.00	54.74	0.50	366	120.00
Omega	60.291	-28.00	-28.00	90.00	54.74	0.50	366	120.00
Omega	60.291	-28.00	-28.00	180.00	54.74	0.50	366	120.00
Omega	60.291	-28.00	-28.00	270.00	54.74	0.50	366	120.00

Wavelength/ Å	Voltage/kV	Current/mA	Temperature/K
0.71073	50.00	30.00	n/a
0.71073	50.00	30.00	n/a
0.71073	50.00	30.00	n/a
0.71073	50.00	30.00	n/a

A total of 1464 frames were collected. The total data collection time was 48.80 hours. The frames were integrated with the Bruker SAINT software package using a narrow-frame algorithm. The integration of the data using a monoclinic unit cell yielded a total of 33314 reflections to a maximum θ angle of 28.56° (0.74 Å resolution), of which 13085 were independent (average redundancy 2.546,

completeness = 94.2%, $R_{\text{int}} = 8.80\%$) and 3832 (29.29%) were greater than $2\sigma(F^2)$. The final cell constants of $a = 8.855(4) \text{ \AA}$, $b = 28.605(14) \text{ \AA}$, $c = 11.190(5) \text{ \AA}$, $\beta = 96.194(7)^\circ$, volume = $2818.(2) \text{ \AA}^3$, are based upon the refinement of the XYZ-centroids of 38 reflections above $20 \sigma(I)$ with $6.747^\circ < 2\theta < 26.19^\circ$. Data were corrected for absorption effects using the empirical multi-scan method (SADABS). The calculated minimum and maximum transmission coefficients (based on crystal size) are 0.9500 and 1.0000.



Sample and crystal data for 197.

Identification code	197	
Chemical formula	$C_{18}H_{22}O_2Si_2$	
Formula weight	326.54	
Wavelength	0.71073 \AA	
Crystal size	0.03 x 0.25 x 0.46 mm	
Crystal habit	clear colourless Plate	
Crystal system	monoclinic	
Space group	P 1 21 1	
Unit cell dimensions	$a = 8.855(4) \text{ \AA}$	$\alpha = 90^\circ$

	$b = 28.605(14) \text{ \AA}$	$\beta = 96.194(7)^\circ$
	$c = 11.190(5) \text{ \AA}$	$\gamma = 90^\circ$
Volume	$2818.(2) \text{ \AA}^3$	
Z	6	
Density (calculated)	1.154 Mg/cm^3	
Absorption coefficient	0.193 mm^{-1}	
F(000)	1044	

Data collection and structure refinement for 197.

Theta range for data collection	1.42 to 28.56°
Index ranges	$-11 \leq h \leq 11, -38 \leq k \leq 37, -15 \leq l \leq 14$
Reflections collected	33314
Independent reflections	13085 [R(int) = 0.0880]
Coverage of independent reflections	94.2%
Absorption correction	empirical multi-scan
Max. and min. transmission	1.0000 and 0.9500
Structure solution technique	direct methods
Structure solution program	SIR92 (Altomare et al., 1994)
Refinement method	Full-matrix least-squares on F
Refinement program	CRYSTALS (Betteridge et al., 2003)
Function minimized	$\sum w(F_o^2 - F_c^2)^2$
Data / restraints / parameters	13085 / 1 / 599
Goodness-of-fit on F	0.807
Δ/σ_{\max}	0.000

Final R indices	3832 data; $I > 2\sigma(I)$	R1 = 0.0346, wR2 = 0.0267
	all data	R1 = 0.1700, wR2 = 0.0267
Weighting scheme	Method= Modified Sheldrick $w = 1/[\sigma^2(F^2) + (0.00P)^2 + 0.00P]$, where $P = (\max(F_o^2, 0) + 2F_c^2)/3$	
Absolute structure parameter	-0.0(1)	

Atomic coordinates and equivalent isotropic atomic displacement parameters (\AA^2) for 197.

U(eq) is defined as one third of the trace of the orthogonalized U_{ij} tensor.

	x/a	y/b	z/c	U(eq)
Si11	0.4290(2)	0.16799(6)	0.93379(17)	0.07
Si12	0.4793(2)	0.28264(6)	0.67728(16)	0.0616
Si21	0.9717(2)	0.30580(6)	0.37073(17)	0.0598
Si22	0.8369(2)	0.42316(6)	0.13143(16)	0.0647
Si31	0.0899(2)	0.54832(6)	0.69792(18)	0.0754
Si32	0.1217(2)	0.58915(6)	0.32036(18)	0.0742
O11	0.4425(4)	0.17676(12)	0.7909(2)	0.0654
O12	0.3474(4)	0.27325(12)	0.7676(2)	0.0688
O21	0.8333(5)	0.31717(12)	0.2645(2)	0.0688
O22	0.8665(4)	0.41608(12)	0.2784(2)	0.0634
O31	0.1691(4)	0.53105(13)	0.5799(2)	0.0657
O32	0.9778(4)	0.57814(12)	0.3987(4)	0.0724
C111	0.5993(5)	0.1932(2)	0.0203(5)	0.1102
C112	0.4171(8)	0.1044(2)	0.9656(7)	0.1333
C113	0.2519(5)	0.1984(2)	0.9622(5)	0.0563
C114	0.1873(8)	0.1930(2)	0.0705(5)	0.0741
C115	0.0567(9)	0.2168(2)	0.0897(7)	0.0825
C116	0.9886(7)	0.2469(2)	0.0048(8)	0.0819
C117	0.0524(7)	0.2523(2)	0.8985(5)	0.0613

	x/a	y/b	z/c	U(eq)
C118	0.1810(7)	0.2284(2)	0.8752(5)	0.0489
C119	0.2443(5)	0.2354(2)	0.7569(5)	0.0507
C121	0.6696(5)	0.2796(2)	0.7610(5)	0.1013
C122	0.4510(7)	0.34165(18)	0.6076(5)	0.0816
C123	0.4463(7)	0.2358(2)	0.5625(5)	0.0585
C124	0.4966(7)	0.2383(2)	0.4478(7)	0.0803
C125	0.4632(10)	0.2033(2)	0.3642(7)	0.1069
C126	0.3810(10)	0.1657(2)	0.3900(7)	0.1041
C127	0.3296(8)	0.1616(2)	0.5012(7)	0.0815
C128	0.3630(7)	0.1964(2)	0.5869(5)	0.0535
C129	0.3140(5)	0.1907(2)	0.7113(5)	0.0526
C211	0.1551(5)	0.3134(2)	0.3095(5)	0.0823
C212	0.9502(7)	0.24490(18)	0.4258(5)	0.0832
C213	0.9411(7)	0.3484(2)	0.4935(5)	0.0491
C214	0.0158(7)	0.3434(2)	0.6099(7)	0.0676
C215	0.9848(8)	0.3735(2)	0.7017(5)	0.0778
C216	0.8767(8)	0.4080(2)	0.6778(5)	0.0672
C217	0.8042(5)	0.41347(18)	0.5651(5)	0.0547
C218	0.8366(5)	0.3844(2)	0.4707(5)	0.0435
C219	0.7614(5)	0.3918(2)	0.3453(5)	0.0487
C221	0.9999(7)	0.4009(2)	0.0600(5)	0.0939
C222	0.8132(8)	0.4866(2)	0.0978(5)	0.1014
C223	0.6627(7)	0.3899(2)	0.0857(5)	0.0559
C224	0.5707(9)	0.3976(2)	0.9780(5)	0.08
C225	0.4389(10)	0.3717(2)	0.9487(7)	0.0957
C226	0.3963(8)	0.3377(2)	0.0226(8)	0.0956
C227	0.4843(8)	0.3291(2)	0.1319(7)	0.068
C228	0.6150(7)	0.3555(2)	0.1625(5)	0.0533
C229	0.7077(7)	0.3468(2)	0.2817(5)	0.0533
C311	0.1502(8)	0.6096(2)	0.7313(5)	0.1184
C312	0.1514(8)	0.5108(2)	0.8281(5)	0.1186
C313	0.8832(7)	0.5429(2)	0.6533(7)	0.0652
C314	0.7749(10)	0.5433(2)	0.7351(5)	0.0856
C315	0.6229(10)	0.5389(2)	0.6972(9)	0.101

	x/a	y/b	z/c	U(eq)
C316	0.5702(9)	0.5338(2)	0.5769(9)	0.0973
C317	0.6759(8)	0.5328(2)	0.4949(5)	0.0741
C318	0.8306(7)	0.5367(2)	0.5321(7)	0.0589
C319	0.9412(7)	0.5323(2)	0.4382(5)	0.0577
C321	0.2464(7)	0.6337(2)	0.3981(5)	0.1137
C322	0.0522(7)	0.6094(2)	0.1671(5)	0.1059
C323	0.2163(5)	0.5314(2)	0.3106(5)	0.0607
C324	0.3107(7)	0.5207(2)	0.2211(5)	0.0832
C325	0.3715(8)	0.4761(2)	0.2128(7)	0.0956
C326	0.3405(8)	0.4425(2)	0.2930(8)	0.0898
C327	0.2474(7)	0.4521(2)	0.3794(5)	0.074
C328	0.1867(5)	0.4959(2)	0.3888(5)	0.0532
C329	0.0843(5)	0.5057(2)	0.4847(5)	0.0549

Bond lengths (Å) for 197

Si11-O11	1.635(4)	Si11-C111	1.849(6)
Si11-C112	1.857(6)	Si11-C113	1.851(6)
Si12-O12	1.646(4)	Si12-C121	1.840(5)
Si12-C122	1.865(5)	Si12-C123	1.858(6)
Si21-O21	1.644(4)	Si21-C211	1.842(5)
Si21-C212	1.865(5)	Si21-C213	1.878(6)
Si22-O22	1.649(4)	Si22-C221	1.838(6)
Si22-C222	1.860(6)	Si22-C223	1.838(6)
Si31-O31	1.637(4)	Si31-C311	1.858(6)
Si31-C312	1.844(6)	Si31-C313	1.851(6)
Si32-O32	1.654(4)	Si32-C321	1.842(6)
Si32-C322	1.851(6)	Si32-C323	1.860(6)
O11-C129	1.424(5)	O12-C119	1.414(6)
O21-C229	1.428(6)	O22-C219	1.435(6)
O31-C329	1.432(6)	O32-C319	1.432(6)
C113-C114	1.403(7)	C113-C118	1.395(7)
C114-C115	1.378(8)	C119-C129	1.529(6)
C115-C116	1.373(8)	C123-C124	1.405(7)
C116-C117	1.380(7)	C124-C125	1.379(8)

C117-C118	1.376(7)	C125-C126	1.347(9)
C118-C119	1.506(7)	C126-C127	1.375(8)
C123-C128	1.390(7)	C127-C128	1.391(7)
C213-C218	1.390(6)	C128-C129	1.511(7)
C219-C229	1.523(6)	C213-C214	1.403(7)
C223-C224	1.398(7)	C214-C215	1.390(7)
C224-C225	1.392(8)	C215-C216	1.382(7)
C225-C226	1.356(9)	C216-C217	1.360(7)
C226-C227	1.399(8)	C217-C218	1.398(7)
C227-C228	1.394(7)	C218-C219	1.502(7)
C228-C229	1.509(7)	C223-C228	1.400(7)
C313-C314	1.396(7)	C313-C318	1.397(7)
C314-C315	1.372(8)	C319-C329	1.520(7)
C315-C316	1.383(8)	C323-C324	1.405(7)
C316-C317	1.380(8)	C324-C325	1.391(8)
C317-C318	1.393(7)	C325-C326	1.364(8)
C318-C319	1.517(7)	C326-C327	1.364(8)
C323-C328	1.385(7)	C327-C328	1.372(7)
C328-C329	1.505(7)		

Bond angles (°) 197.

O11-Si11-C111	108.1(3)	O11-Si11-C112	110.4(3)
C111-Si11-C112	109.9(3)	O11-Si11-C113	104.4(3)
C111-Si11-C113	112.7(3)	C112-Si11-C113	111.1(3)
O12-Si12-C121	110.6(3)	O12-Si12-C122	109.4(3)
C121-Si12-C122	109.3(3)	O12-Si12-C123	103.7(3)
C121-Si12-C123	112.6(3)	C122-Si12-C123	111.1(3)
O21-Si21-C211	109.0(3)	O21-Si21-C212	109.2(3)
C211-Si21-	111.0(3)	O21-Si21-	104.2(3)

C212		C213	
C211-Si21-C213	113.4(3)	C212-Si21-C213	109.7(3)
O22-Si22-C221	110.0(2)	O22-Si22-C222	108.9(2)
C221-Si22-C222	109.1(3)	O22-Si22-C223	104.6(3)
C221-Si22-C223	112.0(3)	C222-Si22-C223	112.1(3)
O31-Si31-C311	107.9(3)	O31-Si31-C312	110.2(3)
C311-Si31-C312	109.7(3)	O31-Si31-C313	104.7(3)
C311-Si31-C313	112.9(3)	C312-Si31-C313	111.3(3)
O32-Si32-C321	109.8(3)	O32-Si32-C322	110.6(3)
C321-Si32-C322	110.1(3)	O32-Si32-C323	103.9(3)
C321-Si32-C323	113.0(3)	C322-Si32-C323	109.3(3)
Si11-O11-C129	121.1(3)	Si12-O12-C119	124.6(3)
Si21-O21-C229	123.4(4)	Si22-O22-C219	122.5(3)
Si31-O31-C329	121.1(3)	Si32-O32-C319	123.4(3)
Si11-C113-C114	121.9(6)	Si11-C113-C118	119.7(5)
C114-C113-C118	118.4(6)	C113-C114-C115	120.5(7)
C114-C115-C116	121.0(7)	C115-C116-C117	118.5(7)
C116-C117-C118	122.1(6)	C113-C118-C117	119.5(6)
C113-C118-C119	120.8(6)	C117-C118-C119	119.7(6)
C118-C119-O12	109.0(5)	C118-C119-C129	112.6(5)
O12-C119-	112.8(4)	Si12-C123-	119.8(5)

C129		C128	
Si12-C123-C124	123.6(6)	C123-C124-C125	121.1(7)
C124-C123-C128	116.6(6)	C125-C126-C127	120.1(8)
C124-C125-C126	120.9(8)	C127-C128-C123	121.5(6)
C126-C127-C128	119.7(7)	C123-C128-C129	118.6(6)
C127-C128-C129	119.9(6)	C119-C129-O11	110.4(4)
C119-C129-C128	112.6(5)	Si21-C213-C218	119.5(5)
C128-C129-O11	108.5(4)	C213-C214-C215	120.8(6)
Si21-C213-C214	121.5(5)	C215-C216-C217	120.6(6)
C214-C213-C218	118.9(6)	C217-C218-C213	119.3(5)
C214-C215-C216	119.2(6)	C213-C218-C219	119.7(5)
C216-C217-C218	121.1(6)	C218-C219-C229	113.7(5)
C217-C218-C219	121.0(6)	Si22-C223-C228	119.5(5)
C218-C219-O22	108.0(4)	C223-C224-C225	121.0(7)
O22-C219-C229	110.7(4)	C225-C226-C227	119.6(8)
Si22-C223-C224	123.5(6)	C223-C228-C227	121.8(6)
C224-C223-C228	117.0(6)	C227-C228-C229	119.0(6)
C224-C225-C226	121.3(8)	C219-C229-O21	110.8(5)
C226-C227-C228	119.3(7)	Si31-C313-C318	119.3(5)
C223-C228-C229	119.2(6)	C313-C314-C315	121.1(7)
C219-C229	112.6(5)	C315-C316	117.8(8)

C228		C317	
C228-C229-O21	109.7(5)	C313-C318-C317	120.9(6)
Si31-C313-C314	123.5(6)	C317-C318-C319	118.3(7)
C314-C313-C318	117.2(6)	C318-C319-C329	112.4(5)
C314-C315-C316	121.9(8)	Si32-C323-C328	119.8(5)
C316-C317-C318	121.1(7)	C323-C324-C325	120.8(7)
C313-C318-C319	120.7(6)	C325-C326-C327	120.2(7)
C318-C319-O32	108.8(5)	C323-C328-C327	121.3(6)
O32-C319-C329	110.8(4)	C327-C328-C329	119.8(6)
Si32-C323-C324	122.8(6)	C319-C329-O31	110.6(5)
C324-C323-C328	117.2(6)		
C324-C325-C326	119.7(7)		
C326-C327-C328	120.7(7)		
C323-C328-C329	118.9(6)		
C319-C329-C328	113.1(5)		
C328-C329-O31	108.5(4)		

REFERENCES

1. Ed.: Christmann, M.; Brase, S. *Asymmetric Synthesis – The Essentials*. Wiley-VCH, Weinheim, **2007**, p. 47.
2. For the beneficial pharmaceutical properties of the (*R*)-enantiomer of thalidomide see: Høglund, P.; Eriksson, T.; Bjorkman, S. *J. Pharmacomet. Biopharm.* **1998**, *26*, 363. For the adverse pharmaceutical properties of the (*S*)-enantiomer of thalidomide see: Wnendt, W.; Finkam, M.; Winter, W.; Ossig, J.; Raabe, G. Zwingenberger, K. *Chirality.* **1996**, *8*, 390.
3. Nobel lectures for catalytic asymmetric synthesis: a) Knowles, W.S. *Angew. Chem. Int. Ed. Engl.* **2002**, *41*, 1998; b) Noyori, R. *Angew. Chem. Int. Ed. Engl.* **2002**, *41*, 2002; c) Sharpless, K.B. *Angew. Chem. Int. Ed. Engl.* **2002**, *41*, 2024.
4. Evans, D.A.; Bartroli, J.; Shih, T.L. *J. Am. Chem. Soc.* **1981**, *103*, 2127.
5. Brunel, J.M. *Chem. Rev.* **2005**, *105*, 857. For other examples of the reduction of carbonyl functions using BINAL see: Kells, K.W.; Ncube, A.; Chong, J.M. *Tetrahedron.* **2004**, *60*, 2247.
6. 1) Gage, J.R.; Evans, D.A. *Org. Synth.* **1990**, *68*, 83. 2) Evans, D.A.; Britton, T.C.; Ellman, J.A. *Tetrahedron Lett.* **1987**, *28*, 6141.
7. Shibasaki, M.; Matsunaga, S. *Chem. Soc. Rev.* **2006**, *35*, 269.
8. Kizirian, J.-C. *Chem. Rev.* **2008**, *108*, 140.
9. Zhang, W.; Chi, Y.; Zhang, X. *Acc. Chem. Res.* **2007**, *40*, 1278.
10. Kagan, H.B.; Dang, T.P. *J. Am. Chem. Soc.* **1972**, *94*, 6429.
11. Blaser, H.-U.; Studer, M. *Chirality*, **1999**, *11*, 459.

-
12. Broecker, J.; Knollmueller, M.; Gaertner, P. *Tetrahedron: Asymmetry*, **2006**, *17*, 2413.
13. Andrus, M.B.; Sekhar, B.B.V.S.; Meredith, E.L.; Dalley, N.K. *Org. Lett.* **2000**, *2*, 3035.
14. Kim, K.S.; Lee, Y.J.; Kim, J.H.; Sung, D.K. *Chem. Commun.* **2002**, 1116.
15. Mazé, F.; Purpura, M.; Bernaud, F.; Mangeney, P.; Alexakis, A. *Tetrahedron: Asymm.* **2001**, *12*, 1957.
16. Marshall, J.A.; Xie, S. *J. Org. Chem.* **1995**, *60*, 7230.
17. Ceder, O.; Hansson, G. *Acta. Chem. Scand.* **1970**, *24*, 2693.
18. Loncharick, R.J.; Schwartz, T.R.; Houk, K.N. *J. Am. Chem. Soc.* **1987**, *109*, 14.
19. Wallace, T.W.; Wardell, I.; Li, K.-D.; Leeming, P. Redhouse, A.D. Challand, S.R. *J. Chem. Soc. Perkins Trans. 1.* **1995**, 2293.
20. Caramella P.; Rondan N.G.; Paddon-Row M.N., Houk K.N. *J. Am. Chem. Soc.* **1981**, *103*, 2438.
21. Fujioka, H.; Kitagawa, H.; Nagatomi, Y.; Kita, Y. *Tetrahedron: Asymmetry*, **1995**, *6*, 2113.
22. Rauniyar, V.; Zhai, H.; Hall, D.G. *J. Am. Chem. Soc.* **2008**, *130*, 8481.
23. Mlynarski, J.; Mitura, M.; *Tetrahedron Lett.* **2004**, *45*, 7549.
24. For an example of a polyketide containing a 1,2-anti-, 1,3-anti relationship see: Corey, E.J.; Nicolau, K.C.; *J. Am. Chem. Soc.* **1974**, *96*, 5614.
25. Mlynarski, J.; Jankowska, J.; Rakiel, B. *Tetrahedron: Asymmetry.* **2005**, *16*, 1521.

-
26. Denmark, S.E.; Beutner, G.L. *Angew. Chem. Int. Ed. Engl.* **2008**, *47*, 1560.
27. Amurrio, D.; Khan, K. Kundig, E.P. *J. Org. Chem.* **1996**, *61*, 2258.
28. Tomioka, K.; Shindo, M.; Koga, K. *J. Am. Chem. Soc.* **1989**, *111*, 8266.
29. McMurry, J.E.; Fleming, M.P. *J. Am. Chem. Soc.* **1974**, *96*, 4708.
30. Jacobsen, E.N.; Marko, I.; Mungall, W.S.; Schroder, G.; Sharpless, K.B. *J. Am. Chem. Soc.* **1988**, *110*, 1968.
31. Mori, Y.; Manabe, K.; Kobayashi, S. *Angew. Chem. Int. Ed.* **2001**, *40*, 2815.
32. Paterson, I.; Delgado, O.; Florence, G.J.; Lyothier, I.; Scott, J.P.; Sereinig, N. *Org. Lett.* **2003**, *5*, 35.
33. Snieckus, V. *Chem. Rev.* **1990**, *90*, 879.
34. Gilman, H.; Bebb, R.L. *J. Am. Chem. Soc.* **1939**, *61*, 109.
35. Wittig, G.; Fuhrman, G. *Chem. Ber.* **1940**, *73*, 1197.
36. a) Langer, A.W. *Adv. Chem. Ser.* **1974**, No. 130. b) Halesa, A.F.; Schulz, D.N.; Tate, D.P.; Mochel, V.D. *Adv. Organomet. Chem.* **1980**, *18*, 55.
37. Gschwend, H.W.; Rodriguez, H.R. *Org. React. (N.Y.)* **1979**, *26*, 1.
38. Hay, D.R.; Song, Z.G.; Smith, S.G.; Beak, P. *J. Am. Chem. Soc.* **1988**, *110*, 8145.
39. a) Hommes, N.; Schleyer, P.von R. *Angew Chem.* **1992**, *104*, 768. b) Hommes, N.; Schleyer, P. Von R. *Tetrahedron.* **1994**, *50*, 5903.
40. Bauer, W.; Schleyer, P. Von R. *J. Am. Chem. Soc.* **1989**, *111*, 7191.
41. Saa, J.M.; Deya, P.M.; Suner, G.A.; Frontera, A. *J. Am. Chem. Soc.* **1992**, *114*, 9093.
42. Anderson, D.R.; Faibish, N.C.; Beak, P. *J. Am. Chem. Soc.* **1999**, *121*, 7553.

-
43. Chadwick, S.T.; Rennels, R.A.; Rutherford, J.L.; Collum, D.B. *J. Am. Chem. Soc.* **2000**, *122*, 8640.
44. Collum, D.B. *Acc. Chem. Res.* **1992**, *25*, 448.
45. Buker, H.H.; Nibbering, N.M.M.; Espinosa, D.; Mongin, F.; Schlosser, M. *Tetrahedron Lett.* **1997**, *38*, 8519.
46. Meyer, N., Seebach, D. *Angew. Chem. Int. Ed. Engl.* **1978**, *17*, 521.
47. Hirt, U.H.; Spingler, B.; Wirth, T. *J. Org. Chem.* **1998**, *63*, 7674.
48. Panetta, C.A.; Garlick, S.M.; Durst, H.D.; Longo, F.R.; Ward, J.R. *J. Org. Chem.* **1990**, *55*, 5202.
49. Wang, Z.M.; Sharpless, K.B. *J. Org. Chem.* **1994**, *59*, 8302.
50. Truhlar, D.G.; Cramer, C.J.; Kass, S.R.; Thompson, J.D. *J. Org. Chem.* **2007**, *72*, 2962.
51. a) R.E. Bates, L.M. Kroposki, D.E. Potter, *J. Org. Chem.* **1972**, *37*, 560. b) Clayden, J.; S.A. Yasin, *New J. Chem.* **2002**, *26*, 191-192.
52. Bromn, T.L.; Ladd, J.A.; Newman, G.N. *J. Organometal. Chem.* **1965**, *3*, 1.
53. Mulvaney, J.R.; Groen, S.; Carr, L.J.; Gardlund, Z.G.; Gardlund, S.L. *J. Am. Chem. Soc.* **1969**, *91*, 388.
54. Periasamy, M.; Srinivas, G.; Karunakar, G.V.; Bharathi, P. *Tetrahedron Lett.* **1999**, *40*, 7577.
55. Russell, G.A.; Janzen, E.G.; Thomas, E. *J. Am. Chem. Soc.* **1964**, *86*, 1807.
56. For comparison purposes, the C=O stretch of isobenzofuran-1(3*H*)-one (γ -lactone) = 1765 cm⁻¹. Anzalone, L.; Hirsche, J.A. *J. Org. Chem.* **1985**, *50*, 2128.

-
- The C=O stretch of isochroman-1-one (δ -lactone) is 1720 cm^{-1} . Shaabani, A.; Mirzaei, P.; Naderi, S.; Lee, D.G. *Tetrahedron*, **2004**, *60*, 11415.
57. Gilman, H.; Miles, D.H.; Moore, L.O. *J. Org. Chem.* **1959**, *24*, 219.
58. For ^1H NMR of this ketone see: Kulasegaram, S.; Kulawiec, R.J. *J. Org. Chem.* **1997**, *62*, 6547. Characteristic methylene ^1H NMR peak at δ 4.29 (s, 2H).
59. Comanita, B.M.; Woo, S.; Fallis, A.G. *Tetrahedron Lett.* **1999**, *40*, 5283.
60. Manoso, A.S.; Ahn, C.; Soheili, A.; Handy, C.J. Correia, R.; Seganish, W.M.; Deshong, P. *J. Org. Chem.* **2004**, *69*, 8305. In this paper, the reaction of organolithiums requires cryogenic conditions whereas Grignard reagents afford similar yields at higher temperatures.
61. ^1H NMR of dimethyl diiodo hydrobenzoin **217** (500 MHz, CDCl_3) δ : 7.63 (d, 4H, $J = 5.0\text{ Hz}$), 7.31 (t, 2H, $J = 5.0\text{ Hz}$), 6.88 (t, 2H, $J = 10\text{ Hz}$), 4.80 (s, 2H), 3.19 (s, 6H).
62. Russell, G.A.; Janzen, E.G.; Strom, E.T. *J. Am. Chem. Soc.* **1964**, *86*, 1807.
63. Ocampo, R.; Dolbier Jr., W.R.; *Tetrahedron*, **2004**, *60*, 9325.
64. For example, see: a) Guerinot, A.; Reymond, S.; Cossy, J. *Angew. Chem. Int. Ed.* **2007**, *46*, 6521; b) de Boer, H.J.R.; Akkerman, O.S.; Bickelhaupt, F. *Angew. Chem. Int. Ed.* **1988**, *27*, 687.
65. For the ^1H NMR of compound **232** see: Kabalka, G.W.; Li, N.S.; Yu, S. *Tetrahedron Lett.* **1995**, *36*, 8545.
66. Yamamoto, H.; Kobayashi, S.; Kanemasa, S. *Tetrahedron: Asymmetry* **1996**, *7*, 149.

-
67. Zhang, H.; Cai, Q.; Ma, Dawei. *J. Org. Chem.* **2005**, *70*, 5164.
68. Brastianos, H.I Sturgeon, C.M.; Roberge, M. Andersen, R.J. *J. Nat. Prod.* **2007**, *70*, 287.
69. Taniguchi, N.; Hata, T.; Uemura, M. *Angew. Chem. Int. Ed.* **1999**, *38*, 1232.
70. Baker, K.M.; Csetenyi, J. Frigerio, A.; Morselli, P.L. *J. Med. Chem.* **1973**, *16*, 703.
71. Reichert, S., Breit, B. *Org. Lett.* **2007**, *9*, 899.
72. Hassa, J.; Sevignon, M.; Gozzi, C.; Schulz, E. Lemaire, M. *Chem. Rev.* **2002**, *102*, 703.
73. Fürstner, A.; Martin, R. *Chem. Lett.* **2005**, *34*, 624 and references therein.
74. Zhang, S.; Zhang, D.; Liebeskind, L.S. *J. Org. Chem.* **1997**, *62*, 2312.
75. Campeau, L.-C.; Rousseaux, S.; Fagnou, K. *J. Am. Chem. Soc.* **2005**, *127*, 18020.
76. Byers, P.K.; Canty, A.J.; Crespo, M.; Puddephatt, R.J.; Scott, J.D. *Organometallics*, **1988**, *7*, 1363.
77. Maruoka, K.; Itoh, T.; Shirasaka, T.; Yamamoto, H. *J. Am. Chem. Soc.* **1988**, *110*, 310.
78. Chen, Y.; Yekta, S.; Yudin, A.K. *Chem. Rev.* **2003**, *103*, 3155.
79. Still, W.C.; Kahn, M.; Mitra, A. *J. Org. Chem.* **1978**, *43*, 2923.
80. Gottlieb, H.E.; Kotlyar, V.; Nudelman, A. *J. Org. Chem.* **1997**, *62*, 7512.
81. Lin, H; Paquette, L.A. *Synth. Commun.* **1994**, *24*, 2503.
82. The ratio of total hexane-ether in this reaction was 2:1 (v/v)
83. Andrus, M.B.; Soma S.B.B.V.; Meredith, E.L.; Dalley, N.K. *Org. Lett.* **2000**, *2*, 3035.

84. Wyatt, P.; Warren, S.; McPartlin, M.; Woodroffe, T. *J. Chem. Soc.; Perkin Trans 1*, **2001**, 279.

85. Solid CO₂ was warmed in a round bottom flask (heat gun) and the resulting gas was passed through a column of drierite then bubbled directly into the reaction mixture.

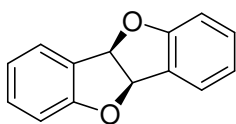
86. When the ¹H NMR spectrum of **196** was recorded in CDCl₃, additional resonances attributed to dimeric or trimeric forms of **196** were observed.

87. Mass spectrometry methods attempted: CI, EI, ESI (negative and positive ion), FAB. The ethanolamine complex also failed to provide a parent ion using these techniques.

88. Dale, W.J.; Rush, E.J. *J. Org. Chem.* **1962**, 27, 2598.

89. Alo, B.I.; Kandil, A.; Patil, P.A.; Sharp, M.J.; Siddiqui, M.A.; Snieckus, V. Josephy, P.D. *J. Org. Chem.* **1991**, 56, 3763.

90. When this cross coupling was attempted without protection of the alcohol functions, *cis*-4b,9b-dihydrobenzofuro[3,2-b]-benzofuran was formed as the major product. For an unrelated synthesis of this compound see: Clerici, A.; Porta, O. *J. Org. Chem.* **1990**, 55, 1240.



¹H NMR (500 MHz, CDCl₃) δ: 7.55 (d, 2H, *J* = 7.5 Hz), 7.29 (t, 2H, *J* = 8.0 Hz), 6.98 (t, 2H, *J* = 7.5 Hz), 6.89 (d, 2H, *J* = 8.0 Hz), 6.29 (s, 2H). ¹³C NMR (125 MHz, CDCl₃) δ: 160.1, 131.5, 126.7, 124.5, 121.3, 110.9, 86.6. IR (KBr pellet):

3050, 2923, 1601, 1481, 1463, 958, 746 cm⁻¹. Exact mass calcd. for C₁₄H₁₁O₂: 211.0759; found: 211.0755. $[\alpha]_D^{25} = +371^\circ$ (*c* = 0.50, CHCl₃). Melting Point: 154 °C.

91 Stang, P.J.; Treptow, W. *Synthesis*, **1980**, 283.

92 Scheiper, B.; Bonnekessel, M.; Krause, H.; Fürstner, A. *J. Org. Chem.* **2004**, *69*, 3943.

93. Simon, J.; Salzbrunn, S.; Prakash, G.K.S.; Petasis, N.A.; Olah, G.A. *J. Org. Chem.* **2001**, *66*, 633.

94. For an unrelated synthesis of this compound see: Annunziata, R.; Benaglia, M.; Cinquini, M.; Raimondi, L. *Eur. J. Org. Chem.* **1999**, 3369.